PAPAIN CRYSTALLIZATION USING SOLVENT FREEZE-OUT TECHNIQUE

CHONUT XAIYATHOUMMA

A Thesis Submitted in Partial Fulfillment of the Requirements for the

Degree of Master of Engineering in Mechanical and Process System Engineering

Suranaree University of Technology

Academic Year 2025

การตกผลึกเอนไซม์ปาเปนโดยใช้เทคนิคการเยือกแข็งตัวทำละลาย

นายโจนัด ไซยะทุมมา

วิทยานิพนธ์นี้เป็นส่วนหนึ่งของการศึกษาตามหลักสูตรปริญญาวิศวกรรมศาสตรมหาบัณฑิต

สาขาวิชาวิศวกรรมเครื่องกลและระบบกระบวนการ

มหาวิทยาลัยเทคโนโลยีสุรนารี

ปีการศึกษา 2568

PAPAIN CRYSTALLIZATION USING SOLVENT FREEZE-OUT TECHNIQUE

Suranaree University of Technology has approved this thesis submitted in partial fulfillment of the requirements for a Master's degree.

Thesis Examining Committee

.....

(Asst. Prof. Dr. Atthaphon Maneedaeng)
Chairperson

.....

(Assoc. Prof. Dr. Lek Wantha)
Member (Thesis Advisor)

.....

(Prof. Dr. Adrian Evan Flood)
Member

.....

(Prof. Dr. Hongxun Hao)
Member

.....

(Assoc. Prof. Dr. Yupaporn Ruksakulpiwat)
Acting Vice Rector for Academic Affairs
and Quality Assurance

.....

(Assoc. Prof. Dr. Pornsiri Jongkol)
Dean of Institute of Engineering

โจนัด ไชยะทุมมา: การตกผลึกเอนไซม์ปาเปนโดยใช้เทคนิคการเยือกแข็งตัวทำละลาย (PAPAIN CRYSTALLIZATION USING SOLVENT FREEZE-OUT TECHNIQUE) อาจารย์ที่ปรึกษา: รองศาสตรจารย์ ดร. เล็ก วันทา, 88 หน้า.

คำสำคัญ: ความสามารถในการละลายของปาเปน เทคนิคการเยือกแข็งตัวทำละลาย การตกผลึกด้วยสารต้านการละลาย การตกผลึกด้วยการลดอุณหภูมิสารละลาย กิจกรรมของเอนไซม์

ในงานวิจัยนี้ได้ศึกษาการตกผลึกเอนไซม์ปาเปน (Papain) ด้วยสามวิธีได้แก่ การลดอุณหภูมิสารละลาย การใช้สารต้านการละลาย และการเยือกแข็งตัวทำละลาย (Solvent Freeze-Out, SFO) เบื้องต้นได้การศึกษาความสามารถในการละลายของปาเปน พบว่าความสามารถในการละลายลดลงตามปริมาณที่เพิ่มขึ้นของเมทานอล (0–60% w/w) และตามอุณหภูมิที่ลดลง แต่ไม่มีผลกระทบจากค่า pH (5–7) การตกผลึกด้วยสารต้านการละลายเมทานอลได้ผลผลิตเฉพาะเป็นของแข็งแบบอสัณฐาน (Amorphous) เท่านั้น ในขณะที่การตกผลึกด้วยการลดอุณหภูมิสารละลายแบบควบคุมอัตราการลดลงของอุณหภูมิที่ 0.005 °C/นาที ได้ผลึกปาเปนคล้ายเข็มจากการป้อนสารละลายเข้มข้น 0.97 g/mL และ 0.77 g/mL โดยมีอุณหภูมิการเกิดผลึก (Crystal nucleation) ตั้งแต่ 12.5 °C ถึง –3 °C ตามลำดับ ผลการศึกษาพบว่าเทคนิค SFO มีประสิทธิภาพเหนือกว่าทั้งสองวิธี โดยประสบความสำเร็จในการตกผลึกสารละลายปาเปนเจือจาง (0.33–0.472 g/mL) ที่อุณหภูมิใกล้เยือกแข็ง (1 °C ถึง –1.5 °C) ด้วยการควบคุมอัตราการโตของน้ำแข็งอย่างแม่นยำ โดยอุณหภูมิสุดท้ายของคอยล์แช่แข็ง (Freeze coil) คือ –14 °C และ –12.6 °C ผลึกที่ได้จาก SFO มีทั้งแบบเข็มและแผ่นผสมกัน ที่มีความเป็นผลึกสูง (ซึ่งยืนยันด้วย PXRD) และ ผลกิจกรรมของผลึกเอนไซม์ปาเปนยังคงไม่เปลี่ยนแปลงเมื่อเทียบกับปาเปนเชิงพาณิชย์ ในขณะที่ร้อยละการผลิตผลึกปาเปนได้ มากกว่า 55% การสูญเสียปาเปนในน้ำแข็ง น้อยกว่า 30% ผลลัพธ์เหล่านี้ทำให้เทคนิค SFO เป็นแนวทางที่มีประสิทธิภาพในการผลิตผลึกโปรตีนที่ออกฤทธิ์ทางชีวภาพ (ผลึกเอนไซม์) ซึ่งจัดการกับข้อจำกัดที่สำคัญของวิธีการทั่วไป วิธีการนี้เป็นกรอบสำหรับการตกผลึกปาเปนที่สามารถประยุกต์ใช้ตรงกับการผลิตยาได้ในอนาคต

สาขาวิชา วิศวกรรมเคมี ลายชื่อนักศึกษา .....

ปีการศึกษา 2568 ลายชื่ออาจารย์ที่ปรึกษา .....

CHONUT XAIYATHOUMMA: PAPAIN CRYSTALLIZATION USING SOLVENT FREEZE-OUT TECHNIQUE

THESIS ADVISOR: ASSOC. PROF. LEK WANTHA, Ph.D., 88 PP

Keyword: PAPAIN SOLUBILITY, SOLVENT FREEZE-OUT, ANTISOLVENT CRYSTALLIZATION, COOLING CRYSTALLIZATION, ENZYMATIC ACTIVITY

This work systematically evaluates the solvent freeze-out (SFO) crystallization for producing functional papain crystals. Through phase behavior analysis, we demonstrate that papain solubility decreases predictably with increasing methanol content (0–60% w/w) and decreasing temperature, but shows no measurable effect of pH (5–7); solubility in acetate buffer (pH 5) is comparable to that in water. Preliminary antisolvent crystallization with methanol recovered only amorphous aggregates, while controlled cooling crystallization (0.005 °C/min) generated metastable needle-like crystals from concentrated solutions (0.97 g/mL; 0.77 g/mL), with nucleation temperatures ranging from 12.5 °C to −3 °C. The SFO technique outperformed both methods, successfully crystallizing dilute solutions (0.33–0.472 g/mL) at near-freezing temperatures (1 °C to −1.5 °C) with precise ice-growth control (freezing coil: −14 °C to −12.6 °C). The SFO-derived crystals exhibited defined mixed needle/plate like morphology, high crystallinity (PXRD-confirmed), and preserved enzymatic activity (specific activity unchanged vs. commercial papain), while achieving greater than 55% recovery and less than 30% solute loss in ice. These results establish SFO as a robust approach for producing bioactive protein crystals, addressing critical limitations of conventional methods and serving as an alternative for initially low-concentration feeds. The methodology provides a framework for crystallizing papain, with direct relevance to pharmaceutical manufacturing.

School of Chemical Engineering

Academic Year 2025

Student's Signature .....

Advisor's Signature .....

ACKNOWLEDGEMENT

This thesis was successfully completed with invaluable support and assistance from many individuals, both academically and in the research process, as well as emotionally. I would like to express my deepest gratitude to the following people:

Assoc. Prof. Dr. Lek Wantha, my thesis advisor from the School of Chemical Engineering at Suranaree University of Technology, provided me with educational opportunities, offered invaluable guidance in my research, and assisted in every aspect of my academic and personal life. He consistently supported various research endeavors, meticulously reviewed, and corrected this thesis, ensuring its successful completion.

I would like to thank my thesis committee members, Asst. Prof. Dr. Atthaphon Maneedaeng, Prof. Dr. Adrian Evan Flood and Prof. Dr. Hongxun Hao for agreement to the part of my committee for my thesis defense. Thank you for your valuable comments and recommendations.

I extend my sincere thanks to all faculty members of the School of Chemical Engineering at Suranaree University of Technology for their dedicated teaching, guidance, and support throughout my academic journey.

Special thanks to Mr. Saran Dokmaikun, a staff member at the Center for Scientific and Technological Equipment, for facilitating the finding of instruments and providing essential guidance during the research process.

Thank you to Mrs. Amphorn Ladnongkhun for her assistance, coordination, and advice on documentation throughout my studies.

I sincere thanks to Prof. Hongxun Hao and members of research group (National Engineering Research Center of Industrial Crystallization Technology, NERCICT) at Tianjin University, China for exchange program of practical research process.

The author would like to thank you to the National Science and Technology Development Agency (NSTDA) according to the Thailand Graduate Institute of Science and Technology (TGIST) scholarship agreement No. SCA-CO-2563-12080-EN for financial

support and Suranaree University of Technology research fund. The authors also acknowledge the research funding from (i) Suranaree University of Technology (SUT), (ii) Thailand Science Research and Innovation (TSRI), and (iii) National Science, Research and Innovation fund (NSRF)-Grant No. 195675.

Finally, I would like to extend my heartfelt thanks to my parents for their unwavering support, encouragement, and financial assistance throughout my studies. Additionally, I am grateful to my fellow graduate students and members of chemical engineering in National University of Laos for their continuous support, motivation, and advice, which has been vital to the completion of this thesis. I am profoundly appreciative and would like to express my highest gratitude to everyone mentioned here.

Chonut Xaiyathoumma

TABLE OF CONTENTS

Page

TABLE OF CONTENTS (Continued)

Page

TABLE OF CONTENTS (Continued)

Page

LIST OF TABLES

Table **Page**

LIST OF FIGURES

Figure **Page**

LIST OF FIGURES (Continued)

Figure **Page**

LIST OF FIGURES (Continued)

Figure **Page**

LIST OF FIGURES (Continued)

Figure **Page**

LIST OF FIGURES (Continued)

Figure **Page**

CHAPTER I

INTRODUCTION

1.1 Background and Significance

The demand for therapeutic proteins and industrial enzymes in chemical, food, and pharmaceutical industries is increasing (Motoki & Seguro, 1998). Therefore, efficient methods for protein extraction and purification from their original source are necessary on an industrial scale (Tam, Chan, & Ng, 2011). Chromatography and precipitation often require many steps to achieve high purity and stability and can be cost-intensive at industrial scale (Chisti & Moo-Young, 1990; Wiencek, 1999). Protein crystallization can be a relatively economical purification step for industrial applications. Crystalline proteins offer advantages compared to the dissolved or amorphous solid in terms of drug release, handling, stability, purity, and shelf life (Drenth & Haas, 1992; Schmidt, Havekost, Klaus Kaiser, Kauling, & Henzler, 2005). Moreover, the crystallization can serve as a cost-effective and highly selective purification step in downstream processing and possibly as an alternative method to replace one or more chromatographic steps. However, the classical crystallization theory does not fully capture the behavior of all protein systems due to protein has highly complex structure that can make purification challenging. Proteins may fail to crystallize under small temperature variations, incompatible reagents, or inadequate hygiene conditions, all of which can negatively affect purity.

An industrial technique for separation and purification known as solid-layer melt crystallization, has been introduced (Ulrich, Bierwirth, & Henning, 1996). This method has been adapted to introduce solvent freeze-out (SFO) crystallization as a novel protein crystallization approach in industrial applications (Borbon & Ulrich, 2013; Ming et al., 2021). More work on SFO crystallization by Diaz Borbon and Ulrich improved this method and applied it to the separation of proteins such as lysozyme crystallized from lysozyme-ovalbumin mixture (Borbón & Ulrich, 2012; Yu, Wang, & Ulrich, 2014),

complex urease crystallized from jack bean meal (Xiaoxi Yu, Jingkang Wang, & Ulrich, 2015). Recombinant l-asparaginase II was also purified by SFO crystallization technique and the original enzymatic activity was preserved by this process (Müller, Liu, Migge, Pietzsch, & Ulrich, 2011; Yu, Wu, Huang, Ulrich, & Wang, 2017). Therefore, SFO crystallization can be considered as an alternative innovation method for protein crystallization, affordability, low environment impact (low salt requirement), low temperature operation, and the potential to preserve protein quality in this study (Ming et al., 2021).

Furthermore, the SFO method was applied for papain crystallization which included an ice-layer (solid) combined with solution crystallization to produce protein crystals. At laboratory scale, an SFO crystallizer was constructed comprising a double-walled vessel and a freezing coil (−14 ± 2 °C). During the crystallization process, the solvent in the papain solution was removed by freezing on a freeze coil as the ice layer. The solution was concentrated and became supersaturated, which promoted the formation and growth of papain crystals within the solution. By removing solvent from the system, the desired supersaturation of papain was achieved with minimal precipitant use. Therefore, this study concerns the recovery, loss of papain to the ice, and loss of enzymatic activity, which before and after using the SFO crystallizer. Accordingly, enzyme activity was quantified spectrophotometrically; solubility and nucleation were mapped; and crystal structure was examined by microscope and X-ray diffraction, in order to compare with previous conventional crystallization methods. In this study, papain was selected as a representation commercialized protein due to its valuable enzymatic properties. Papain is a cysteine protease from papaya latex, shows antimicrobial potential and has been widely used in pharmaceutical products, cosmetics, foods industry even as well-known in meat tenderization (Amri & Mamboya, 2012; Parsaeimehr, Chen, & Sargsyan, 2014). In Thailand, there are a lot of papaya cultivation. To add value to papaya-derived products and promote their use in high-value chemical industries. This study was initiated, especially considering the relatively high market price of purified papain. We hope our study contributed to the development at a cost-effective following the upstream production process.

The crystallization process begins with primary nucleation, which is influenced by various factors, including supersaturation level, agitation parameters, processing time, and the nature of antisolvent agents (Giulietti, Seckler, Derenzo, Re, & Cekinski, 2001; Mullin, 2001; Nyvlt, 1984). Although papain had been crystallized using methanol at pH 5.0 (Kamphuis, Kalk, Swarte, & Drenth, 1984), yielding needle-like crystals (Harris, 1983) and its industrial-scale crystallization behavior remains underexplored. Recent studies on batch antisolvent crystallization have identified ethanol, acetone, and acetonitrile as antisolvents, with ethanol (1:4 solvent-to-antisolvent ratio) achieving high activity retention (Boonkerd & Wantha, 2024). However, comprehensive studies the phase-diagram mapping, nucleation control, and process modeling for papain are still lacking.

This study aims to determine solubility and nucleation zones and to strengthen understanding of SFO crystallization as a purification unit for commercial papain. Scale-up supported by process modeling is proposed for future work.

1.2 Research Objectives

1.2.1. To quantify papain solubility versus temperature and methanol in water and acetate buffer.

1.2.2. Construct pseudo phase diagrams (solubility and nucleation boundaries) for cooling, antisolvent, and SFO; establish an SFO operating window minimizing ice entrapment while preserving activity.

1.3 Scope and limitations of the research

The investigation of the crystallization potential of papain using SFO was studied by setting up a series of experimental procedure to clarify its feasibility. The experimental study steps on this crystalline papain are obtained in Figure 1.1, which shows the overall work flow performed in this study.

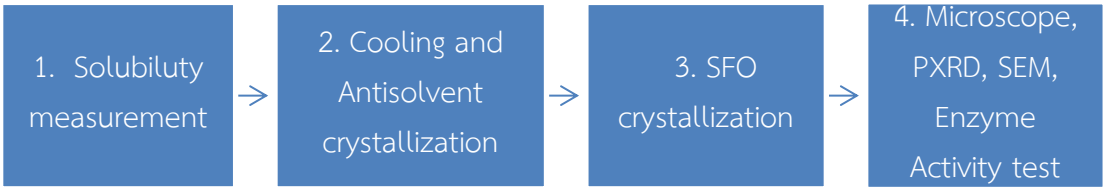

Figure 1.1: Overall workflow of papain crystallization.

First, the saturation concentration (solubility) of crystalline papain in water, acetate buffer (pH 5) and buffer with methanol (0 - 60% w/w) was measured by gravimetric method and monitored with a refractometer. Experiments were investigating at various temperature ranging from –8 to 30°C.

Second, preliminary cooling crystallization (at rate of 0.005 °C/min) and antisolvent crystallization using methanol (dropping rate of 0.2 mL/20min) were conducted along saturation lines.

Third, the SFO crystallization process was studied by conducting experiments under a controlled freezing rate of 0.02 °C/min, stepwise reduction.

Fourth, the resulting crystal was analyzed by microscope, X-ray powder diffraction (PXRD) and Scanning electron microscopy (SEM). The activity of enzyme was evaluated by the reaction efficiency of papain with the BAPNA substrate where the amount of product formation from substrate decompositions quantified over time.

1.4 Expected outcomes

This study aims to deliver: (i) pseudo phase diagrams for papain, (ii) an SFO operating window (coil –14 to –12.6 °C; bulk –1.5 to 1 °C) minimizing ice entrapment, (iii) PXRD/SEM-verified crystalline products, and (iv) activity benchmarks versus commercial references. Furthermore, it is expected to support Thailand's bioindustries in producing high-value enzyme crystals via crystallization, suitable for sale and specified application using crystallization process.

CHAPTER II

LITERATURE REVIEWS

2.1 Overview of the literature

Enzyme crystallization is a cornerstone of structural biology and bioprocessing, pivotal for both structure elucidation and the purification of biocatalysts at industrial scales (Grossmann & McClements, 2023; Wegner et al., 2024). The practice has evolved from niche laboratory techniques to scalable processes, reaching as far as the production of high-purity enzymes such as papain, lysozyme, catalase (Mitsuda & Yasumatsu, 1955), glucose isomerase, asparaginases and α-amylase...et.al for food, pharmaceutical, and other high-value applications (Boonkerd & Wantha, 2024; Liu, Hou, & Li, 2020; Y. Liu, M. Pietzsch, & Ulrich, 2013). In recent years, solvent freeze-out (SFO) crystallization has emerged as a promising, energy-efficient method for enzyme crystallization that addresses many limitations of traditional techniques (Ming et al., 2021).

This chapter provides a comprehensive literature review focusing on papain crystallization using SFO, including a rigorous treatment of enzyme crystallization theory—encompassing supersaturation, nucleation mechanisms, and kinetics. It further discusses the construction and application of phase diagrams, methods for solubility measurement and nucleation mapping, and provides comparative analysis of cooling, antisolvent, and SFO methods. Finally, it synthesizes recent studies (2020–2024) on the crystallization of papain and other benchmark enzymes, connecting theory to practical outcomes with exhaustive support from contemporary peer-reviewed literature.

2.1.1 Crystallization technologies

Normal crystallization process is part of the nature, taking place in several natural phenomena, for instance in the formation of solid such as snowflakes, sugar and salts. Moreover, biological lives parts are also included calcium carbonate and calcium phosphate combine in bones, teeth and cell eggs of animals.

Crystallization is known as a purification technique, as a separation process, as a branch of particle technology, but in its physical definition it is a supramolecular phenomenon of molecules, ions or atoms randomly arranged to form ordered three-dimensional ions or a matrix molecule called crystal (Davey & Garside, 2001). This phenomenon can occur inside a liquid and consequently a phase change occurs in a solution, then solid crystalline material is obtained there.

The crystallization is fundamentally governed by thermodynamic principles: a solid (crystal) will form spontaneously from a solution when the Gibbs free energy change (ΔG) for the process is negative. Crystallization proceeds only when the solution is supersaturated, that is, when the actual solute concentration exceeds the equilibrium solubility at a given temperature and composition (Lewis, Seckler, Kramer, & Rosmalen, 2015; Mullin, 2001). The magnitude and method of supersaturation generation whether by cooling, addition of antisolvent, evaporation, or SFO—determines the crystallization kinetics and thus the attainable crystal size and purity.

Phase diagrams provide essential maps indicating the regions of solubility, metastable, and precipitation for a given protein under specified conditions (protein and precipitant concentration, pH, temperature, ionic strength) (Asherie, 2004; Mullin, 2001; Nyvlt, 1984).

- Solubility curve: Boundary where solution and crystal are in equilibrium (no net growth or dissolution).
- Nucleation curve: Separates the metastable and labile zones—nucleation becomes statistically observable.
- Labile/precipitation zone: Rapidly formed aggregates/out-of-order structures dominate; this is a zone to avoid if high-quality crystals are sought.

1) Measuring solubility

The typical approach to determine a phase diagram involves stepwise variation of one or more parameters, incubating until equilibrium, and then measuring protein concentration or phase transitions using:

- Spectroscopic methods (e.g., UV absorbance).

- Dynamic light scattering for aggregation.
- Thermal analysis (DSC) for phase transitions.
- Cloud-point method for LLPS mapping.

The van't Hoff equation (2.1) is routinely used for temperature & solubility relationships (Hentschel, Hansen, Egelhaaf, & Platten, 2021):

$$\ln(C_2/C_1) = (\Delta H/R)\cdot(1/T_1 - 1/T_2) \quad (2.1)$$

Where C_1, C_2 are equilibrium concentrations at temperatures T_1, T_2, ΔH is enthalpy of dissolution.

2) Nucleation mapping and metastable zone width:

Between the solubility curve (where crystals dissolve) and the nucleation limit (labile zone), lies the metastable zone: supersaturated but nucleation is kinetically hindered. Crystals grow in this zone only if seeds are present. Metastable zone width (MSZW) is strongly dependent on process parameters like cooling or antisolvent addition rates and agitation intensity (Noor, Camacho, Ma, & Mahmud, 2020). MSZW can be measured by techniques such as:

- Polythermal experiments (heating/cooling cycles).
- Induction time analysis (e.g., detection of light scattering or turbidity increase).
- On-line sensors (FBRM, Raman).

These experiments define the quasi-kinetic boundaries of the phase diagram, which depend on cooling or antisolvent addition rates and system scale. Pseudo-phase diagrams combine solubility, nucleation, and aggregate formation data, providing pragmatic guides for crystallization protocol design (Sacher, Bolf, & Sejdi, 2024).

2.1.1.1 Cooling crystallization and phase diagram

Phase diagrams map temperature (T) and solute concentration (c) to liquid–solid equilibrium in heterogeneous systems. Since pressure has little effect, the equilibrium data appear as a single line in a T vs c plot, often called a solubility diagram (Ulrich & Stelzer, 2014). This solubility curve separates undersaturated solutions (below) from supersaturated ones (above), the latter being

necessary for crystallization since c exceeds the equilibrium solubility. Supersaturation drives both nucleation and growth. At high supersaturation, primary nucleation begins along the nucleation curve (labile-zone boundary), whereas the region between the solubility and nucleation curves is the metastable zone. The metastable zone permits growth of existing crystals without new nuclei forming. The width of this metastable zone represents the maximum supersaturation achievable before nucleation occurs (Giulietti et al., 2001). In cooling crystallization, lowering T reduces the equilibrium solubility, moving the system sequentially from undersaturated into metastable and then labile regions (Figure 2.1). By controlling the cooling rate and agitation, one can target either gentle crystal growth (within the metastable zone) or rapid nucleation (crossing into the labile zone).

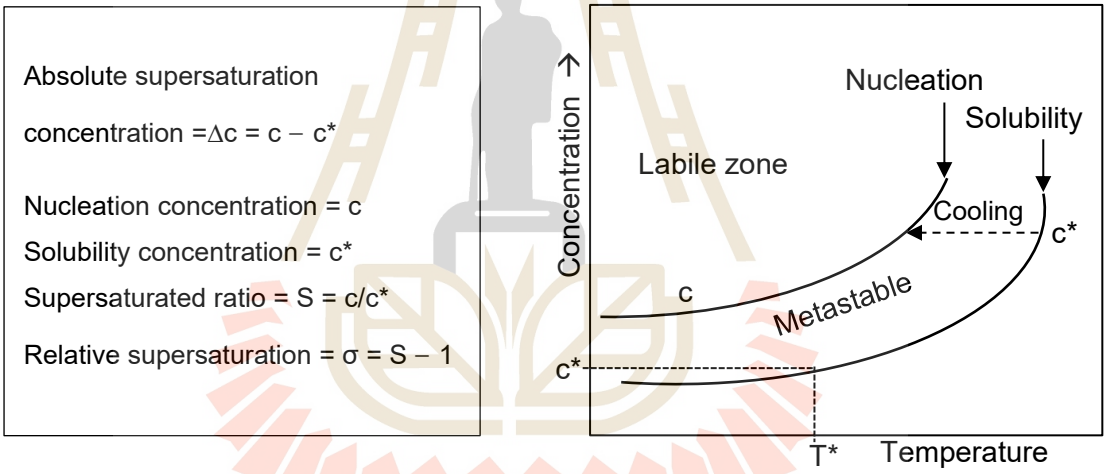

Figure 2.1: Conceptual solubility and nucleation diagram for cooling crystallization. Adapted from (Giulietti et al., 2001).

Supersaturation is achieved by lowering the temperature, exploiting the temperature dependence of protein solubility. This method is simple, common, and adaptable for scale-up.

1) Key parameters:
   - Initial and final temperature.
   - Cooling rate (slower rates favor larger crystals and less nucleation).

- Agitation (influences secondary nucleation and crystal habit).

2) Advantages:

- No need for organic or additional chemicals.
- Reversible: if no crystals form, system can be reheated and retried.
- Well suited to temperature-sensitive proteins.

3) Limitations:

- Some proteins have weak or atypical temperature dependence in solubility.
- High minimum nucleation supersaturation.
- Thermal denaturation risk for sensitive enzymes (mitigated by mild temperature windows).

4) Example (lysozyme):

Well-characterized lysozyme crystallization at 4 to 20 °C in sodium acetate buffer with NaCl is a standard benchmark system. Cooling rate in the range 0.03–0.2 °C/min is typically optimal for tetragonal crystals with narrow size distributions (Maosoongnern, Flood, Flood, & Ulrich, 2016; Tang, XH, Liu, JJ, & Zhang, 2018; Wang, Li, Zhang, & Wang, 2023).

2.1.1.2 Antisolvent crystallization

A miscible antisolvent (ethanol, acetone, acetonitrile., et.al) is added to the protein solution. Because the protein is much less soluble in the antisolvent, its supersaturation abruptly increases, triggering nucleation (Jia et al., 2022). The solubility at a temperature and an agitation are controlled. Crystallizing agents (anti-solvent) addition drive to the supersaturation region by different mode as in Figure 2.2. The metastable zone permits growth of existing crystals without new nuclei forming.

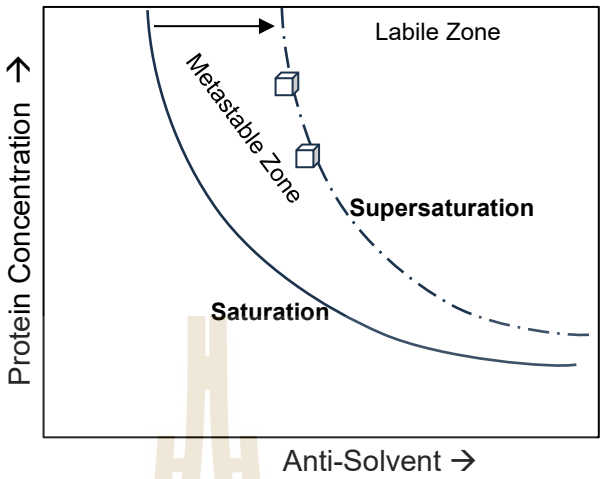

Figure 2.2: Conceptual solubility/nucleation diagram for the antisolvent technique. Adapted from (Jia et al., 2022).

1) Key process parameters:
   - Type of antisolvent and ratio to solvent.
   - Addition rate, mode (batch, dropwise, gradient).
   - Mixing and agitation.
   - Temperature.
2) Advantages:
   - Operational at ambient temperature: suited for thermally labile proteins.
   - Rapid supersaturation: enables formation of nano- or micro-scale crystals.
   - Polymorph, morphology, and particle size can be controlled by process optimization.
3) Limitations:
   - Local supersaturation inhomogeneity; possible aggregation and wide particle size distributions if mixing is suboptimal.
   - Purification and recovery of antisolvent required.
   - Potential for partial denaturation if harsh antisolvents or excessive concentration are used.

4) Example (papain):

Recent studies report ethanol as an effective antisolvent for papain (1:4 S:AS, into 30 mg/mL papain solution) yielding nanosized particles with retained activity under controlled addition and mixing (in Figure 2.3). Acetone and acetonitrile were less effective, often producing amorphous aggregates (Boonkerd, Hao, & Wantha, 2024; Boonkerd & Wantha, 2024).

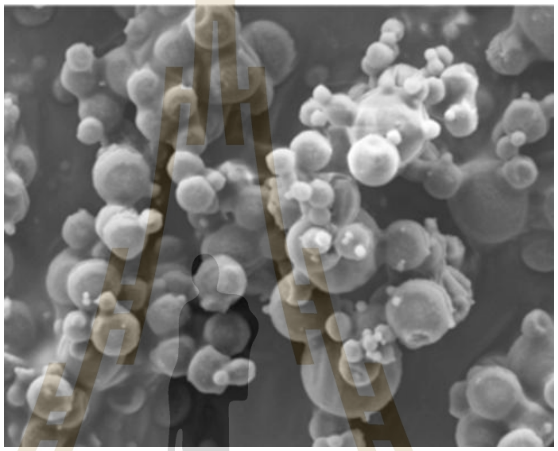

Figure 2.3: SEM photomicrographs of nanoparticle papain precipitated at different solvent-to-antisolvent ratios (1:4); reproduced from with permission (Boonkerd et al., 2024; Boonkerd & Wantha, 2024).

2.1.1.3 Solvent freeze-out crystallization (SFO) technology

Solid layer crystallization has been applied for decades to recover target compounds from mixtures by forming a crystalline layer on a cooled surface. In this process, a component of the melt undergoes a phase change and deposits as a solid layer on the heat exchanger surface. Crystal growth proceeds perpendicular to the cooled surface toward the bulk liquid (mother liquor), driven by the temperature gradient between the equilibrium temperature at the crystal–liquid interface and the bulk melt temperature. This gradient represents the difference in equilibrium conditions between the solid and liquid phases (Ryu & Ulrich, 2018; Ulrich et al., 1996).

In a typical setup (Figure 2.4), a tube cooled internally by a circulating coolant is immersed in a temperature-controlled vessel containing the feed melt. A thermostat regulates the surface temperature. Because the temperature

difference controls both growth rate and product purity, an optimal cooling program is essential. As the crystal layer thickens, it acts as a thermal insulator, reducing heat transfer. To maintain a constant driving force and steady growth rate, the cooling intensity must be gradually increased. Without this adjustment, the process slows and eventually stops when thermal equilibrium is reached. The growing layer experiences a thermal gradient due to the release of latent heat of crystallization, which must pass through the crystal layer and crystallizer wall (Borbón & Ulrich, 2012).

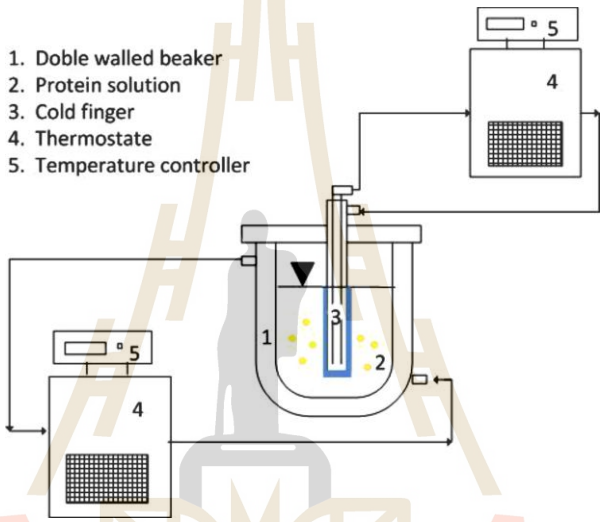

Figure 2.4: Set up of a simple equipment for solvent freeze out crystallization of proteins. Adapted from (Borbón & Ulrich, 2012).

In suspension crystallization, crystals are formed directly in the bulk liquid. These crystals are typically of high purity, but even small amounts of entrained mother liquor can significantly reduce product quality. Efficient solid–liquid separation is therefore critical. Temperature and supersaturation control are particularly important for concentrated feeds, where supersaturation is highly temperature-dependent. In suspension systems, a large surface area for crystallization (on the order of 10^{4} m²/m³) allows relatively low growth rates (10^{-7} to 10^{-9} m/s) to achieve acceptable production rates. Such low growth rates reduce impurity incorporation, enabling high separation efficiency in a single step (Ulrich et al., 1996). Suspension crystallization also offers high crystal production rates per unit equipment volume.

In SFO crystallization, two processes occur simultaneously:

- Solvent crystallization (e.g., water) as a solid layer on the cooled surface — analogous to melt crystallization.
- Solute crystallization (e.g., proteins) within the remaining liquid phase — analogous to suspension crystallization.

Ice formation is governed by the phase separation between ice and dissolved substances in water, while protein crystallization is dictated by the phase behavior of the aqueous protein solution (e.g., enzymes). Only when system conditions fall within the respective crystallization regions will nucleation and growth occur. For solid-layer melt crystallization, the solution adjacent to the cooled surface must be below the A–B line in the simplified binary phase diagram of water and solute (Figure 2.5, left). For protein solution crystallization, the bulk conditions must lie between the solubility curve and the metastable liquid–liquid boundary in the generic protein phase diagram (Figure 2.5, right) (Borbon & Ulrich, 2013).

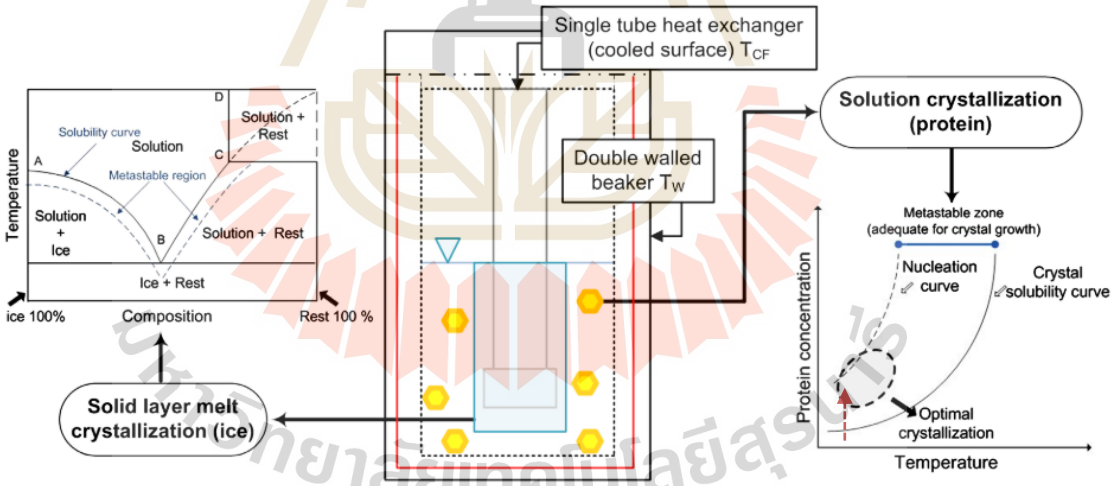

Figure 2.5: Mechanism of the solvent freeze out (SFO) crystallization process. Two crystallization processes take place. One is the crystallization of melt (water-ice) on a cooled surface. The other is the crystallization of the protein within the solution. Adapted from (Borbon & Ulrich, 2013).

SFO integrates aspects of freeze concentration and crystallization. The process involves controlled freezing of the solvent (usually water), thus concentrating the protein and promoting supersaturation. As the "ice" of solvent

separates, the unfrozen solution becomes supersaturated, allowing the protein to crystallize (Ryu & Ulrich, 2018).

1) Key process parameters:
   - Cooling rate and cold surface temperature (cold finger or freeze coil).
   - Ice growth rate/time at fixed temperature.
   - Initial protein concentration and ionic strength (salt type/concentration).
   - Agitation and mixing regime.
2) Advantages:
   - Low-temperature operation preserves protein activity and structure.
   - Significantly reduced salt/precipitant usage compared to traditional methods.
   - High yields and high purity due to the concurrent purification during ice crystallization.
   - Scalable and suitable for industrial bioprocessing.
   - Offers a mild environment; minimal chemical exposure; unlike salt-heavy traditional methods.
3) Limitations:
   - Requires precise thermal control.
   - Potential for protein inclusion (entrapment) in ice, reducing yield; requires optimized ice growth and agitation conditions for maximal protein exclusion.
   - May be less documented for certain enzyme classes and complex feeds.
4) Recent industrial relevance of SFO:

The SFO has been used for purification of industrial enzymes such as lysozyme showing high activity retention and eco-friendly profiles (Ming et al., 2021; Ryu & Ulrich, 2018). Previous works success the proteins purification

from mixtures by SFO method for three in here review as lysozyme, urease and recombinant l-asparaginase.

In approach, the solid layer formed on the cooled surface is composed primarily of the solvent, while the remaining liquid phase contains the target protein and other solutes. A key challenge is that small droplets of protein solution can become trapped within the frozen solvent layer, leading to product loss. Ryu *et al.* (2012) investigated how cooling rate and protein concentration influence this phenomenon. For an ice layer approximately 1 cm thick, reducing the cold-finger cooling rate from 0.4 K/min to 0.1 K/min lowered protein loss to ice from ≈40 % to ≈23 % (Ryu & Ulrich, 2018).

For hen egg-white lysozyme (HEWL), crystallization conditions were first identified through screening experiments and represented in pseudo-phase diagrams. These data guided the selection of initial SFO parameters. In this system, ice formation generated supersaturation in the remaining liquid, enabling lysozyme to crystallize. Using a feed containing 15 mg/mL lysozyme and 1.7 mg/mL ovalbumin, the SFO process achieved a crystallization yield of 69 %, producing crystals with an average size of 77.8 µm in ≈15 h. SDS-PAGE confirmed the identity of the crystals as lysozyme, and enzymatic assays verified that activity was retained (Borbón & Ulrich, 2012).

Urease was crystallized from jack bean meal extracts using SFO, and product purity was evaluated by specific activity measurements and SDS-PAGE. Compared with conventional salt-induced crystallization, SFO provided greater control over process conditions. Experimental variation of operating parameters highlighted the importance of ice-layer quality in determining crystallization performance. Although the process was not fully optimized, it yielded urease crystals of satisfactory purity and reasonable recovery, with higher enzyme activity preserved relative to traditional methods (Xiaoxi Yu et al., 2015).

Recombinant L-asparaginase II from *Escherichia coli* fermentation broth was also purified at laboratory scale using SFO. Initial crystallization parameters were determined via batch screening. Subsequent freeze-out crystallization with ethanol as the solvent produced rhombic (diamond-shaped)

protein crystals. Purity was assessed by SDS-PAGE and UV spectrophotometry, which confirmed effective removal of DNA contaminants. Enzymatic activity assays showed that the catalytic function of L-asparaginase II was maintained after purification (Yu et al., 2017).

2.1.2 Direct methodological comparisons

From the above sections of crystallization methodologies review that can summary in short comparison the advantages and weakness of each method under table 2.1.

Table 2.1: Summary comparison of crystallization methods.

Crystallization Method →	Cooling	Antisolvent	SFO
Supersaturation Source	Lowering temperature	Compositional (adding non-solvent)	Solvent solidification/removal
Temperature Profile	Decreasing	Constant/Ambient	Decreasing
Speed	Moderate	Rapid	Moderate
Activity Retention	High	High (if controlled)	High
Scalability	High	High	High
Process Complexity	Simple	Moderate	Moderate–Complex
Salt/Additive Use	Low	Moderate	Very low

*Note: “low/moderate/very low” relative to salt/additive mass per unit product.

2.2 Protein crystallization

Proteins are linear polymers of amino acids linked by peptide bonds, folding into defined secondary (α-helices, β-sheets), tertiary, and, for multimeric proteins, quaternary structures through a combination of hydrogen bonding, hydrophobic

interactions, and disulfide bridges (Bennema, 1992; M., Tymoczko, & Stryer, 2007). Their surface charge depends on ionizable side chains and solution pH, reaching zero net charge at the isoelectric point (pI), where solubility is minimal (M. et al., 2007; Mcpherson, 1990).

Water molecules hydrating protein surfaces are essential for solubility. Removing this hydration layer drives "salting-out" and can precipitate the proteins by adding salts or polymers; conversely, low concentrations of certain salts enhance solubility ("salting-in") in figure 2.6 (Mcpherson, 1990). Crystallization occurs when the system's free energy is minimized by transferring protein molecules from solution into an ordered crystal lattice; analogous to the fully hydrated state satisfying charge and bonding requirements.

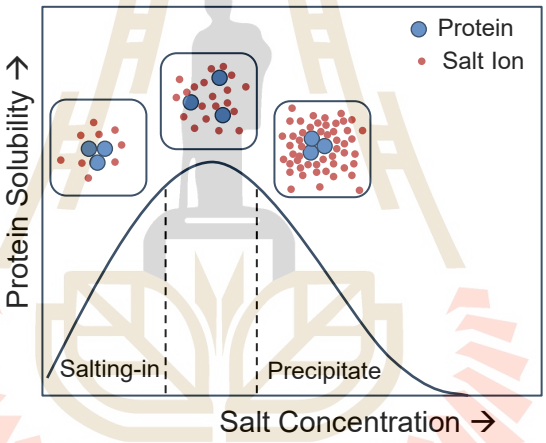

Figure 2.6: Effect of salt on macromolecule solubility (Mcpherson, 1990).

The thermodynamic driver is supersaturation ($S=C/C_{eq}$), achieved by altering temperature, protein concentration, pH (Wang et al., 2023), or adding precipitants (Weber, 1997). Crystallization requires ($S>1$) mild supersaturation promotes growth of existing crystals, while higher supersaturation triggers primary nucleation.

Phase diagrams (temperature vs. concentration) map liquid–solid equilibrium and define three regions:

- Undersaturated ($C<C_{eq}$) — no crystallization.
- Metastable (between solubility and nucleation curves) — crystal growth only.

- Labile (beyond the nucleation curve) — spontaneous nucleation (Alderton & Fevold, 1946).

Accurate phase-boundary data guide process design. The width of the metastable zone quantifies the allowable supersaturation before unwanted nucleation occurs as shown in Figure 2.7.

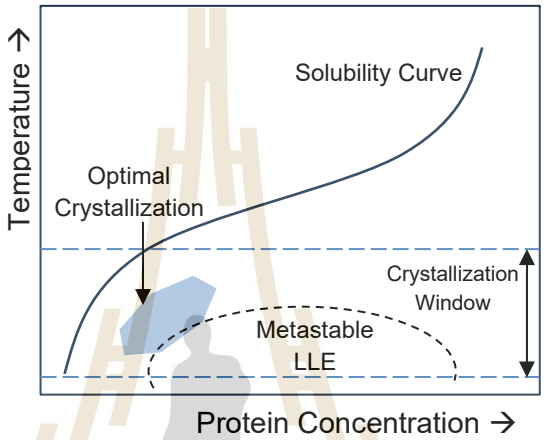

Figure 2.7: Typical phase diagram with crystallization window where the optimal crystallization region is found near the metastable liquid–liquid equilibrium (LLE) (Curtis & L.Lue, 2005).

At the molecular level, crystallization behavior correlates with protein–protein and protein–salt interactions, often described by the osmotic second virial coefficient (B_2). A narrow "crystallization window" exists between the solubility limit and the onset of liquid–liquid phase separation, within which optimal nucleation and growth occur (Curtis & L.Lue, 2005).

Because each protein's phase behavior depends on its unique surface chemistry and solution environment, empirical screening across pH, ionic strength, temperature, and precipitants and representation as pseudo–phase diagrams, it is essential (Wang et al., 2023). Only a few model proteins (e.g., lysozyme) (Alderton & Fevold, 1946) have well–characterized thermodynamic parameters, underscoring the need for systematic condition mapping in novel systems.

In this kind of experiments the conditions of the protein systems are varied in a wide range and the results are observed and analyzed. Furthermore, results can be summarized in pseudo–phase diagrams. The conditions under determined phase were

observed that is located on them and then a broader knowledge of the phase behavior is available.

2.3 Industrial crystallization of protein

Protein crystallization plays a vital role across pharmaceutical, cosmetic, and food industries. Crystalline proteins offer enhanced stability, purity, and handling properties, making them valuable in both formulation and processing. Studies show that protein crystals can be thermodynamically more stable than their dissolved counterparts, with stabilization energies (Drenth & Haas, 1992). Biopharmaceuticals, including therapeutic proteins and industrial enzymes, are high-value products. For example, lysozyme (from egg white) and papain (from papaya) are widely used for food preservation and antibacterial applications. Proteins are also incorporated into cosmetics for skin and hair protection, and in food processing to improve texture, elasticity, and nutritional value — such as through transglutaminase-mediated cross-linking (Grzonka, Kasprzykowski, & Wiczk, 2007; Kieliszek & Misiewicz, 2013).

Industrial crystallization, or mass crystallization, is employed to produce crystalline intermediates or final products with controlled purity, morphology, and physical properties (Giulietti et al., 2001; Nyvlt, 1984). Crystallization techniques vary by how supersaturation is achieved — commonly through evaporation, cooling, salting-out, or antisolvent addition (Albert M. Schwartz, 2000; Borbon & Ulrich, 2013; Drenth & Haas, 1992; Hekmat, Hebel, Joswig, Schmidt, & Weuster-Botz, 2007; Liu et al., 2020; Schmidt et al., 2005; Tam et al., 2011; Weber, 1997; Wiencek, 1999; Yi-Bin Lin et al., 2008).

Designing a crystallization process requires consideration of product specifications: purity, activity, crystal size and distribution, polymorphism, and downstream compatibility (Nyvlt, 1984; Roy & Abraham, 2003). Supersaturation is still the key variable, governing nucleation and growth kinetics. Its control determines crystal quality, yield, and reproducibility. Because crystallization occurs in a dynamic liquid–solid interface, managing non-equilibrium conditions is essential for process optimization.

2.4 Papain and crystallization of papain

2.4.1 Papain

The solvent freeze-out (SFO) technique has demonstrated effective protein purification across several model systems, including lysozyme, urease, and recombinant L-asparaginase, as outlined in the preceding section. These studies highlight SFO's potential for producing high-purity protein crystals while retaining enzymatic activity. Building on this foundation, the present work extends the application of SFO to papain, a cysteine protease of significant industrial and biomedical importance.

Papain is a proteolytic enzyme belonging to the cysteine protease family (molecular mass 21–30 kDa), characterized by a catalytic dyad of Cys25 and His159 (Figure 2.8) and stabilized by three disulfide bonds (Kamphuis et al., 1984). It is primarily sourced from the latex of *Carica papaya* L. (family Caricaceae), though it can also be obtained from the fruit's skin, leaves, or sap. Dried papaya latex contains approximately 57 % protein, with the protease fraction comprising papain (10 %), chymopapain (45 %), and other proteases (20%), each with a molecular weight near 23 kDa (Chaiwut, Nitsawang, & Shank, 2007; Macalood, Vicente, Boniao, Gorospe, & Roa, 2013). Crude latex papain exhibits protease activities of 2655 U/g at pH 5.5 and 285 U/g at pH 9.0.

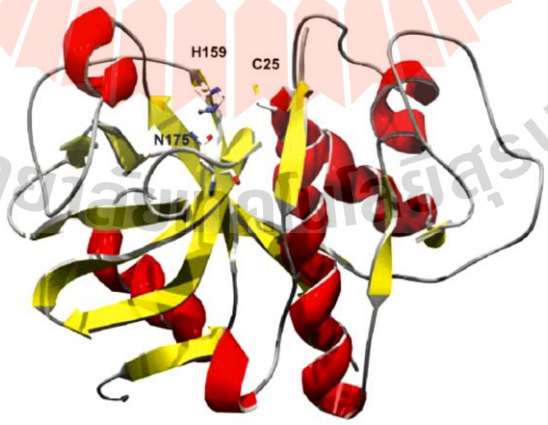

Figure 2.8: Ribbon representation of the three-dimensional structure of papain active site at His159 and Cys25 (Amri & Mamboya, 2012; Grzonka et al., 2007; Kamphuis et al., 1984).

An isoelectric point (pI) of 8.75, papain is optimally active between pH 5.0 and 7.0 at 50–60 °C, retaining most of its activity under moderate heating but showing progressive loss at higher temperatures. Commercial papain, often sold as a yellowish-white powder, is typically stored at ≤ 4 °C to preserve activity. Reported kinetic parameters include a Michaelis–Menten constant K_m and V_{max} (Mathias Elsson, Anondho Wijanarko, Heri Hermansyah, & Sahlan, 2019).

Papain's versatility underpins its widespread use in detergents, leather processing, brewing, meat tenderization, pharmaceuticals, and waste treatment. Medically, it has been applied to manage conditions such as leaky gut syndrome, hypochlorhydria, and gluten intolerance, and has shown analgesic and anti-inflammatory effects in allergic sinusitis without reported side effects (Amri & Mamboya, 2012). In drug discovery, papain has served as a model enzyme for developing selective inhibitors of cathepsin K and cathepsin L. Antimicrobial studies have demonstrated that papain from papaya seeds can inhibit *Bacillus cereus*, *Escherichia coli*, *Enterococcus faecalis*, *Staphylococcus aureus*, *Proteus vulgaris*, and *Shigella flexneri* (Parsaeimehr et al., 2014).

As showed in Mathias Elsson study characteristic of commercial papain in papain-casein mixture and used the Lowry protein assay method (Mathias Elsson et al., 2019). Commercial preparations, such as the "Paya" brand meat tenderizer (Figure 2.9), contain papain mixed with sugar and salt. Although the exact enzymatic activity of such products is often unknown, they have been used in experimental studies and present an interesting candidate for crystallization trials.

Figure 2.9: Commercial enzyme Papain brand "Paya" reaction with casein (Mathias Elsson et al., 2019).

Notably, a 2016 study compared lyophilized latex and purified papain from *C. papaya* for activity against *Strongyloides venezuelensis* eggs and larvae. High latex concentrations exhibited partial toxicity to parasite forms, suggesting that compounds other than papain contributed to the observed effects. Purified papain at 2.8 mg/mL produced similar egg-hatching inhibition to latex diluted 1:1000 in the egg hatching test (EHT) (Moraes, Levenhagen, Costa-Netto, Costa-Cruz, & Rodrigues, 2016).

Studies on papain (2025) show that organic cosolvents can markedly affect its kinetics and structure. In BAPNA hydrolysis assays (with 10 % DMSO for substrate solubility), methanol and ethanol raised K_m without altering V_{max}, lowering catalytic efficiency. Acetonitrile acted as a reversible mixed-competitive inhibitor (IC_{50} in the low millimolar range) and induced a blue shift in tryptophan fluorescence, implying conformational tightening. Molecular dynamics simulations confirmed that acetonitrile competes with BAPNA at the active site and that solvent polarity modulates substrate binding. These insights inform optimal solvent selection for papain-based biosensor design (Sirirak, Tamdee, Sawatthitileat, Thaithong, & Sirasunthorn, 2025).

1) Productions and exportation of Thailand's papaya:

From website List of countries by papaya production - Wikipedia according to the list of countries by papaya production (Wikipedia), Thailand produced 165,605 tons of papaya in 2022, while India produced 5,341,000 tons. The estimated global production that year was 13,822,328 metric tons, representing a 1.9 % decrease from 14,086,181 tons in 2021. India remained the dominant producer, contributing over 38 % of the world's total output. These figures highlight both the agricultural capacity and the global demand for papaya, underscoring the importance of research across multiple fields that including agricultural technology, extraction processes, and production methods for applications in food, cosmetics, and pharmaceuticals.

In Asia, many universities continue to investigate the benefits of papaya latex. In Thailand, for example, Chiang Mai University has conducted extensive studies on extraction techniques (Chaiwut et al., 2007; Manosroi, Chankhampan, Pattamapun, Manosroi, & Manosroi, 2014), culminating in dissertations focused on modifying papaya-derived enzymes for use in cosmetic and pharmaceutical products

(Nekoueinaeini, Aliahmadi, & Soleimani, 2024). Given this context, advancing research on papain purification, particularly its crystallization, would be highly valuable for Thailand, enabling the development of high-purity enzyme products for diverse industrial applications.

2) The conclusion of papain proteolytic activity determination as review in table 2.2:

Table 2.2: Papain enzymatic activity studies.

Buffers	Sources	Enzymatic activity	pH	Max, T (°C)	Method/ Substrate
	Liquid papain by Arinor Limited, Belfour House 46-54, Great Titchfield Street, London	250.0 U/g	5.0-7.0	60	Caseinolytic method (casein digestion) (Lukin, 2020)
Acetate 0.2M	Dried crude latex of C. papaya L (code P-1301)	2655.0 U/g	5.5	55	Caseinolytic method (Macalood et al., 2013)
In water	Boonkerd's work. Commercial papain	Residual activity >90%	7	25	Ruth's method, BAEE, BAPNA hydrolysis (Boonkerd & Wantha, 2024)
In water, methanol, ethanol, DMSO, acetonitrile.	Sirirak's work. Commercial papain activity effected by different solvents	Catalytic efficiency reduced by acetonitrile	-	25	Ruth's method, BAPNA hydrolysis (Sirirak et al., 2025)

Given papain's industrial relevance, biochemical stability, and prior evidence of successful crystallization in other proteins via SFO, it represents a

compelling target for further investigation. The following sections detail the experimental strategies employed to achieve high purity papain crystals using the SFO method.

2.4.2 Papain crystallization review

First, papain represents another useful protein for studying electron microscopically the fibre to crystal transformation process, as well as for the understanding of the formation of varying crystalline state. The crystals of papain exhibit longitudinal and transverse periodicities and are clearly shown to be formed like needle (Figure 2.10) by the coalescence of parallel bundles of individual fibrils. Thin cross-sections of the thicker crystals show a complex honeycomb structure with pronounced aqueous channels (Harris, 1983).

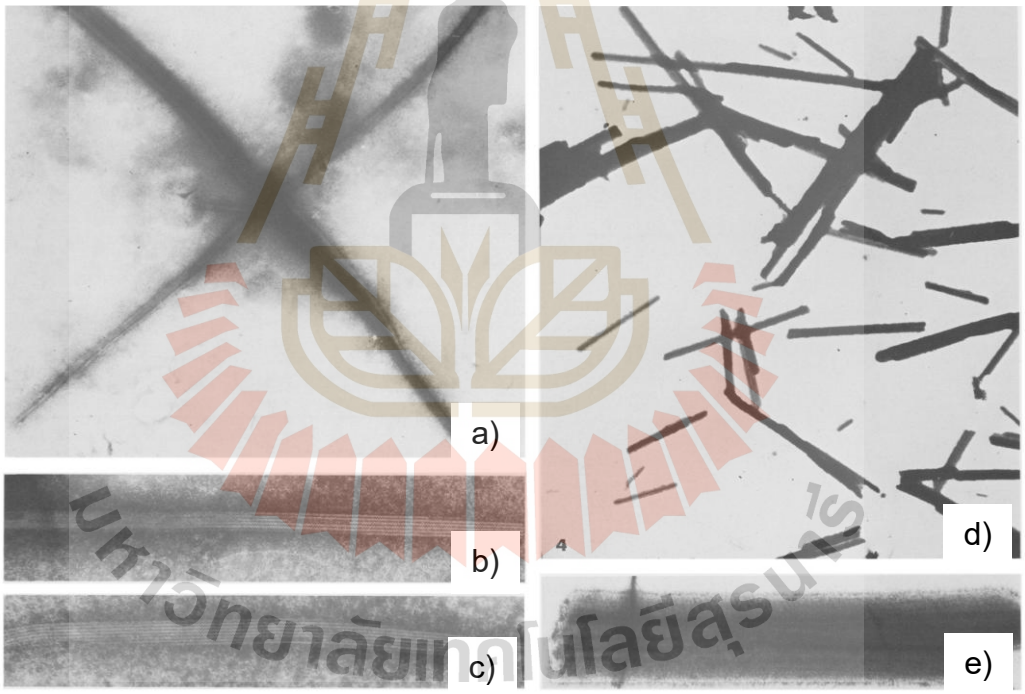

Figure 2.10: Needle-like crystals of papain present in the suspension originating from Sigma. The needles contain parallel fibrils, which exhibit a pronounced zigzag helical periodicity. Negatively stained with 2% sodium phosphor tungstate (pH 7.0). (a) x18,000, (b) x78,000, (c) x78,000, (d) x6,000, (e) x30,000, respectively. Adapted from (Harris, 1983).

Second, the crystallization of a Kunitz-type Papain Protease Inhibitor (PPI) that was isolated from the latex of green Carica papaya fruits. PPI has a molecular weight of 23 kDa and two disulfide bridges. PPI was crystallized by the hanging-drop vapour-diffusion method using Hampton Research Crystal Screen and checked with X-ray by a merohedral twin law of diffraction method. The Prismatic crystals (crystal form I) were obtained after a week of incubation in 2.0 M ammonium sulfate. Crystals diffract resolution of 2.6 Å (Mohamed Azarkan et al., 2006) as shown in Figure 2.11.

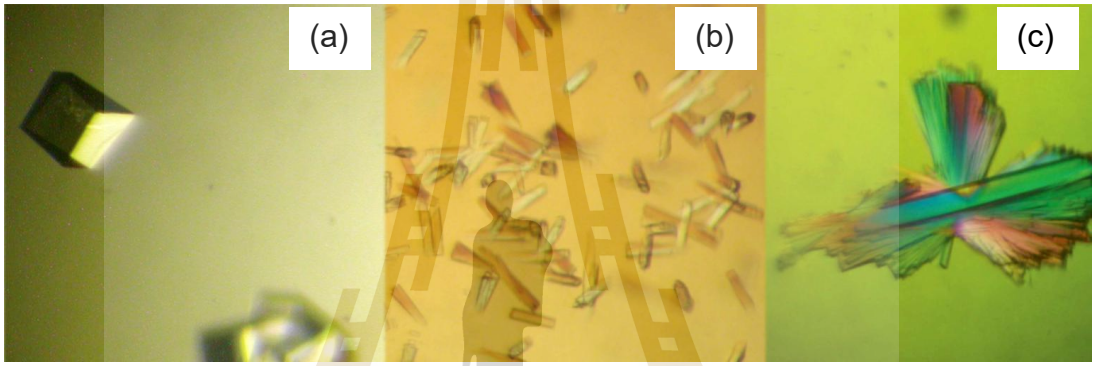

Figure 2.11: Crystals of papain protease inhibitor (PPI). (a) Crystal form I (prismatic) grown in 2.0 M sodium formate, 20 mM sodium acetate pH 4.6. (b) Original crystals of crystal form II grown at 293 K in 1.8 M ammonium sulfate, 100 mM MES pH 6.5, 10 mM cobalt chloride. (c) Typical growth crystals of crystal form II of PPI grown at 283 K after optimization. The clusters of needles are only loosely attached to each other and the large single crystal in the middle was picked out for data collection. Adapted from (Mohamed Azarkan et al., 2006).

Ethanol antisolvent protocols for papain (1:4 S:AS, controlled addition/mixing) (Boonkerd & Wantha, 2024) report nanoscale particles with retained activity, whereas methanol under similar droplet-addition regimes frequently yields amorphous aggregates and gelation; this contrast underscores solvent-specific protein–solvent interactions and mixing-driven local supersaturation as key determinants. In contrast, SFO builds supersaturation by solvent removal at near–freezing bulk temperatures, decoupling protein nucleation from harsh compositional shocks and minimizing denaturation risk.

2.4.2.1 Phase diagram of papain

Papain (papaya latex from Sigma/Aldrich) was studied solubility and nucleation in polyethylene glycol (PEG) reagent solution at three points temperature in Figure 2.12 (Yi-Bin Lin et al., 2008).

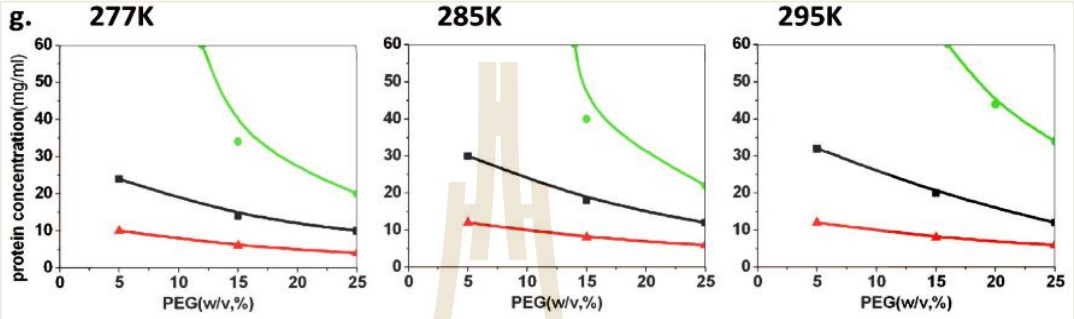

Figure 2.12: Phase-diagrams of papain: Red solubility curve was determined from the residual concentration in equilibrium with crystals 50-days after the initiation of crystallization at varying temperatures from 4 °C, 12 °C and 22 °C, left to right respectively. Nucleation and precipitation curves are plotted in black and green, respectively. Adapted from (Yi-Bin Lin et al., 2008).

2.4.2.2 Related studies of papain using XRD and SEM

In Figure 2.13 (a) X-ray diffraction (XRD) analysis was conducted using a Da Vinci PXRD instrument (Germany) with a scan range of 2θ = 5–60°; step size of 0.05°; scan rate 4°/min. Papain crystals were prepared using three different precipitation conditions: 50% unsaturation ammonium sulfate, 20% w/w PEG 6000, and a combination of both. The XRD patterns revealed distinct peaks at 23.29 degree and 28.47 degree for crystals precipitated with ammonium sulfate, which matched the raw papain profile. Crystals obtained from the combined precipitant exhibited a prominent peak at 20.69 degree, indicating enhanced crystallinity. In contrast, PEG 6000 alone produced weaker and broader peaks, suggesting lower crystallinity (Qi Hao et al., 2024).

Scanning electron microscopy (SEM) imaging (Figure 2.13, b) was performed using a Quanta 450 FEG-SEM. Air-dried crystals were sputter-coated and mounted on stubs for observation. The SEM micrographs showed block-shaped crystals with sharp, well-defined edges and corners. A uniform crystal habit was

consistently observed across batches prepared with the combined precipitant and L-cysteine dosing (Qi Hao et al., 2024). These results were used for discussion.

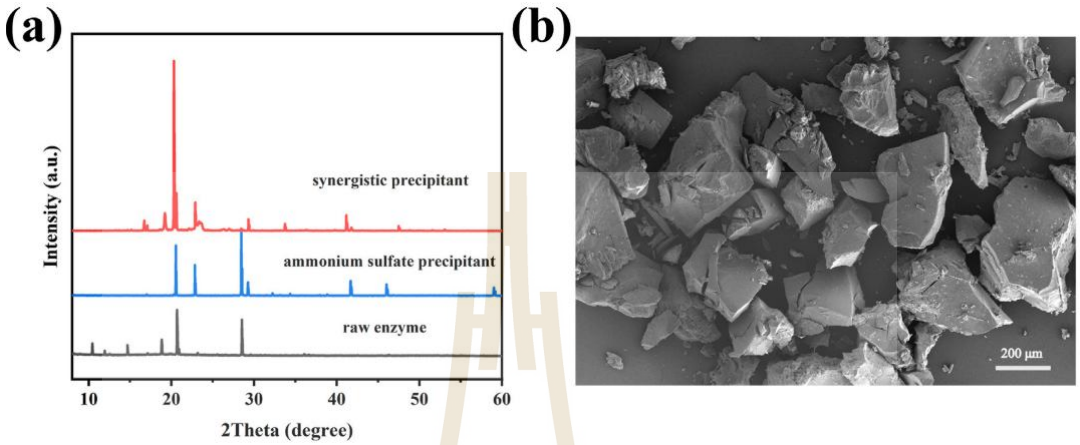

Figure 2.13: a) XRD pattern of papain crystals under different precipitation conditions. b) SEM micrographs showing crystal morphology of papain under combined precipitant. Adapted from (Qi Hao et al., 2024).

2.5 Conclusion

Advances in enzyme crystallization science have produced a toolkit of methods: from classical cooling and antisolvent techniques to solvent freeze-out (SFO) are suitable for a diversity of protein systems and industrial requirements. Each method offers unique strengths: cooling for simplicity and gentleness, antisolvent for rapidity and small size control, and SFO for environmental friendliness, reduced additive use, industrial scalability, and enzyme integrity retention.

In the context of papain, antisolvent crystallization with ethanol at a 1:4 ratio yields highly active, uniform nanocrystals-like, as validated by robust gravimetric and activity assays. Lysozyme now serve as models for SFO and precipitant-free crystallization, underscoring the generality and transferability of modern approaches. Urease, asparaginase, lysozyme, et.al though more complex, also benefit from these advances, with stabilization agents and solvent systems broadening the operational window for successful, high-yield crystallization.

Future directions include expanded mechanistic modeling (linking thermodynamic and kinetic parameters to process outcomes), digital twin and machine-learning–guided process optimization, seamless integration with downstream

purification, and further scale-up studies to ensure industrial impact and environmental sustainability.

To our knowledge, quantitative solubility and nucleation boundaries for papain in water/buffer–methanol systems have not been reported; this gap is addressed here using gravimetry and pseudo–phase mapping. Preliminary of cooling, antisolvent technique were conducted to comparison with SFO. Methanol is using for antisolvent. Enzyme activity determination was followed Ruth's method and PXRD also analyst with reference works (Boonkerd, Sirilak, ...et.al).

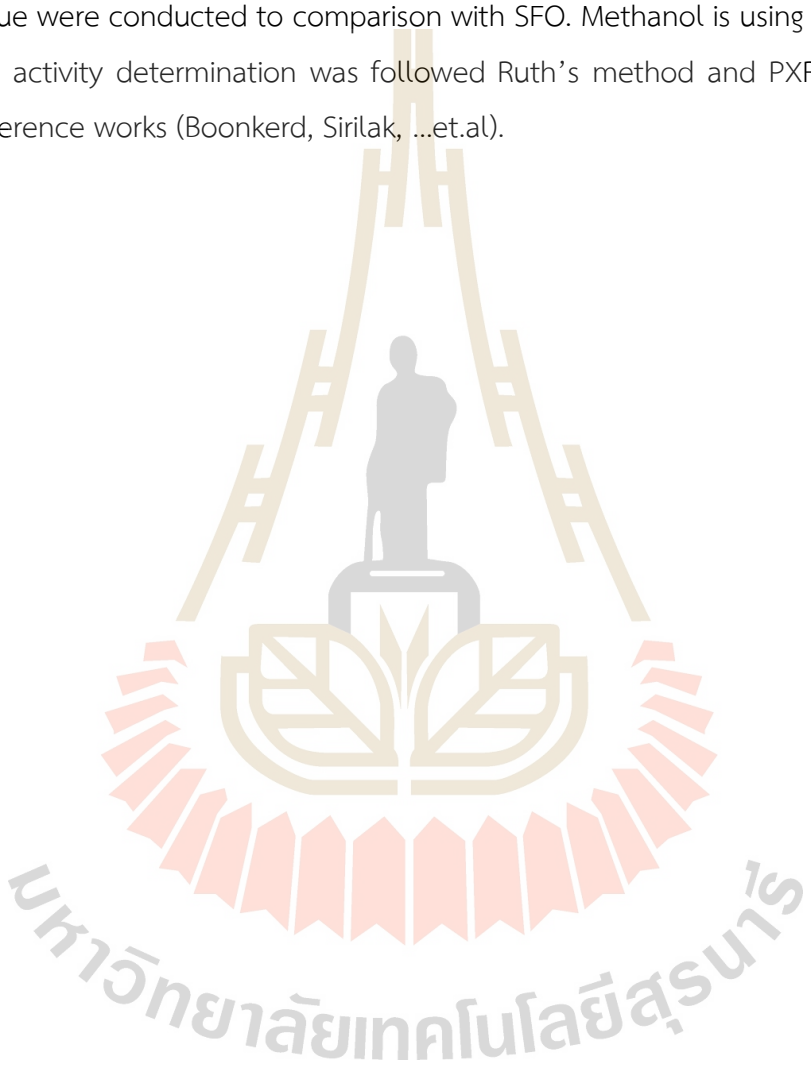

CHAPTER III

RESEARCH METHODOLOGY

3.1 Chemicals and reagents

Crystalline papain (white powder; CAS No. 9001–73–4) was obtained from three suppliers: a) Shaanxi Yuantai Biological Technology Co., Ltd. (YT0829), b) Tianjin HEOWNS Biochemical Technology Co., Ltd. (P–01102; provided with support from NERCICT, Tianjin University), c) Sisco Research Laboratories Pvt. Ltd (SRL; 2× USP grade, 14049), and d) Crystalline Lysozyme from Sigma-Aldrich (62971-50G-F) as following in Figure 3.1.

Sodium acetate trihydrate, ethylenediaminetetraacetic acid (EDTA), dimethyl sulfoxide (DMSO), hydrochloric acid, ammonium sulfate, and methanol were purchased from RCI LabScan Limited (Thailand). Tris(hydroxymethyl)aminomethane was purchased from Carlo Erba. Glacial acetic acid was purchased from QReC (New Zealand).

Nα–Benzoyl–DL–arginine–4–nitroanilide hydrochloride (BAPNA; B4875–1G) was obtained from Sigma–Aldrich, and L–cysteine hydrochloride monohydrate (GRM046) from Himedia. All Chemicals and reagents were of analytical grade and used without further purification.

Figure 3.1: Papain powder from a) Shaanxi Yuantai Biological Technology Co., Ltd (YT0829), b) Tianjin HEOWNS Biochemical Technology Co., Ltd (P-01102), c) Sisco Research Laboratories Pvt. Ltd (SRL) (papain 2xUSP, 14049) and d) Lysozyme powder from Sigma-Aldrich.

3.2 Methods and apparatus

3.2.1 Preliminary lysozyme study to validate SFO setup and phase mapping tools

The phase-diagram is important information for crystallization. In this case of enzyme crystallization, the solubility of lysozyme was measured by Focused Beam Reflectance Measurement (FBRM) to study the effect of temperatures and salt concentration, and then solvent freeze-out (SFO) process was applied.

FBRM is an industry-standard measurement technique used for in-process measurement of particles. A highly precise chord length distribution (CLD), which is sensitive to both particle size and count, is reported in real-time without the need for sampling or sample preparation. No shape is assumed and the measurement can be applied at full process concentrations in opaque or translucent slurries and

emulsions. It is capable of monitoring particles from ranging 0.5-1000 μm at most process concentrations and within a temperature range of −10 to 120 °C. As showed in Figure 3.2 is the Particle Track™ G600B with FBRM® technology from METTLER TOLEDO used in lysozyme solubility study.

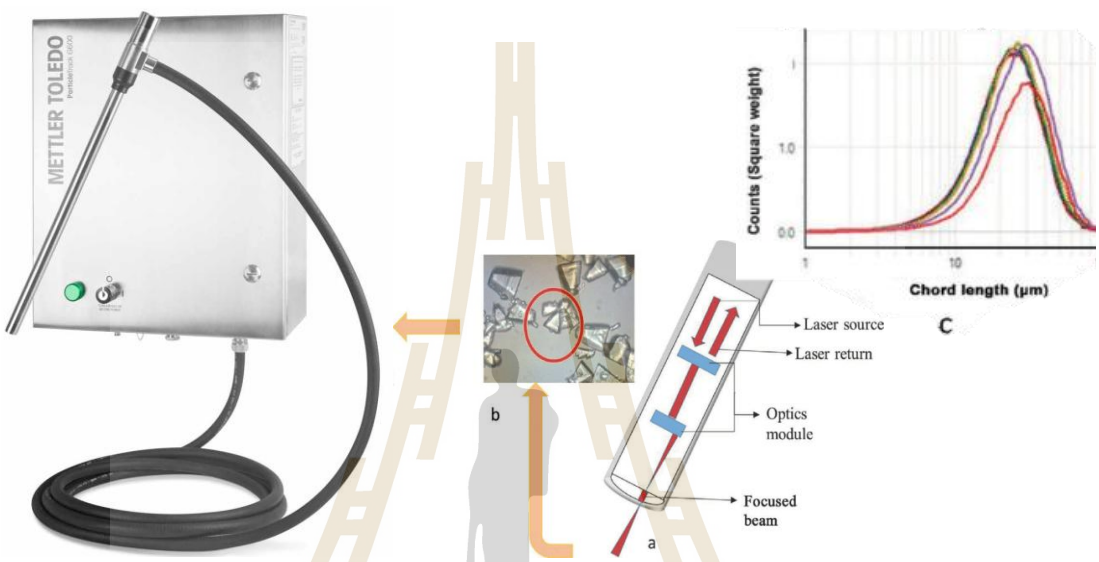

Figure 3.2: The Particle-Track™ G600B with FBRM (technology from METTLER TOLEDO) and its working principle.

The focus beam (probe a) was dived into solution b to measure the number and size of all the particles. The data were then displayed on the PC monitor as show in diagram C, which presents square wight versus particle size in micron.

The solubility measurement of lysozyme was conducted in 50 mL crystallizer which temperature was controlled by circulate water bath. The FBRM probe was positioned into solution in crystallizer and experiment began at −10 °C. The temperature was then gradually increased at a rate of 0.1 °C/min, negative temperatures were of particular interest as previous work (Yi-Bin Lin et al., 2008) have only reported lysozyme crystallization at temperatures no less than 4 degree C. Temperatures were recorded in real-time using a thermocouple. Complete dissolution of solid lysozyme was confirmed by FBRM that showed the zero particle count at the corresponding time. Those are the solubility points. Amount of solid lysozyme and salt (ammonium sulphate) were prepared in gram. The salt used were 0.4, 0.6, 0.7 M

dissolved in deionize water. These were to determine how different salt concentrations affected in the solubility (mg/mL) of lysozyme at various temperature. For each concentration, the temperature was increased until the solubility point was record. This process is illustrated in Figure 3.3. The highest temperature was 6 ℃. The result was plotted as concentration versus temperatures each salt concentration.

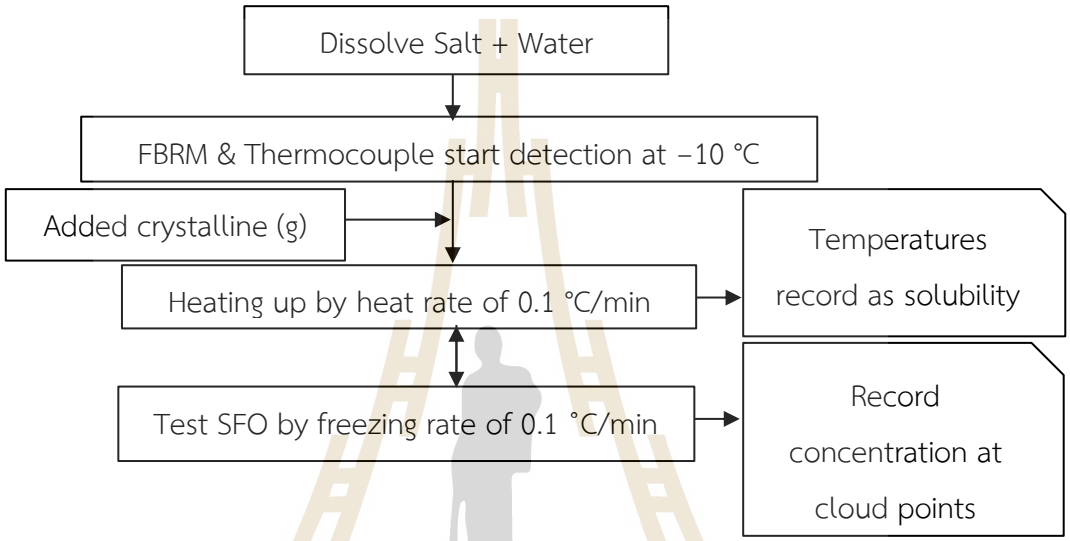

Figure 3.3: The process of solubility measurement for lysozyme and crystallization by the SFO technique.

The SFO crystallizer set up is shown in Figure 3.4. It consisted of a double wall beaker size as 100 mL and a freeze coil made from glass tube with an outside diameter of 2 cm. The first circulating water bath that controlled temperature of beaker was set up at 0 ℃. The freeze coil was controlled the temperature by second cooling system, which gradually decreased the temperature step-by-step initiating the formation of ice. The cooling rate was set to 0.1 ℃/min from 0 ℃ and decreasing to −10 ℃ (held at −10 ℃ for five minutes), to −15 ℃ (held for ten minutes) and finally down to −18 ℃ (held for approximately 14hours). By these controlled cooling process, the solution temperature of gradually decreased from 0 ℃ to minimum approximately −8 ℃ to avoid protein loss to the ice phase. At solution temperature between −1 ℃ to −4 ℃, the nucleation was observed by visually through the crystallizer and under a microscope. After 15hours, all crystals were collected by filtration as soon as possible while ensuring that the temperature did not higher than 5 ℃ in order to avoid re-

dissolution. Solid collected on the filter paper was stored in a desiccator for 4 days. The result was presented in a solution temperature and time diagram.

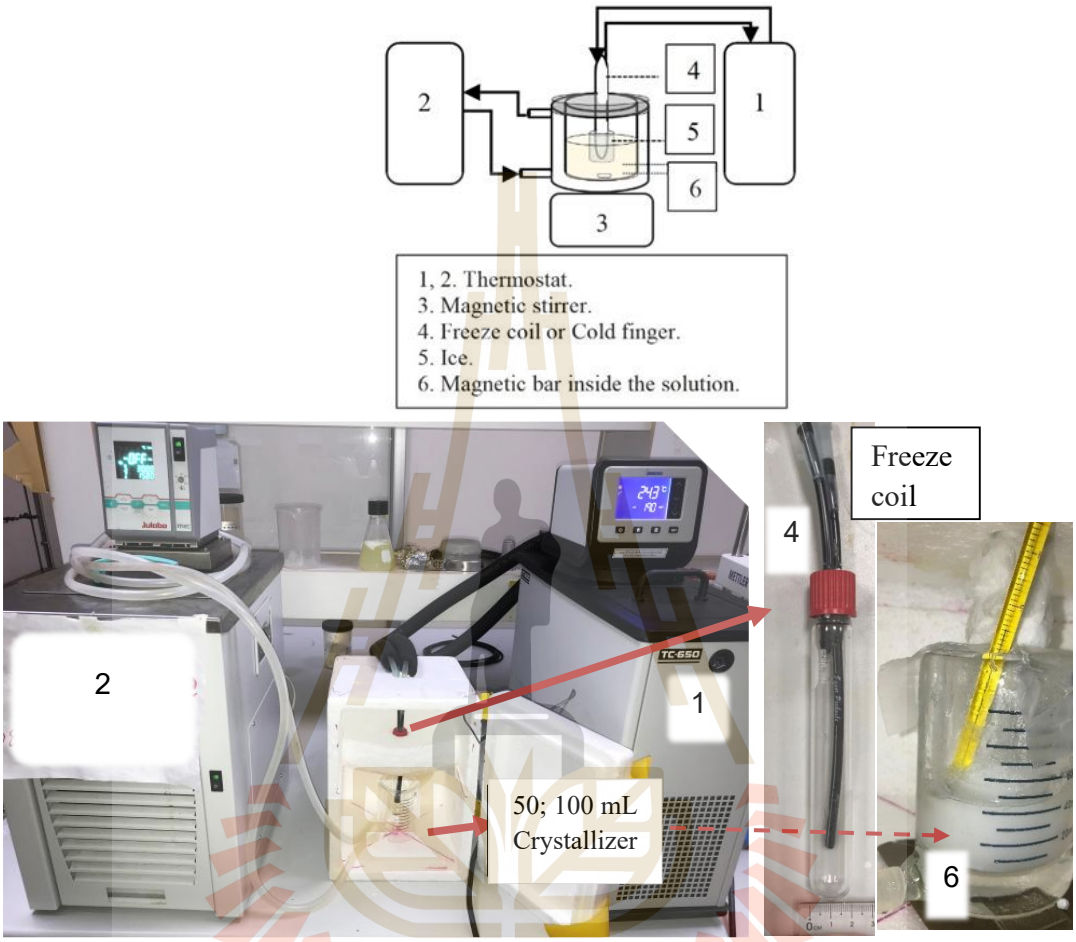

Figure 3.4: SFO crystallizer setup.

3.2.2 Solubility of papain (gravimetric and RI correlation)

The solubility (saturation concentration) of commercial crystalline papain was determined using the gravimetric method (Yu et al., 2017). An excess amount of papain powder was dissolved in three different solvents: DI water, acetate buffer (0.05M, pH5), and acetate buffer mixed methanol (0–60 % w/w). The mixtures were stirred at set controlled temperatures ranging from −8 to 30 °C for at least 48 hours to ensure saturation as shown in Figure 3.6. The saturated solutions were then filtrated using 0.22 micron syringe filters and analyzed using a digital refractometer (Refractive Index, RI) (Mat Yunus W. Mahmood & Azizan, 1988). To validate relationship between the RI and concentration, parallel filtrated samples were evaporated to

complete dryness at 60 °C, 48 hours, and the residual mass was determined gravimetrically. A linear correlation between RI and concentration was then plotted as shown in Figure 3.5. Notably, all solvents without papain exhibited a baseline RI of 1.3330.

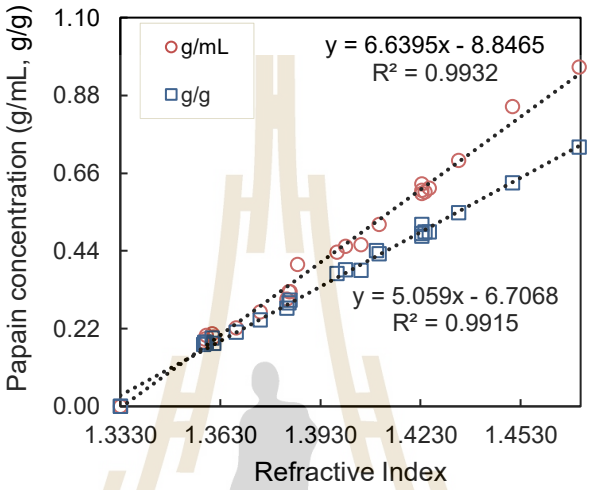

Figure 3.5: Refractive index (RI) vs. papain concentration (g/mL, g/g) in DI water, acetate buffer (pH 5.0), and buffer-methanol mixtures.

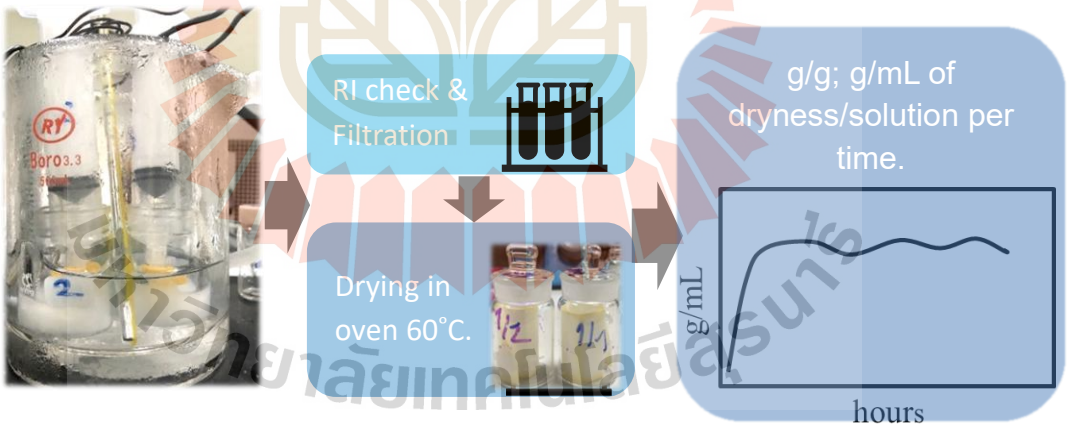

Figure 3.6: The process of solubility measurement for papain by gravimetric method. At −8, 0, 10, 20, 30 °C, in water, acetate buffer, and buffer mixed methanol (0–60 % w/w). Using a 0.22 µm syringe filter prior to drying.

3.2.3 Cooling crystallization of papain

To test the cooling crystallization, saturated papain solutions were prepared in two solvent systems: DI water (natural pH 6.7–7), 0.05 M acetate buffer

(pH 5.0, used to stabilize catalytic activity (Kamphuis et al., 1984)). Due to the elevated viscosity of concentrated papain solutions at 20–30 °C, a controlled slow-cooling protocol was employed to ensure reproducible nucleation. Filtered solutions (1 mL aliquots in sealed vials) were cooled from 30 °C to 5 °C at a rate of 0.005 °C/min using a programmable recirculating thermostat. A micro magnetic stir bar provided intermittent agitation 100 rpm and zero speed. The cloud point was slowly occurred. Therefore, the solution was monitored using a handheld camera and samples were taken for microscope observation. The temperature at which cloudiness first appeared was measured as the nucleation point. The cooling crystallizer set up is shown in Figure 3.7.

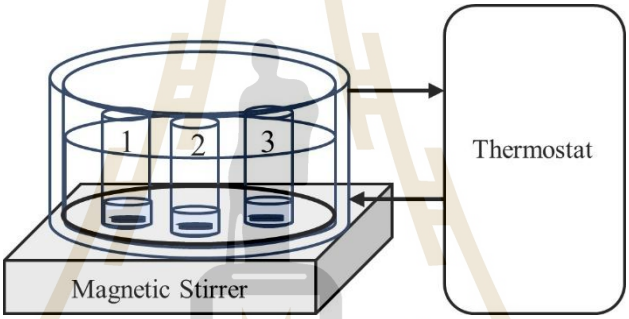

Figure 3.7: Cooling crystallizer set up.

3.2.4 Antisolvent crystallization of papain

Near-saturated papain solutions were prepared in 0.05 M acetate buffer (pH 5.0) and buffer-methanol mixtures (pre-determined via solubility assays). The solutions were equilibrated under agitation 120 rpm for 2 hours to ensure homogeneity, followed by syringe filtration (0.22 μm) to remove undissolved particulates. A jacketed crystallizer (50 mL) was charged with 10 mL of the filtered solution, maintained at 20 and 0 °C (±0.5 °C) via a circulating chiller during methanol addition. Agitation was provided by a PTFE-coated stir bar (Ø0.5 × L2.49 cm) at 120 rpm. The Eazy-Viewer camera (model 400, Mettler-Toledo) was installed for capturing solid cluster in solution and the Dinoe-lite digital camera was for real-time observation to the crystallizer until supersaturation (cloud point) was reached.

Methanol was introduced stepwise at manually rate of 0.2 mL/20 min after a 20-min equilibration period at saturation. Methanol addition continued until

cloud point (nucleation onset) and the gelation threshold (amorphous precipitation) was observed. Methanol consumption was minimized by terminating addition at gelation onset, which methanol was quantified as the weight fraction (w/w) of total solution.

3.2.5 Solvent freeze-out crystallization of papain

The solvent freeze-out (SFO) crystallization technique was applied for papain solution at pH 5 to induce supersaturation near the freezing point of water (Borbon & Ulrich, 2013). The experimental setup (Figure 3.4) consisted of 50 mL jacketed crystallizer integrated with a glass cold finger (freezing coil) and dual thermostatic controls. The first recirculating chiller cooled the freeze coil at a rate of 0.02 °C/min (−0.2 °C per 10 min manually) via stepwise temperature reduction protocol to minimize papain entrapment in ice until the final temperature (Ming et al., 2021; Ryu & Ulrich, 2018). The second thermostat stabilized the bulk solution at near-equilibrium conditions.

An initial 7 mL of near-saturated papain solution (pre-filtered, through a 0.22 µm syringe filter) was loaded into the crystallizer. Final cold finger temperatures were constrained to −12.6 °C (bulk solution temperature ranging from −1.5 to 0 °C) and −14 °C (bulk solution at 1 °C) to prevent excessive ice formation and minimize papain loss. These conditions were determined based on our preliminary study of the SFO process for papain. Solvent freezing concentrated the solution to a residual volume of 1-3 mL (60-80% of initial volume), achieving supersaturation levels corresponding to the phase diagram. Cooling below −14 °C resulted in uncontrolled ice propagation greater than 30% solute loss, consistent with previous observations that showed ice formation at lower temperatures (Ming et al., 2021). So, the protocol used in this study followed our earlier previous preliminary study as illustrated in Figure 3.8.

After nucleation occurred, thermal regulation of the freeze coil was terminated, and the solution was maintained at the nucleation temperature until growth ceased. Papain crystals were harvested afterward. The growth continued for approximately 72 hours to maximize crystal recovery. Papain crystals were isolated and dehydration (in silica gel desiccator until completely dry). The weight of papain

lost in the ice and the recovery of papain crystals were quantified using equations 3.1 and 3.2, respectively.

$$\text{Mass lost of papain\%} = \frac{B}{i} \times 100\% \quad (3.1)$$

$$\text{Recovery\% of crystalline papain} = \frac{C}{i} \times 100\% \quad (3.2)$$

where B is the mass (g) of papain per volume of ice (Ice melts and measure volume); i is the initial mass (g) of papain in saturated solution (7mL); C is dry mass (g) of papain crystal after the SFO process. The crystal was captured by microscope.

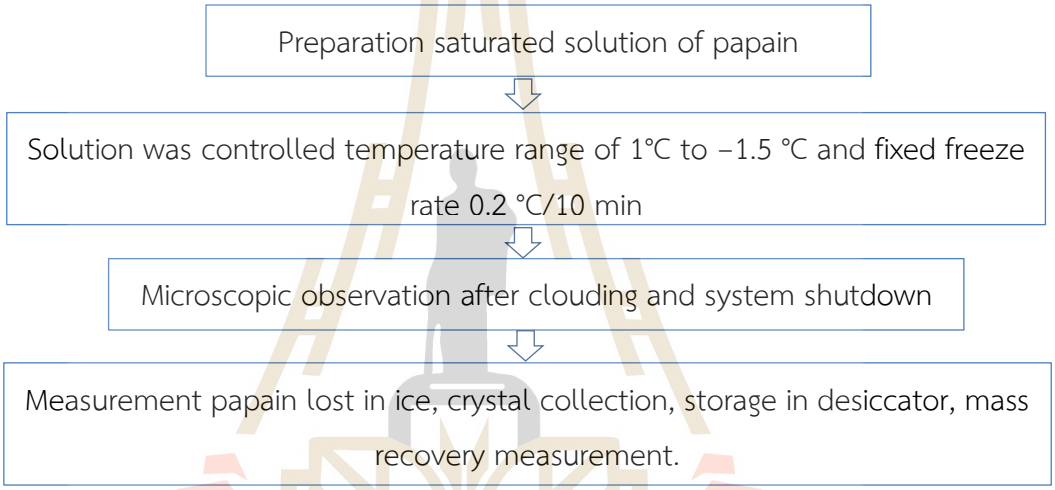

Figure 3.8: Illustration the SFO crystallization procedures for papain.

3.3 Papain concentration determination and characterization

3.3.1 Papain activity assay (BAPNA, UV–vis at 410 nm)

In this part, enzyme activity and protein concentration were determined from the UV absorption value of the protein solution, measured using a spectrophotometer. The most common use of a spectrophotometer is to measure the absorption of light at a specific wavelength. Typically, a spectrophotometer consists of two parts: namely a spectrometer for generating a light beam and a photometer for measuring the light intensity.

Usually, a cuvette containing the liquid sample is placed between the spectrometer and the photometer. The amount of light passing through the cuvette is measured by the photometer. The light absorbance can be read in a display device. The drawing of mechanism of the spectrophotometer is shown in Figure 3.9.

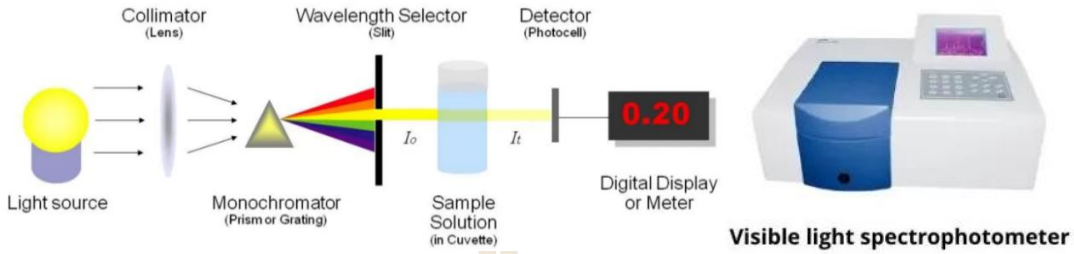

Figure 3.9: UV–vis spectrophotometer principle and equipment. Adapted from (https://microbiologynote.com/spectrophotometer-principle/).

The measurement of light absorbance is based on the Beer-Lambert law. The absorbance (also can be replaced by extinction) of a liquid sample can be expressed in linear equation, as shown in 3.3 (Law). This means that the absorbance becomes linear function with the concentration of the sample.

$$A = -\log_{10}\left(\frac{I}{I_0}\right) = \varepsilon cL \qquad (3.3)$$

Where I_0 and I are the intensities of light before and after passing through the cuvette, respectively. **ε** is the molar extinction coefficient. c is the concentration of sample solution (mol/L). L is the thickness of the cuvette which the light beams passing through (cm).

1) Steps of performing activity estimation consist of:

The enzymatic activity of commercial papain (solid storage and liquid storage at 3°C denature by time) and crystallized samples (from cooling, antisolvent, SFO processes) were quantified using the Anorn-Ruth method with BAPNA (N**α**-benzoyl-DL-arginine 4-nitroanilide hydrochloride) as substrate (Boonkerd & Wantha, 2024; Iván E. Moreno-Cortez et al., 2015; Ruth, 1970). The substrate solution was prepared by first dissolving 43.5 mg of BAPNA in 1 mL of DMSO, then diluting to 100 mL with Tris-buffer (0.05 M Tris, pH 7.5 adjusted with HCl, containing 0.005 M cysteine and 0.002 M EDTA). All solid papain samples were dissolved in DI water at a concentration of 30 mg/mL, with the enzyme concentration verified by measuring absorbance (Abs) at 280 nm (Quartz cuvette) using UV-vis spectroscopy (DR6000, Hach, USA) with DI water as blank as followed standard curve in Figure 3.10.

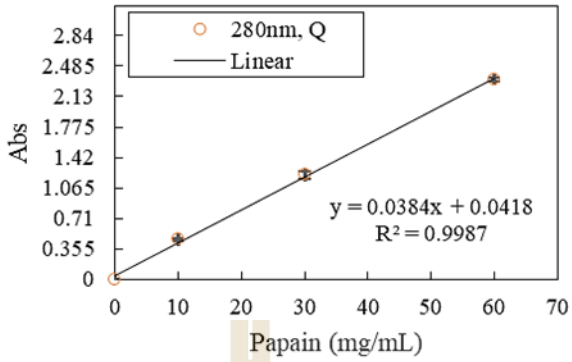

Figure 3.10: The calibration line of papain concentration in water for enzyme activity measurement.

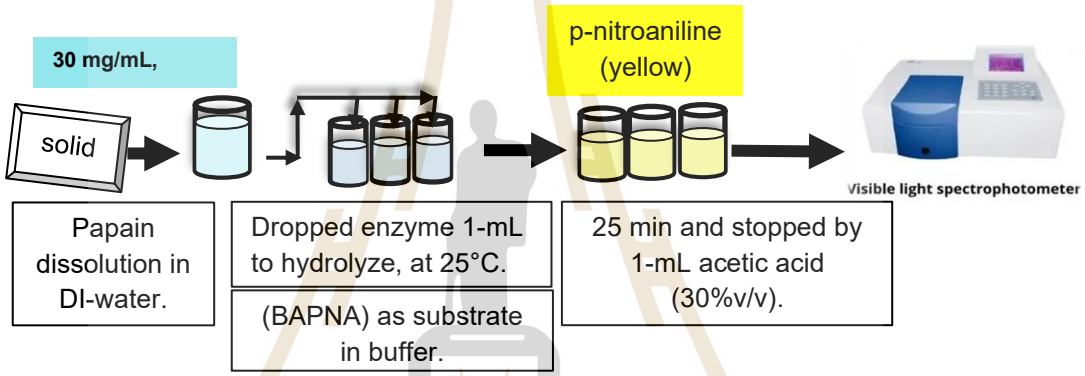

Figure 3.11: The papain activity measurement procedure with BAPNA hydrolyze.

For the activity assay, 1 mL of the papain solution was mixed with 5 mL of BAPNA substrate solution in test tubes and incubated at 25°C for 25 minutes (Figure 3.11). The reaction was terminated by adding 1 mL of 30% (v/v) acetic acid, after which the absorbance at 410 nm was measured against a blank (5 mL substrate mixed 1 mL acetic acid as the blank). The measured absorbance values, corresponding to liberated p-nitroaniline, were used to calculate BAPNA units and specific activity according to equations 3.4 and 3.5 respectively. One BAPNA units was defined as the amount of enzyme required to hydrolyze 1 micromole of substrate per minute under the specified conditions.

$$\text{BAPNA Units} = \frac{\text{Abs}_{410\text{nm}}}{25\text{min}} \times \frac{3 \times 1000}{8800} \quad (3.4)$$

$$\text{Specific activity} = \frac{\text{Unit}}{\text{mg}} = \frac{\text{BAPNA Units}}{30\text{mg}} \quad (3.5)$$

where Abs_{410nm} is the absorbance of product p-nitroaniline (yellow); t is reaction time (25 min); and 8800 M^{-1} cm^{-1} is molar extinction coefficient of p-nitroaniline at 410 nm. The enzyme activity was measured immediately after complete dissolution.

3.3.2 Crystal characterizations

The morphology of papain crystal sample was observed by microscope. The crush fine powder by an agate mortar and pestle. The fine powder was carefully transferred on a sample holder. The crystal was examined by powder X-ray diffraction (D2 Phaser, Bruker) using Cu Kα radiation (λ = 1.5418 Å) with a scan range of 10–50° 2ϑ at 0.0025° step size. The resulting diffraction patterns were compared with reference patterns (Chandran & Nachimuthu, 2018).

Scanning Electron Microscope (JSM-6010LV) was also used to monitor powder structure of commercialize papain, SFO recovery crystal of papain and from others methods.

CHAPTER IV

RESULTS AND DISCUSSION

4.1 Preliminary study of SFO crystallization of lysozyme

4.1.1 The solubility study by FBRM and SFO crystallizer testing

Figure 4.1 the solid dissolution in heating crystallizer until particle disappearance in FBRM monitor. Lysozyme showed the solubility through various temperatures versus amount of ammonium sulfate solution. In Figure 4.1 (a) solid lysozyme was added into crystallizer at −3 ˚C (0.4M) and the temperature gradually increased. The FBRM monitor showed high amount of solid in solution (Figure 4.1 (b)) and slowly decreased to base line with more clearly solution of lysozyme in crystallizer (Figure 4.1 (c)) at −1.5 ˚C.

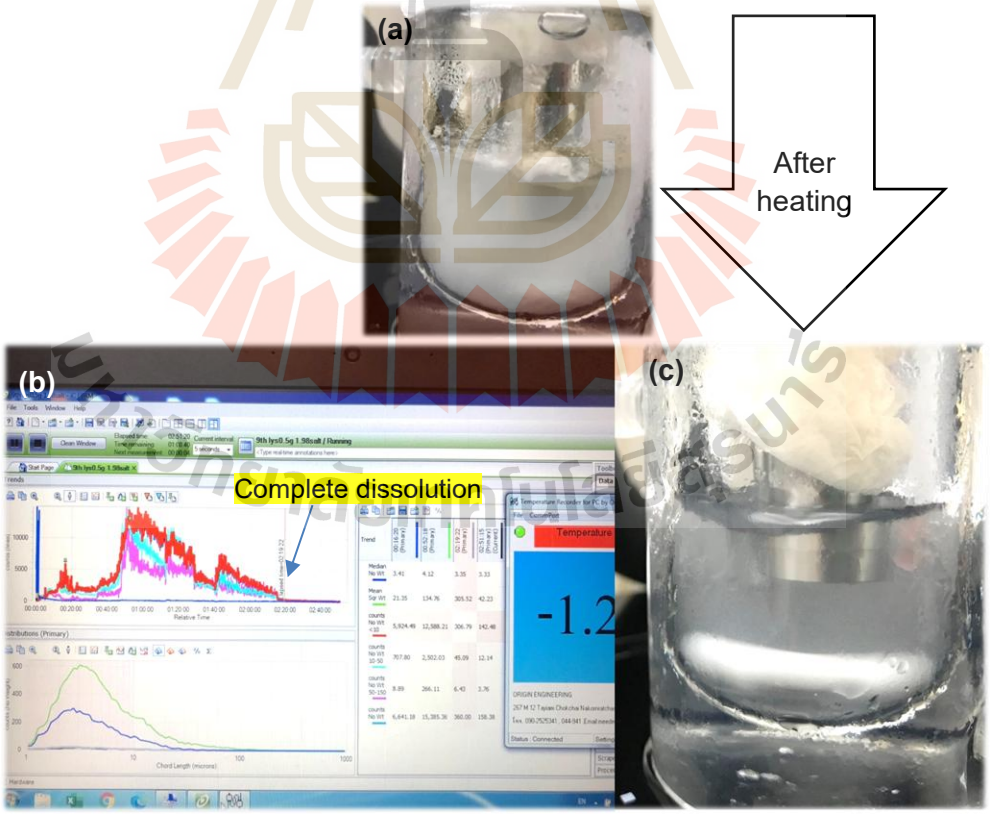

Figure 4.1: The crystallizer with FBRM set-up for measuring lysozyme solubility.

The solubility of lysozyme in different amount of ammonium sulfate is shown in Figure 4.2. The solubility of lysozyme decreased with increasing the concentration of ammonium sulfate and increased with raising temperature (Do et al., 2021; Ferreira & Castro, 2023). The phase-diagram to control SFO process for lysozyme that completed all three different salt concentration are shown in Figure 4.3. The result illustrated freezing the water out and nucleation of lysozyme were reached higher solubility point. Nucleation points at 0.7 M of salt was less than using 0.4 M and 0.6 M. It followed the literature (Elizabeth L. Forsythe, Edward H. Snell, Christine C. Malone, & Pusey, 1999) and solubility of 0.4 and 0.6 M illustrated the over salt drove the less dissolution ability, but the 0.7 M condition uncapable produced crystalline of lysozyme as shown in Figure 4.4 (c).

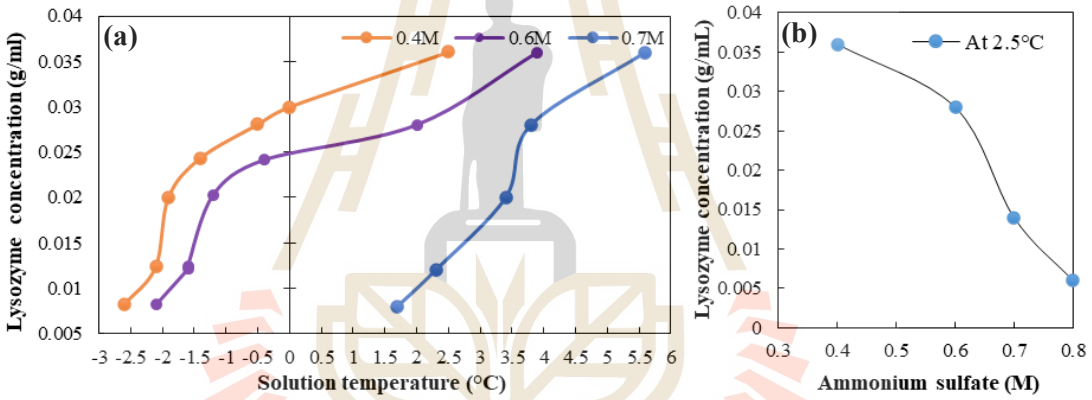

Figure 4.2: Solubility of lysozyme in ammonium sulfate with various temperatures (a-b).

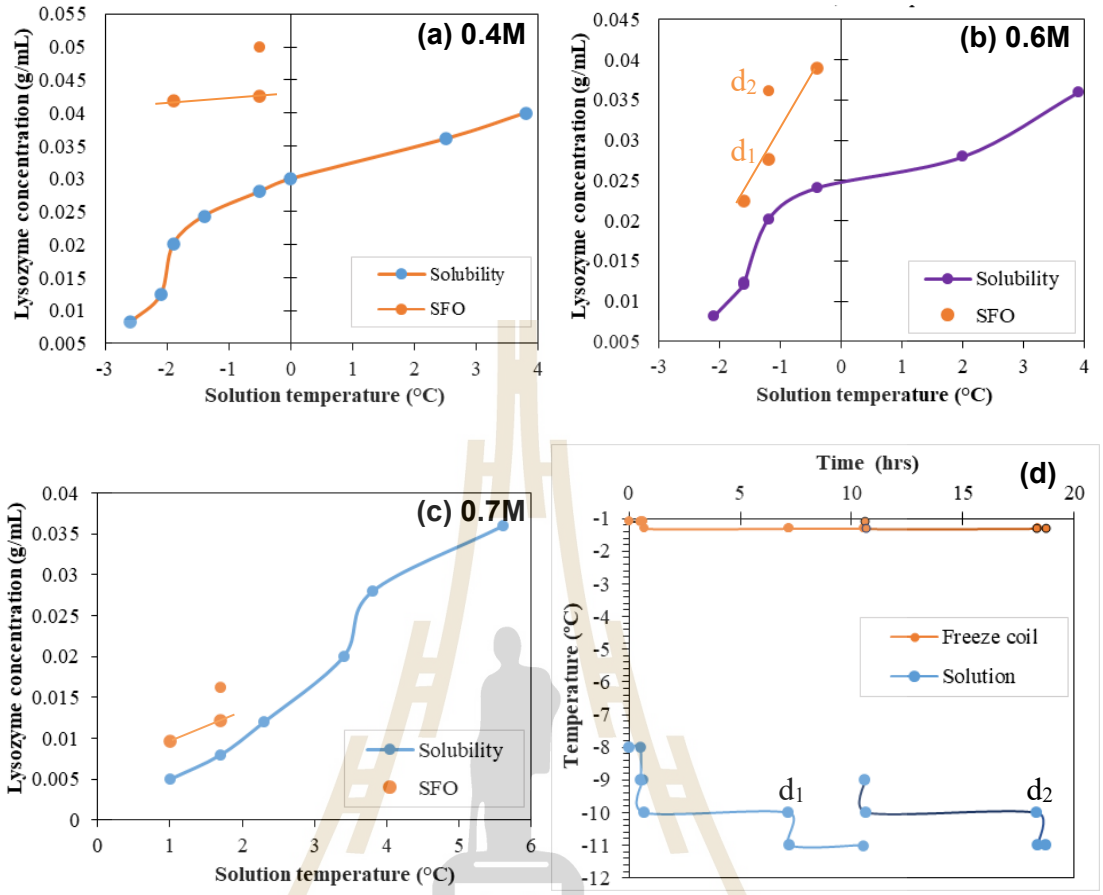

Figure 4.3: The phase-diagrams of lysozyme in ammonium sulfate solution. Solubility and nucleation point using SFO at pH 4.6 with salt concentration of (a) 0.4M, (b) 0.6M, and (c) 0.7M. (d) Freeze-coil and bulk-solution temperature profiles with time.

In Figure 4.4, showed the lysozyme became cloud (nucleation) in SFO crystallizer. Figure 4.4 (a) was before and after freezing the water until clouding of salt 0.7M at 1 ˚C. The observed particle image under microscope in Figure 4.4 (b) and the filtration and dryness in (c). But after filtration the cloud solution became gel-like because over salt addition. After drying, the salt crystal nucleated over the lysozyme.

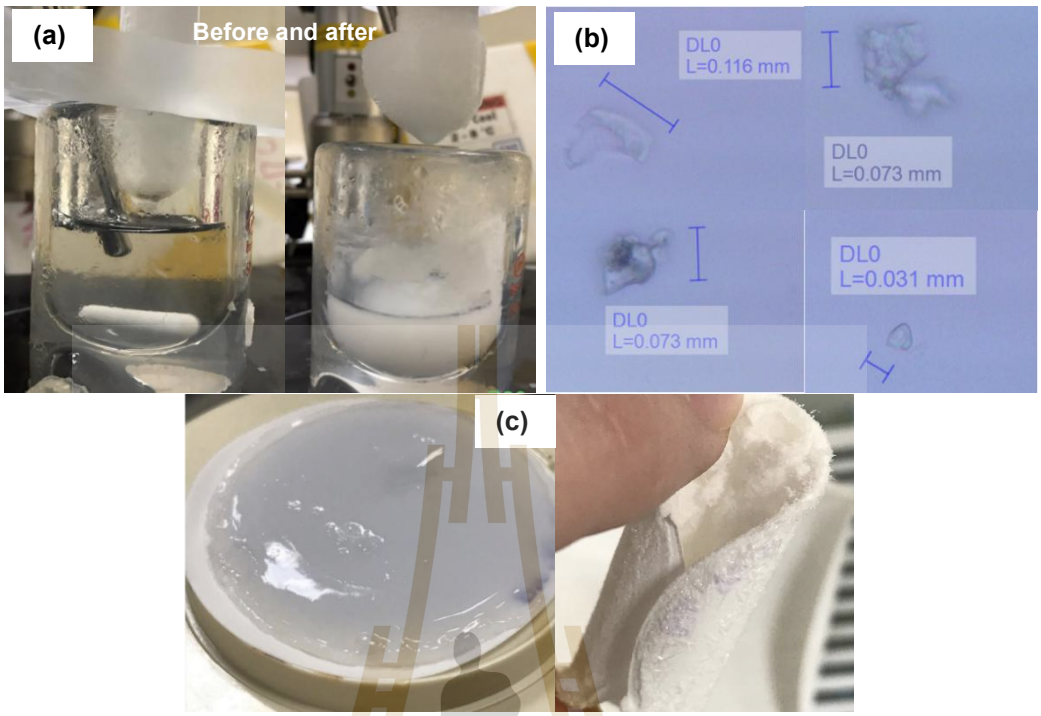

Figure 4.4: (a) The SFO crystallizer at Lysozyme precipitated as a gel in ammonium sulfate (0.7M) from solution at 1 °C. (b) particle images by Microscope,4X. (c) Filtration and dry particle.

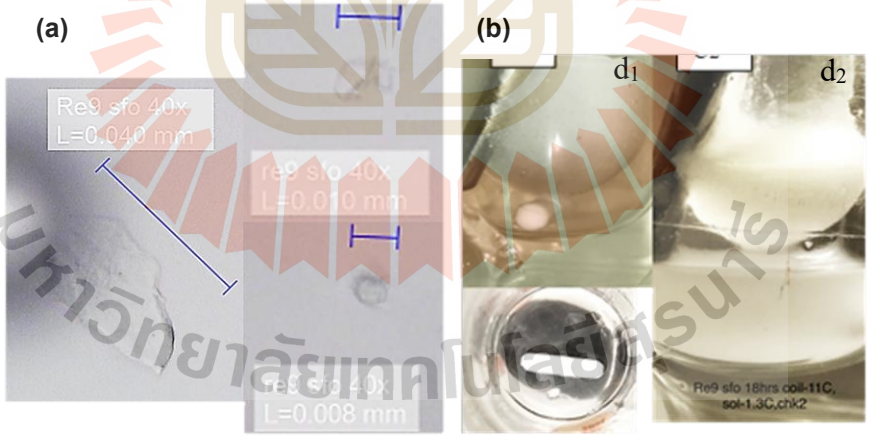

Figure 4.5: The Lysozyme nucleation in ammonium sulfate (0.6M) from SFO crystallization: (a) particle images by Microscope 40X, and (b) Lysozyme cloud in solution but d_1 as a first freezing, d_2 as second freezing.

For 0.6M of salt, the freezing water out required to run for second time due to less cloud occurred at first freezing (Figure 4.5 (b), at points d_1 & d_2). However,

the all particle image showed unlike lysozyme particle when compared to previous work (crystallization of chicken egg white lysozyme from assorted sulfate salts) (Elizabeth L. Forsythe et al., 1999). The final temperature could be controlled to only −11 ˚C for this concentration and by freeze rate of 0.1 ˚C/min for freeze coil. The chosen freezing rate may have been too high, promoting gelation and poor crystal habit; provide comparative runs at slower rates to corroborate.

To summary, solubility of lysozyme decreased with increasing ammonium sulfate concentration. Ammonium sulfate contributed lysozyme cloud in SFO crystallizer, but crystal was still small and disable to observe the monoclinic form by microscope while comparing to case of NaCl. For this study, SFO technique had satisfy efficiently to drive solution to supersaturation and it must be studied more to use in other protein separation/crystallization. However, this need to be careful the final temperature of freeze coil, initial enzyme concentration, and amount of salt or precipitant agent to avoid precipitation and loss of enzyme.

4.2 Results of papain crystallization

4.2.1 Solubility of papain

Solubility studies revealed that papain exhibited similar saturation concentrations in both DI water (pH 6.6-7) and acetate buffer (pH 5.0), as evidenced by the overlapping solubility curves shown in Figure 4.6 (a). This observation suggests that the buffer system at pH 5.0 did not significantly alter the thermodynamic solubility of papain compared to aqueous solution (pH 6.6). Opposite with lysozyme that solubility was increased by raising pH (Wang et al., 2023). But this point suitably studies more. Figure 4.6 (b) presents the solubility profile of papain in methanol-acetate buffer mixtures, showing a clear dependence on both solvent composition and temperature. The solubility decreases progressively with increasing methanol fraction (w/w), following typical antisolvent behavior where the addition of methanol reduces the solubility of papain. Similar solubility suppression has been reported for lysozyme, amino acids and peptides exposed to alcohol–acetate environments, attributed to decreased dielectric constant and disrupted hydrogen bonding networks that promote aggregation (Do et al., 2021; Ferreira & Castro, 2023).

Furthermore, lower temperatures resulted in lower solubility at all methanol fractions, consistent with the exothermic nature of protein dissolution and corroborated by thermodynamic analyses of acetate-buffered protein systems (Grossmann & McClements, 2023; Hentschel et al., 2021; Kenneth P. Murphy, Privalov, & Gill, 1990).

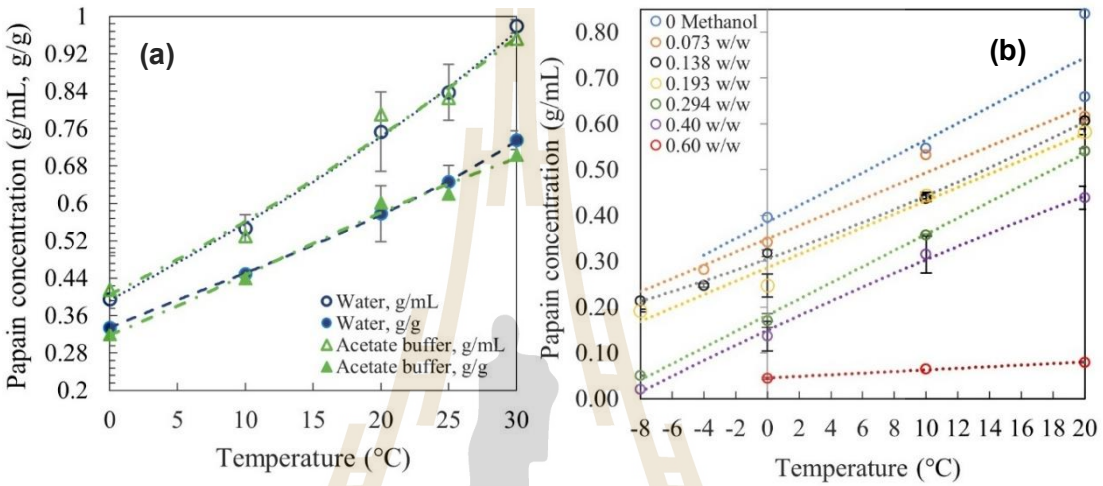

Figure 4.6: The solubility of papain in (a) water and acetate buffer (pH 5.0) at various temperatures. (b) In the mixture of acetate buffer with methanol (0.07-0.6 w/w) at various temperatures.

4.2.2 Cooling crystallization for papain

The cooling crystallization experiments revealed distinct nucleation characteristics under different conditions. When a saturated papain solution (0.97 g/mL) at 30 °C was cooled at rate of 0.005 °C/min with moderate agitation, the cloud point (indicating nucleation onset) was observed at 12.5 °C. The gradual viscosity increased at lower temperatures reduced stirring efficiency, as evidenced by the slower rotation of the magnetic stir bar. In contrast, under static conditions, nucleation was delayed until 9.0 °C, demonstrating the significant impact of agitation on crystallization kinetics (Bartłomiej Filip, Michał Kołodziej, Roman Bochenek, Marcin Chutkowski, & Antos, 2024; Noor et al., 2020). For solutions with lower initial saturation (0.7534 g/mL at 20 °C), nucleation occurred at −3.0 °C, although some batch-to-batch variability was observed. The induction time of cooling crystallization for papain from saturation (at 30 to 9 °C) was evaluated approximately 15 hours for nucleation and growth in case

of smoothly agitation, but in case of none agitation because of high viscosity that induction time was approximately 55 hours (showed in appendix A.1). The complete phase behavior, including the boundaries of the supersaturation zone, is presented in Figure 4.7.

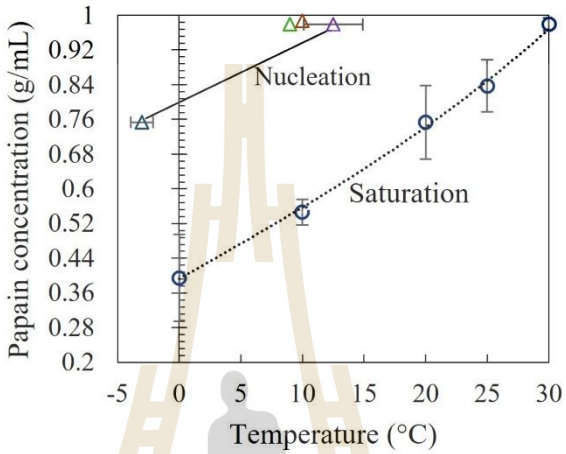

Figure 4.7: The phase-diagram for cooling crystallization of papain.

Crystallization and photomicroscopes analyses (Figures 4.8 and 4.9) suggest that crystal habits are likely dependent on the initial concentration and temperature. The −3 °C system produced metastable needle-like crystals that exhibited partial redissolution, while the 12.5 °C system initially formed sharper needle crystals, which transformed into plate-like or mixed morphologies during extended growth. These observations align with previous reports of papain's needle-like crystalline structure at nucleation point (Harris, 1983). The large temperature difference between the −3 °C system and the ambient environment may explain the observed redissolution under the microscope. However, the plate-like habit of papain crystal has not been reported previously. So, the plate-like habit of papain crystal needs more research for fulfilling the confirmation.

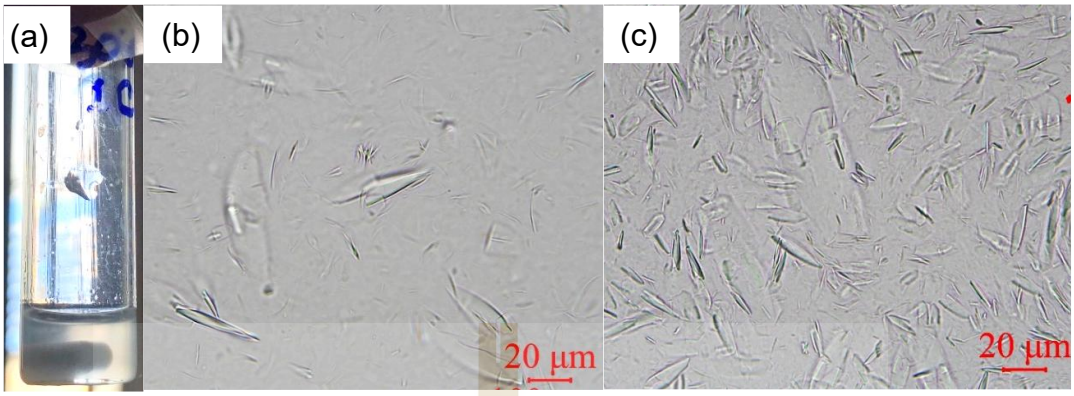

Figure 4.8: Cooling crystallization (cooling from 30 °C to 12.5 °C) of a saturated papain solution: (a) solution clouding in the crystallizer, (b) photomicrograph of crystals at the onset of nucleation, and (c) photomicrograph of crystals after 24 hrs of nucleation and growth.

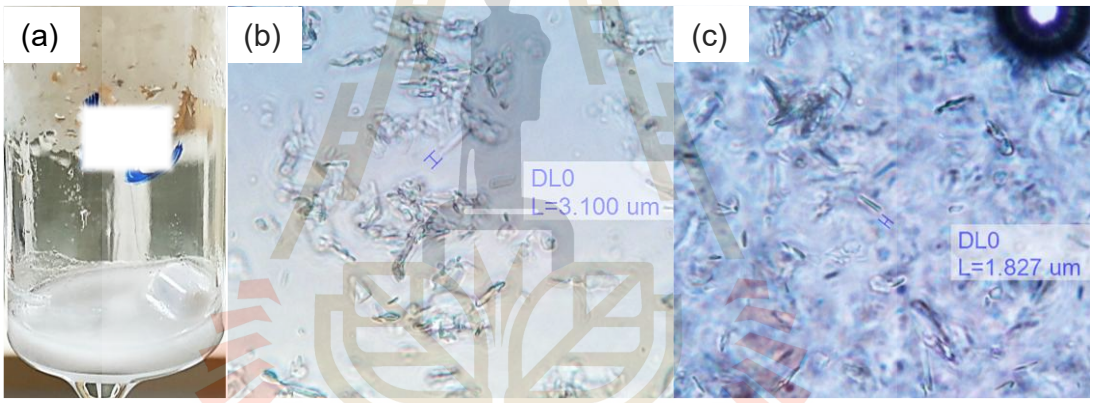

Figure 4.9: Cooling crystallization (cooling from 20 °C to -3 °C) of a saturated papain solution: (a) crystal clouding in the crystallizer after nucleation, (b) photomicrograph of crystals at the onset of nucleation, and (c) photomicrograph of crystals after 24 hrs of nucleation and growth.

4.2.3 Antisolvent crystallization for papain

Phases diagram of antisolvent crystallization for papain using methanol is illustration in Figure 4.10. The antisolvent crystallization of papain was systematically investigated at two fixed temperatures (20 °C and 0 °C) by incrementally adding methanol (0.2 mL/20 min) into saturated solutions until nucleation occurred. At 20 °C, a solution with an initial concentration of 0.67 g/mL reached its cloud point at a methanol weight fraction of 0.231, while a more dilute solution (0.07 g/mL) required significantly more antisolvent (methanol fraction of 0.66) to induce nucleation (Figure

4.10 (b)). In contrast, at 0 °C, nucleation occurred at lower methanol fractions for concentrated solutions (0.4 g/mL at methanol weight fraction of 0.112), but required higher fractions for dilute systems (0.1 g/mL at methanol weight fraction of 0.514) (Figure 4.10 (a)). The different methanol requirements at each temperature (0.231 w/w at 20 °C vs 0.112 w/w at 0 °C for concentrated solutions) demonstrate that temperature significantly affects the antisolvent concentration needed for nucleation. This suggests that methanol's disruption of papain's solvation shell prevents ordered crystallization regardless of temperature (Chayen & Saridakis, 2008; Mullin, 2001).

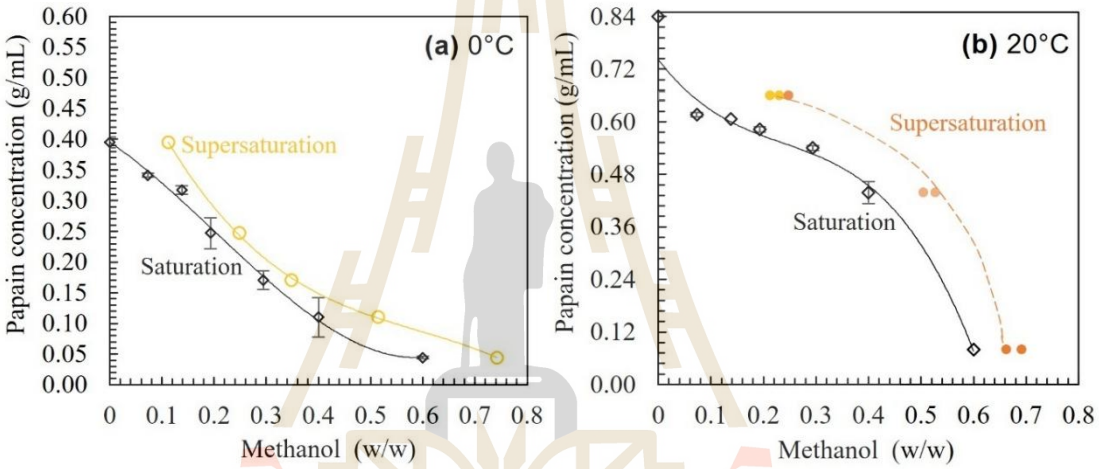

Figure 4.10: The phase diagram of antisolvent crystallization for papain at 0 °C (a) and 20 °C (b).

The real-time monitoring by FBRM and Easy-viewer (PVM) revealed (Figure 4.11) that particle formation began immediately after reaching the cloud point, with turbidity increasing as methanol was added.

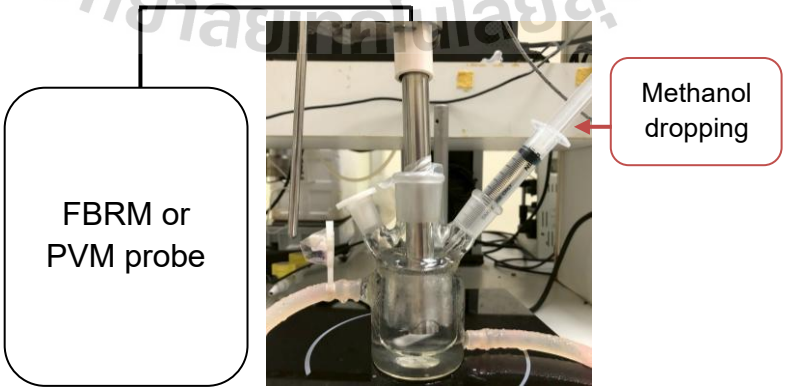

Figure 4.11: Antisolvent crystallizer setup with methanol dropping.

As shown in the photographs of Figure 4.12, the 0.17 g/mL solution at 0 ℃ showed initial nucleation at methanol fraction of 0.31-0.348 w/w, followed by rapid particle growth beyond 0.52-0.56 w/w, eventually forming a gel above 0.57 w/w. In Figure 4.13, the photographs of crystallizer show the solution at supersaturation level upon methanol addition at 0.21-0.23 w/w from a 0.67 g/mL solution at 20 ℃ (Figure 4.13 (a)). Gelation started occurred at 0.64 w/w of addition methanol (Figure 4.13 (c)). However, all conditions ultimately produced amorphous precipitates rather than crystals, consistent with previous reports using ethanol (Boonkerd & Wantha, 2024). Even though, harvesting the particle from cloud points using centrifugal force and gravity separation, the particle became amorphous as evidenced by the PXRD pattern shown in Figure 4.17.

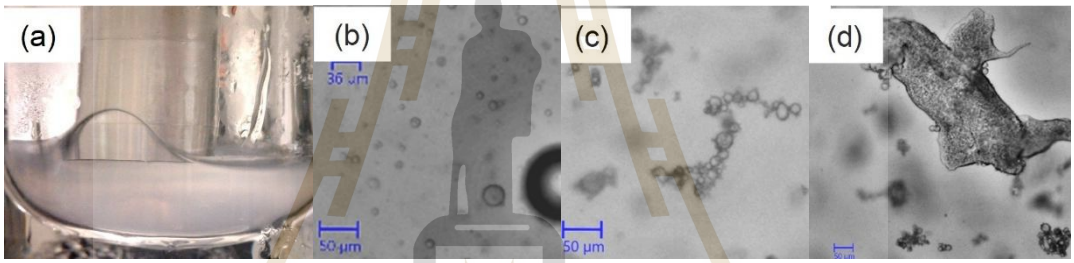

Figure 4.12: (a) Crystallizer image was captured during methanol addition at 0.348 w/w, and photomicrograph of papain crystals in liquor (b) at cloudy point (methanol 0.348 w/w) from saturation concentration of 0.17 g/mL (0 ℃); (c) at point of methanol 0.56 w/w, and (d) the particle became sticky gel at 0.57 w/w.

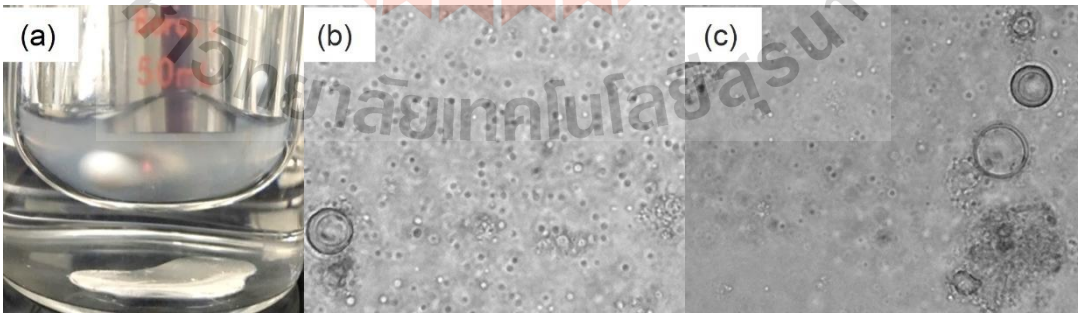

Figure 4.13: (a) Crystallizer captures image was captured during methanol addition at supersaturation of 0.23 w/w, and photomicrograph of papain crystals in liquor (b) at cloudy point (0.23 w/w) from saturation concentration of 0.67 g/mL (20 ℃) and (c) the particle became sticky gel at 0.64 w/w.

4.2.4 SFO crystallization for papain

Solvent freeze-out crystallization was systematically investigated at three initial concentrations 0.47 g/mL, 0.41 g/mL, and 0.33 g/mL; to observe the nucleation points at different temperatures range from −1.5 to 1 °C. The phase diagram for this SFO process of papain is shown in Figure 4.14 (a). The system achieved remarkably high nucleation thresholds, indicating the significant supersaturation required to initiate crystal formation. Crystalline was monitored via optical microscopy (40x magnification) following nucleation after deactivation of the freezing coil.

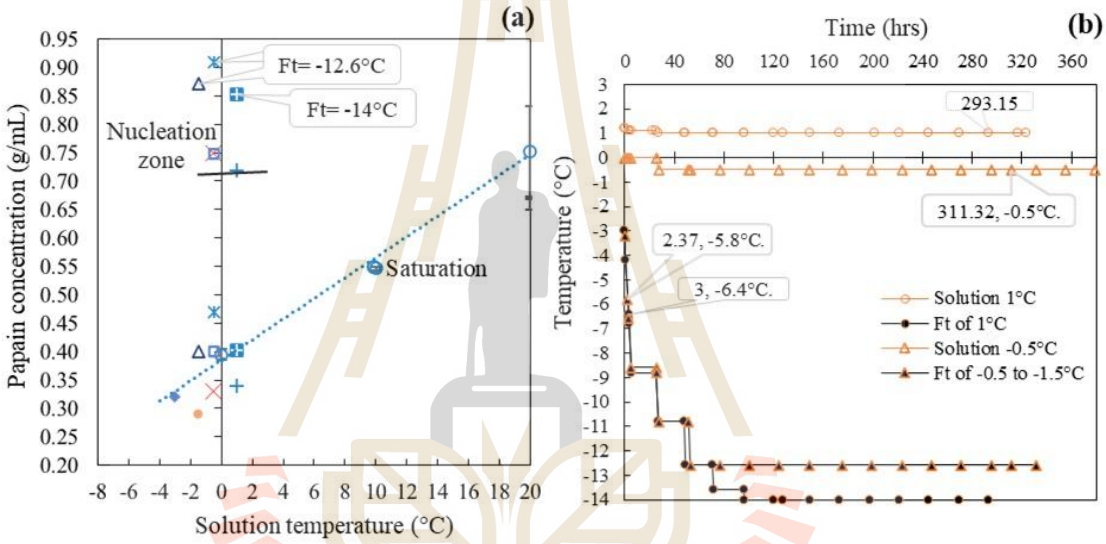

Figure 4.14: (a) The phase diagram of SFO for this papain solution at pH 5.0. (b) the temperature reduction profile of freeze coil (293.15 & 311.32h are time of nucleation). **Ft is final temperature of freeze coil*.

The final temperature of freeze coil terminated at -14 °C for systems maintained at 1 °C of papain solution as shown in Figure 4.14 (b). This is compared to −12.6 °C for both −0.5 °C and −1.5 °C of papain solution. The SFO process at low temperature (close to 0 °C) induced cloud concentration at-least 0.7157 g/mL (feed 0.33 g/mL saturation of 1 °C) in a residual volume 3.15 mL, corresponding to an 18.51% recovery with 13.22% lost in ice, as detailed in Table 4.1. Comparative analysis revealed that reduced final volumes (residual 1.9 mL, 0.7482 g/mL from feed 0.33 g/mL at −0.5 °C) recovered higher percentages (20%), demonstrating the expected concentration-dependent efficiency. Micrographic examination (Figures 4.15)

consistently revealed needle-like crystal morphologies under all experimental conditions, which transformed into a mixed of plate-like after drying as shown in Figure 4.16. The secondary nucleation may be occurred during slowly drying.

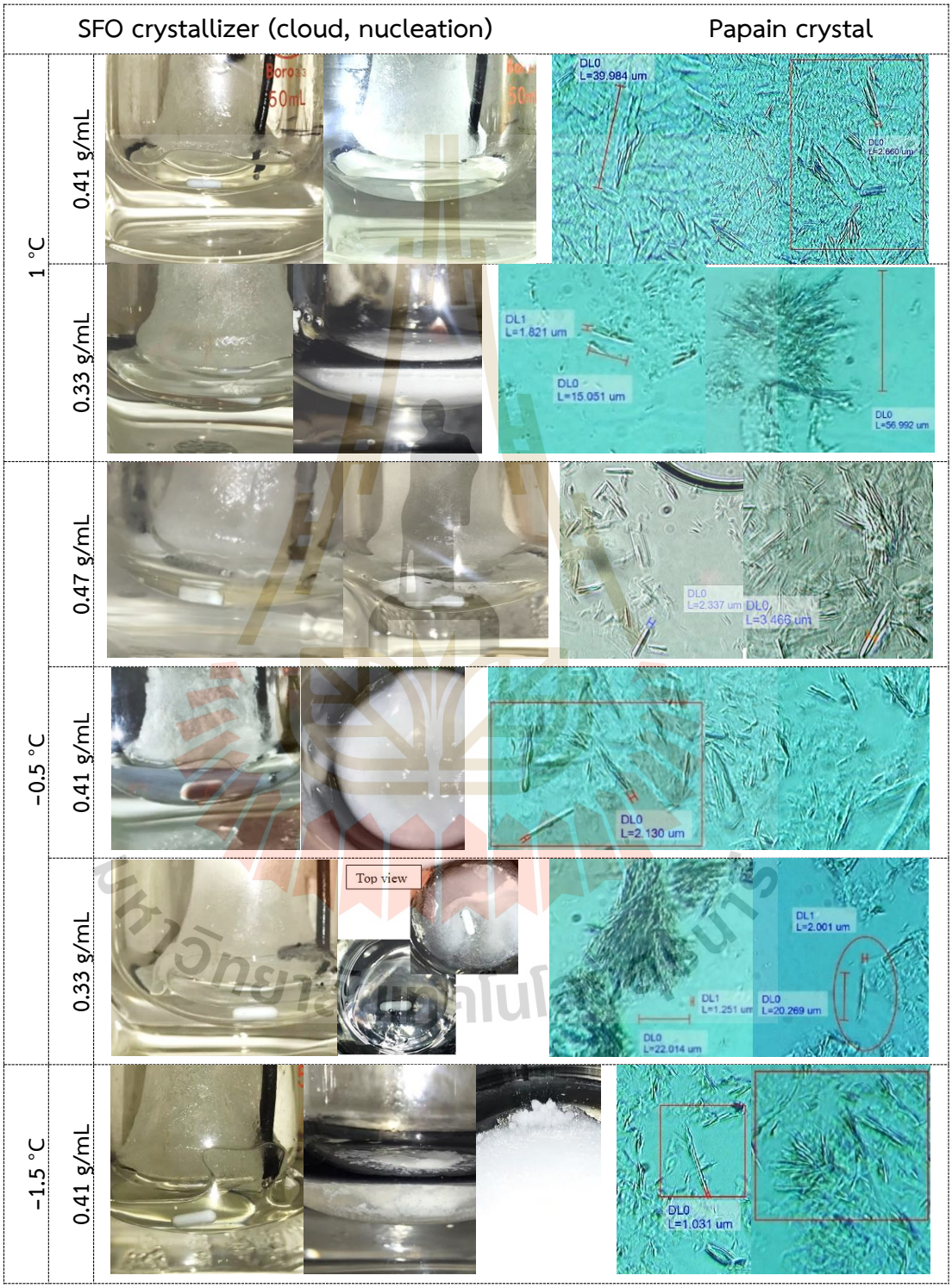

Figure 4.15: The SFO crystallizer and photomicrographs of papain crystal obtained at nucleation point from feed concentrations ranging of 0.33 to 0.47 g/mL.

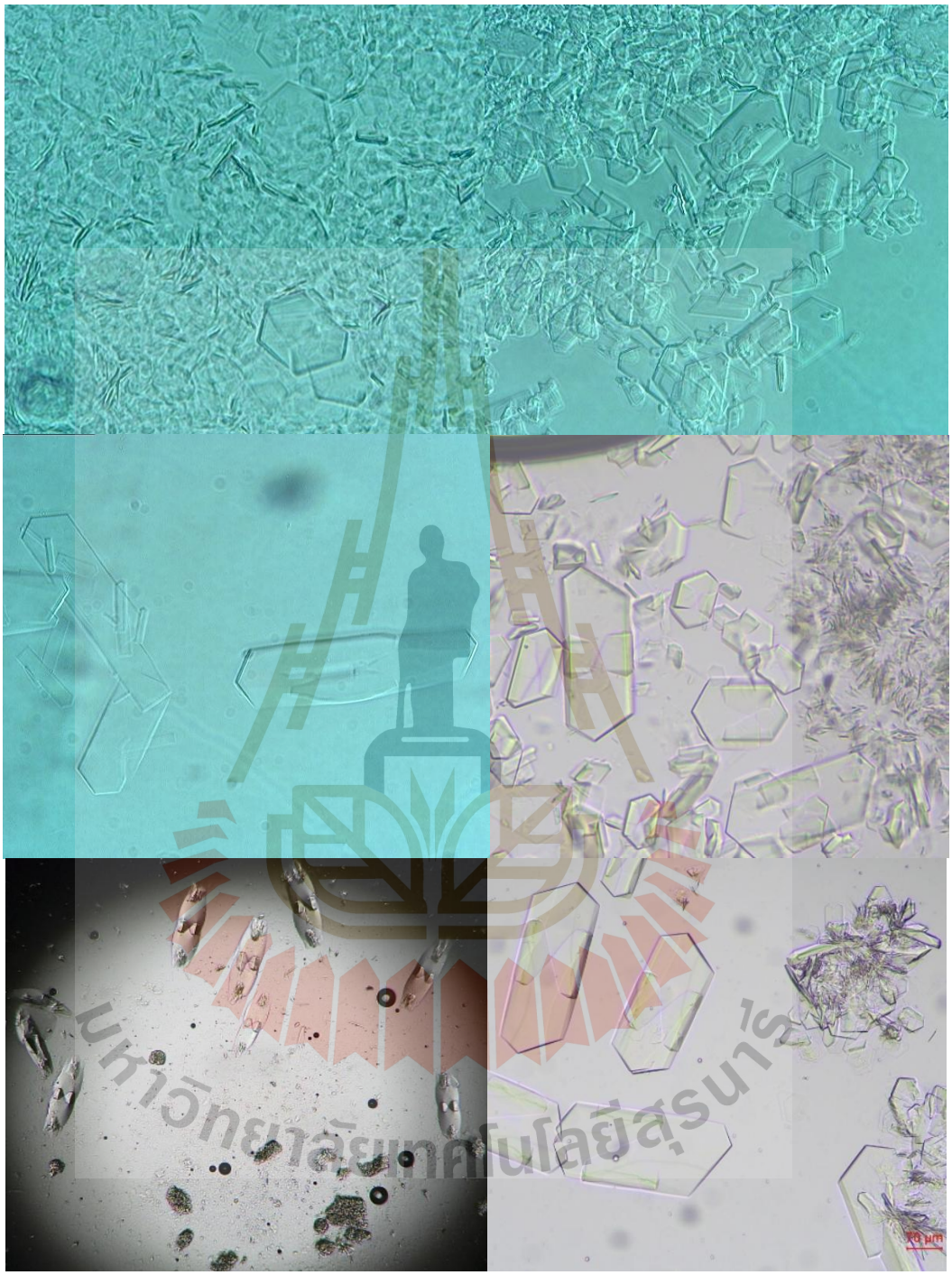

Figure 4.16: Examples of photographs of crystals from all conditions obtained after drying on slide under microscope (room/air temperature) in SUT and TjU.

Table 4.1: The percentage loss and recovery of papain crystallization using SFO in this work.

Papain in acetate buffer (no methanol addition)						
Solution Temp,°C	Initial Solution concentration, g/mL	Concentration at cloud points, g/mL	Residual Volume, mL	Ice Volume, mL	%Recovery of papain	%Lost of papain in ice
1	0.41	0.8472	1.8	5.2	64.74	28.89
−0.5	0.47	0.9222	2.6	4	64.21	21.23
	0.41	0.7449	2	5	57.14	26.02
	0.33	0.7482	1.9	5.1	20.05	20.58
−1.5	0.41	0.8671	1.2	5.75	58.42	26.77

The SFO technique demonstrated particular effectiveness for near saturated concentration systems, achieving recoveries exceeding 55% at all tested temperatures (−1.5, −0.5, and 1 °C) while minimizing solute loss to ice entrapment. Although the process required extended duration to reach nucleation, the reproducible formation of crystalline products (in contrast to the amorphous aggregates observed in antisolvent crystallization) highlights the method's superiority for obtaining structurally defined papain crystals.

This systematic investigation demonstrates that solvent freeze-out (SFO) crystallization enables precise, temperature-programmed control of nucleation while preserving protein tertiary structure and enzymatic activity (Ming et al., 2021), were mention in section 4.2.7. In contrast to traditional salting-out methods that risk structural denaturation at high ionic strengths (Hekmat, 2015; Wang et al., 2023), SFO produces homogeneous, needle-like crystals with sharply defined, temperature-dependent nucleation and growth thresholds (Feng et al., 2024; McArdle & Erxleben, 2024). These thresholds align with lysozyme pseudo-phase boundaries reported by Díaz-Borbón et al., (Borbón & Ulrich, 2012; Borbon & Ulrich, 2013) validating cross-system reproducibility. The observed habit modulation via additive concentration and cooling rate mirrors needle-forming strategies in organic crystallization systems, highlighting SFO's advantage for morphology control in biopharmaceutical scale-up (Xiaoxi Yu et al., 2015).

4.2.5 Powder X-ray diffraction

This work was further examined using PXRD, as shown in Figure 4.17. The papain crystal exhibited the characteristic peaks at 2theta angle of 12.13°, 14.83°, 18.97°, 20.19–20.80°, 23.34°, 28.65° and 36.00°, consistent with patterns of the commercial papain and previous reports (Chandran & Nachimuthu, 2018; Qi Hao et al., 2024). The products obtained from the SFO process and cooling process (pH 5 and 6.7) showed similarly high crystallinity and phase purity, whereas the antisolvent-derived product was amorphous (Boonkerd et al., 2024) due to XRD pattern showed as curve (no peaks).

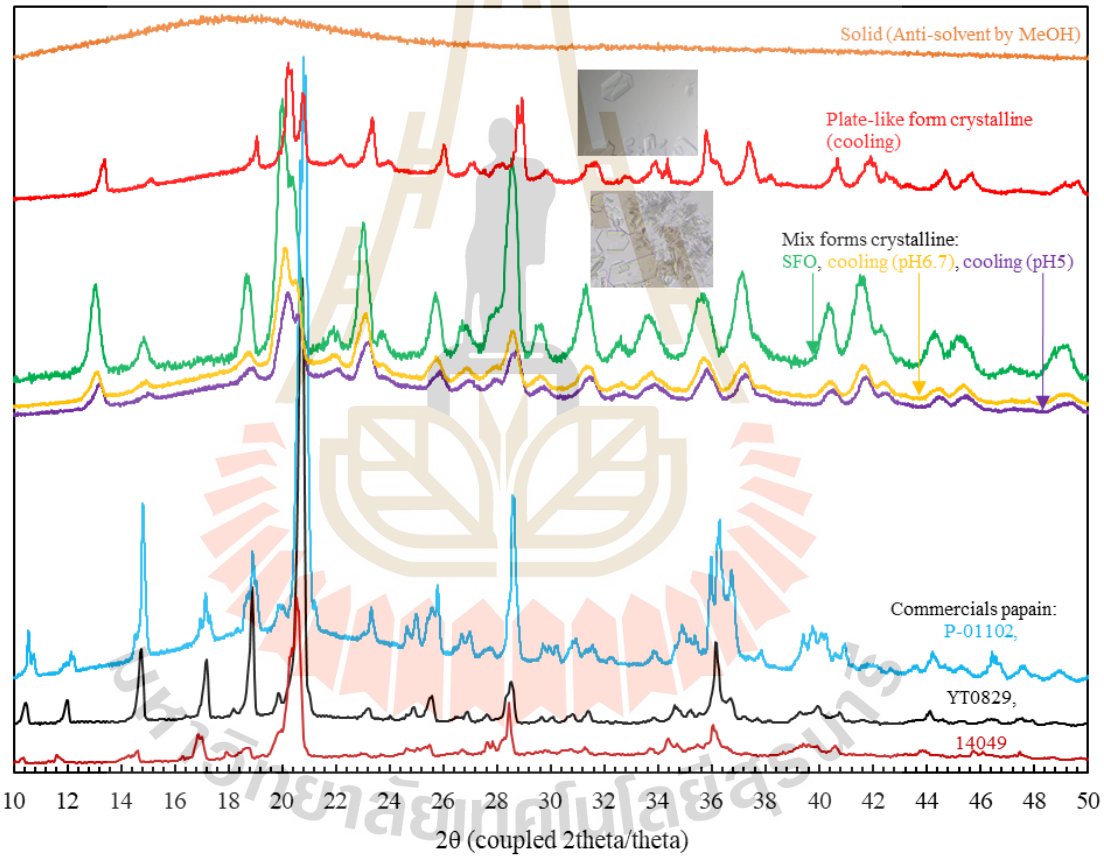

Figure 4.17: PXRD patterns of papain particle obtained from this work: orange) Amorphous papain from antisolvent by methanol; red) Plate-like form from cooling crystallization; green) Mixed needle/plate like habit crystal of papain from SFO process; yellow) Mix form crystal from cooling crystallization without buffer; purple) Mix form crystal from cooling crystallization with buffer (pH 5.0); and commercial crystalline papain: blue) As product no. P-01102; black) YT0829; dark red) 14049.

4.2.6 SEM of papain crystal

The SEM photographs in Figure 4.18 further revealed distinct morphologies. Commercial papain (Figure 4.18 (a)) appears as irregular, smooth-surfaced granules, while SFO-derived papain crystals (Figure 4.18 (b-e)) exhibits two habits: agglomerated plate-like lamellae in panel (c) and agglomerated needle-like crystals in panel (d-e). The crystals in (b-e) contrasted with the SEM observations of antisolvent-precipitated papain which formed agglomerated granule (Boonkerd et al., 2024). The high viscosity of the remaining solvent and slow drying process (in air/room environment) likely drove the agglomeration of the papain crystal (Gao et al., 2024; Qi Hao et al., 2024).

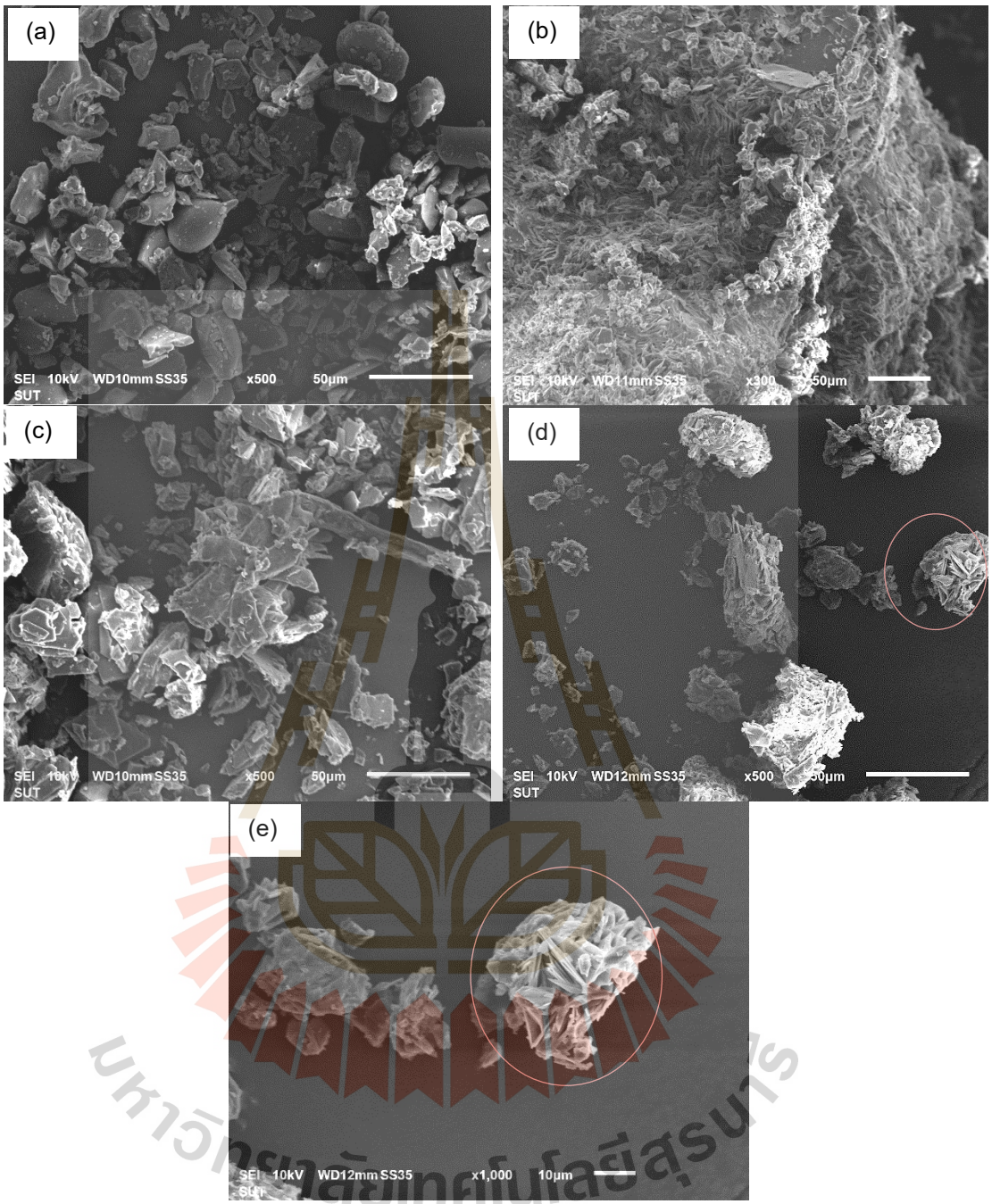

Figure 4.18: The SEM photographic of this work: (a) Commercial crystalline papain, (b-e) Crystal of papain from SFO process. (c) Plate-like form and (d-e) Needle-like form.

4.2.7 The enzyme activity analysis

Papain crystals obtained from the SFO crystallization and commercial papain were each tested at a concentration of 30 mg/mL for their reaction with the substrate, and the resulting product was measured at 410 nm, as shown in Figure 4.19.

The enzyme activity was then calculated, and the specific activity is shown in Table 4.2. The results showed the papain crystal obtained activity from SFO crystallization was 0.001777 BAPNA Units, while commercial papain crystal responded an activity of 0.001811 BAPNA Units. At the same time, papain crystal from the antisolvent crystallization responded the stable enzyme activity. It may cause of antisolvent method consumes shorter processing time (not over 20hrs), but SFO and cooling process maintained longer processing time (over 50 hours) for papain in liquid-phase before the occurrence of nucleation. As consistence with illustration in Figure 4.20 all showed that the papain from liquid-phase storage reduced enzyme activity faster than keeping as solid-phase (crystal) under cool environment during a month. The crystal from SFO (0.0000590 Units/mg) and cooling (0.0000596 Units/mg) were between the commercial papain (0.000060 Units/mg) and liquid-phase storage of papain (0.0000570 Units/mg). These values indicate that the enzymatic function was preserved, consistent with previous studies showing that antisolvent crystallization (particularly using ethanol or methanol) can maintain protease activity when solvent ratios and temperature are controlled (Boonkerd & Wantha, 2024; Sirirak et al., 2025).

The negligible difference in activity between papain crystals obtained from SFO and commercial papain supports the hypothesis that solvent freeze-out crystallization is a gentle, non-denaturing technique suitable for biopharmaceutical applications. Similar findings were reported by Arnon (Ruth, 1970) and Boonkerd (Boonkerd et al., 2024) who demonstrated that papain retains catalytic efficiency post-crystallization when stabilized with cysteine and EDTA, and assayed using BAPNA substrates. These results further reinforce the suitability of crystallization for preserving bioactivity in proteolytic enzymes.

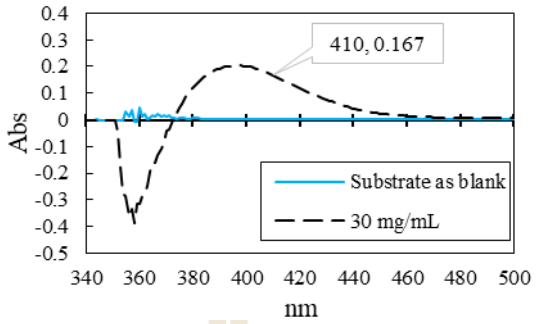

Figure 4.19: The product from reaction of papain with substrate (BAPNA) was analyzed using UV-vis spectroscopy at 410 nm.

Table 4.2: The enzyme activity assay of papain crystal.

Source of papain crystal	BAPNA Units	Units/mg
Commercial (YT0829)	0.001811	0.000060
By cooling crystallization	0.001788	0.0000596
By anti-solvent crystallization using methanol	0.001883	0.000063
By SFO crystallization	0.001777	0.000059

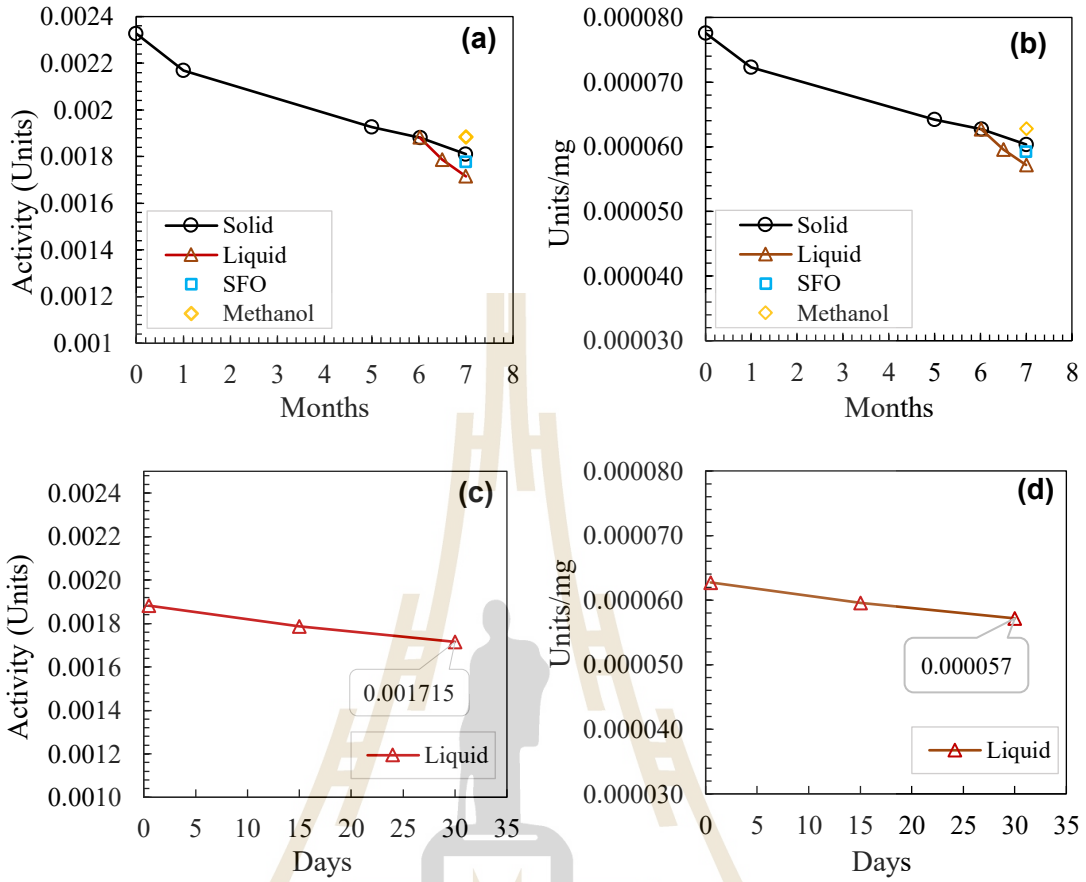

Figure 4.20: The papain activity denatured by time in different phases storage inside refrigerator (solid commercial papain and dissolution in water as liquid) and comparison with products of using antisolvent by methanol, SFO process: (a) as BAPNA Units, (b) as Units/mg. The activity denatured in liquid phase: (c) as BAPNA Units, (d) as Units/mg.

CHAPTER V

CONCLUSION AND RECOMMENDATION

5.1 Conclusion

Papain crystallization behavior depends on the method of nucleation generation and operating conditions. Within measurement uncertainty, solubility in acetate buffer (pH 5) was comparable to water, whereas solubility decreased with increasing methanol fraction and decreasing temperature.

Under the tested methanol addition protocol, antisolvent crystallization predominantly yielded amorphous aggregates and gel, while cooling crystallization at rate of 0.005 °C/min recovered papain crystals (needle-like) from concentrated solutions (saturated >0.77 g/mL, 100 rpm). Needle–like crystals at nucleation that evolved toward mixed needle/plate habits during growth; some plate-like appearance after drying may reflect preparation artifacts.

The SFO crystallization produced crystalline papain (also needle-like and mix plate-like after dryness) from dilute feeds (0.33–0.47 g/mL) at bulk −1.5 to 1 °C when the coil was held at −12.6 °C and −14 °C. The SFO technique achieved over 55% recovery with less than 30% solute loss into the ice phase at a freeze rate of 0.02 °C/min. PXRD indicated similar crystallinity for papain crystals grown in buffer (pH 5) versus water. Specific activity differences among SFO, cooling, and commercial references were not significant under the reported assay conditions, but SFO process uniquely capable crystallized papain from lower feed concentrations while maintaining crystallinity and specific activity, and making it particularly suitable for pharmaceutical applications requiring pure, functional protein crystals.

5.2 Recommendations

1) The pilot scale SFO crystallizer for papain should study with less solute loss than 20% into ice.

2) For separation papain by crystallization, if feed papain concentration is less than solubility, this SFO process is suitable. But for feeds near saturation, the cooling crystallization should be considered with slow cooling rate.

3) The enzyme activity determination should be analyzed in triplicate within the same batch and month of experimental operation to avoid the time dependent decay.

REFERENCES

Albert M. Schwartz, K. A. B. (2000). In situ monitoring and control of lysozyme concentration during crystallization in a hanging drop. *Journal of Crystal Growth 210*(2000), 753-760. Retrieved from https://www.sciencedirect.com/science/article/pii/S0022024899004236

Alderton, G., & Fevold, H. L. (1946). Direct Crystallizaton of Lysozyme from Egg White and some crystalline Salts of Lysozyme. *The Journal of Biological Chemistry, 1*, 1-5. Retrieved from https://www.chem.fsu.edu/chemlab/bch4053l/protein/crystal/Lys%20Crystals%20diff%20salts.pdf

Amri, E., & Mamboya, F. (2012). Papain, A Plant Enzyme of Biological Importance: A Review. *American Journal of Biochemistry and Biotechnology, 8*(2), 99-104. doi:10.3844/ajbbsp.2012.99.104

Asherie, N. (2004). Protein Crystallization and Phase Diagrams. *Methods, 34*, 266–272. doi:10.1016/j.ymeth.2004.03.028

Bartłomiej Filip, Michał Kołodziej, Roman Bochenek, Marcin Chutkowski, & Antos, D. (2024). Computational Fluid Dynamics for Determining the Interplay between Stirring Conditions and Crystal Size Distribution in Small Laboratory Devices. *Industrial & Engineering Chemistry Research, 63*(37), 16208-16219. doi: 10.1021/acs.iecr.4c01816

Bennema, P. (1992). Theory of Growth and Morphology Applied to Organic Crystals; Possible Applications to Protein Crystals. *Journal of Crystal Growth, 122*, 110-119. Retrieved from https://www.sciencedirect.com/science/article/pii/002202489290234A

Boonkerd, S., Hao, H., & Wantha, L. (2024). Preparation and Characterization of Acetylated Starch/papain Composites. *RSC Adv., 14*, 37820. doi: 10.1039/d4ra05814c

Boonkerd, S., & Wantha, L. (2024). Antisolvent Crystallization of Papain. *ChemEngineering, 8*(4). doi:10.3390/chemengineering8010004

Borbón, V. D., & Ulrich, J. (2012). Solvent Freeze Out Crystallization of Lysozyme from a Lysozyme-Ovalbumin Mixture. *Cryst. Res. Technol, 47*(No.5), 541 – 547. doi:10.1002/crat.201200073

Borbon, V. P. D., & Ulrich, J. (2013). SFO-Solvent Freeze Out-Technology for Industrial Proteins. *Journal of Crystal Growth, 373*, 38–44. doi:http://dx.doi.org/10.1016/j.jcrysgro.2012.09.031

Chaiwut, P., Nitsawang, S., & Shank, L. (2007). A Comparative Study on Properties and Proteolytic Components of Papaya Peel and Latex Proteases. *Chiang Mai J. Sci., 34*(1), 109-118. doi:Article/CMJS/10905753

Chandran, S. P., & Nachimuthu, K. (2018). Formulation and Characterization of Papain Loaded Solid Lipid Nanoparticles Against Human Colorectal Adenocarcinoma Cell Line. *Asian J. Pharm Clin Res, 11*(10), 393-399. doi:http://dx.doi.org/10.22159/ajpcr.2018.v11i10.27258

Chayen, N. E., & Saridakis, E. (2008). Protein Crystallization: from Purified Protein to Diffraction-Quality Crystal. *Nature Methods, 5*, 147–153. doi:https://doi.org/10.1038/nmeth.f.203

Chisti, Y., & Moo-Young, M. (1990). Large Scale Protein Separations: Engineering Aspect of Chromatography. *Biotech. Adv., 8*, 699-708. Retrieved from http://tur-www1.massey.ac.nz/~ychisti/ChromatBA.pdf

Curtis, R. A., & L.Lue. (2005). Amolecular Approach to Bioseparations: Protein–Protein and Protein–Salt Interactions. *Chemical Engineering Science, 61*, 907–923.

Davey, R., & Garside, J. (2001). From Molecules to CrystallizerssAn Introduction to Crystallization. *Cryst. Growth Des., 1*, 101. doi:10.1021/cg000012w

Do, H. T., Franke, P., Volpert, S., Klinksiek, M., Thome, M., & Held, C. (2021). Measurement and Modelling Solubility of Amino Acids and Peptides in Aqueous 2-Propanol Solutions. *Phys. Chem. Chem. Phys., 23*, 10852. doi: 10.1039/d1cp00005e

Drenth, J., & Haas, C. (1992). Protein Crystals and Their Stability. *Journal of Crystal Growth 122*, 107-109. Retrieved from https://www.sciencedirect.com/science/article/pii/0022024892902339

Elizabeth L. Forsythe, Edward H. Snell, Christine C. Malone, & Pusey, M. L. (1999). Crystallization of chicken egg white lysozyme from assorted sulfate salts. *Journal of Crystal Growth, 196*, 332—343.

Feng, Y., Wang, H., Wu, D., Chen, K., Wang, N., Wang, T., . . . Hao, H. (2024). Polymorph Transformation of Solid Drugs and Inhibiting Strategies. *CrystEngComm, 26*, 6510. doi:10.1039/d4ce00811a

Ferreira, J., & Castro, F. (2023). Advances in Protein Solubility and Thermodynamics: Quantification, Instrumentation, and Perspectives. *CrystEngComm, 25*, 6388. doi:10.1039/d3ce00757j

Gao, Y., Song, W., Yang, J., Ji, X., Wang, N., Huang, X., . . . Hao, H. (2024). Crystal Morphology Prediction Models and Regulating Methods. *MDPI. Crystals, 14*, 484. doi:https://doi.org/10.3390/cryst14060484

Giulietti, M., Seckler, M. M., Derenzo, S., Re, M. I., & Cekinski, E. (2001). Industrial Crystallization and Precipitation from Solutions: State of the Technique. *Brazilian Journal of Chemical Engineering*, 1-25.

Grossmann, L., & McClements, D. J. (2023). Current Insights into Protein Solubility: A Review of Its Importance for Alternative Proteins. *Food Hydrocolloids, 137*, 108416. doi:https://doi.org/10.1016/j.foodhyd.2022.108416

Grzonka, Z., Kasprzykowski, F., & Wiczk, W. (2007). Chapter 11 Cysteine Proteases. *Industrial Enzymes springer*, 181–195.

Harris, J. R. (1983). Electron Microscopy of Papain Crystals. *Printed in Great Britain, Micron., 14*(2), 147-164. doi:10.1016/0047-7206(83)90017-1

Hekmat, D. (2015). Large-Scale Crystallization of Proteins for Purification and Formulation. *Bioprocess Biosyst Eng, 38*, 1209–1231. doi:10.1007/s00449-015-1374-y

Hekmat, D., Hebel, D., Joswig, S., Schmidt, M., & Weuster-Botz, D. (2007). Advanced Protein Crystallization Using Water-Soluble Ionic Liquids as Crystallization Additives. *Biotechnology Letter ©Springer Science, 29*, 1703-1711. doi: 10.1007/s10529-007-9456-9

Hentschel, L., Hansen, J., Egelhaaf, S. U., & Platten, F. (2021). The Crystallization Enthalpy and Entropy of Protein Solutions: Microcalorimetry, Van't Hoff Determination and Linearized Poisson–Boltzmann Model of Tetragonal Lysozyme Crystals. *Phys. Chem. Chem. Phys., 23*, 2686. doi:10.1039/d0cp06113a

https://microbiologynote.com/spectrophotometer-principle/.

Iván E. Moreno-Cortez, Jorge Romero-García, Virgilio González-González, Domingo I. García-Gutierrez, Marco A. Garza-Navarro, & Cruz-Silva, R. (2015). Encapsulation and Immobilization of Papain in Electrospun Nanofibrous Membranes of PVA Cross-Linked with Glutaraldehyde Vapor. *Materials Science and Engineering, C*(52), 306–314. doi:dx.doi.org/10.1016/j.msec.2015.03.049

Jia, S., Yang, P., Gao, Z., Li, Z., Fang, C., & Gong, J. (2022). Recent Progress in Antisolvent Crystallization. *CrystEngComm, 24*(17), 3122-3135. doi:http://dx.doi.org/10.1039/D2CE00059H

Kamphuis, I. G., Kalk, K. H., Swarte, M. B. A., & Drenth, J. (1984). Structure of Papain Refined at 1.65 A Resolution. *Academic Press Inc. (London) Ltd., 179*, 233-256. doi:10.1016/0022-2836(84)90467-4

Kenneth P. Murphy, Privalov, P. L., & Gill, S. J. (1990). Common Features of Protein Unfolding and Dissolution of Hydrophobic Compounds. *J. Mol. Biol, 247*, 559-561. Retrieved from https://www.jstor.org/stable/2873805

Kieliszek, M., & Misiewicz, A. (2013). Microbial Transglutaminase and its Application in the Food Industry. A review. *Folia Microbiol, springer*. doi:10.1007/s12223-013-0287-x

Law, B. L. Beer Lambert Law. Retrieved from https://teaching.shu.ac.uk/hwb/chemistry/tutorials/molspec/beers1.htm

Lewis, A., Seckler, M., Kramer, H., & Rosmalen, G. v. (2015). *Industrial Crystallization: Fundamentals and Applications. Thermodynamics, Crystallization Methods and Supersaturation*: Cambridge University Press.

Liu, Y., Hou, H., & Li, J. (2020). Direct Crystallization of Proteins from Impure Sources. *Crystal Growth & Design, 20*, 1694–1705. doi:10.1021/acs.cgd.9b01446

Lukin, A. (2020). Application and Comparison of Proteolytic Enzyme Preparations in Technology of Protein Hydrolyzates. *Food Science and Technology, 40*, 287-292. doi:https://doi.org/10.1590/fst.09319

M., B. J., Tymoczko, J. L., & Stryer, L. (2007). Stryer Biochemie. *Elsevier GmbH, München*.

Macalood, J. S., Vicente, H. J., Boniao, R. D., Gorospe, J. G., & Roa, E. C. (2013). Chemical Analysis of Carica papaya L. Crude Latex. *American Journal of Plant Sciences, 4*, 1941-1948. doi:http://dx.doi.org/10.4236/ajps.2013.410240

Manosroi, A., Chankhampan, C., Pattamapun, K., Manosroi, W., & Manosroi, a. J. (2014). Antioxidant and Gelatinolytic Activities of Papain from Papaya Latex and Bromelain from Pineapple Fruits. *Chiang Mai J. Sci., 41(3)*, 635-648. http://epg.science.cmu.ac.th/ejournal/ Contributed Paper

Maosoongnern, S., Flood, C., Flood, A. E., & Ulrich, J. (2016). Crystallization of Lysozyme from Lysozyme-Ovalbumin Mixtures: Separation Potential and Crystal Growth Kinetics. *Journal of Crystal Growth, 469*, 0022-0248. doi:http://dx.doi.org/10.1016/j.jcrysgro.2016.09.049

Mat Yunus W. Mahmood, & Azizan, R. (1988). Refractive Index of Solutions at High Concentrations. *Applied Optics, 27*, 3341-3343. doi:10.1364/AO.27.003341

Mathias Elsson, Anondho Wijanarko, Heri Hermansyah, & Sahlan, M. (2019). *Michaelis-Menten Parameters Characterization of Commercial Papain Enzyme "Paya"*. Paper presented at the IOP Conf. Ser. Earth Environ. Sci. .

McArdle, P., & Erxleben, A. (2024). Crystal Growth and Morphology Control of Needle-Shaped Organic Crystals. *CrystEngComm, 26*, 416. doi:10.1039/d3ce01041d

Mcpherson, A. (1990). Current approaches to macromolecular crystallization. *Eur. J. Biochem, 189*, 1-23.

Ming, H., Zhu, M.-F., Li, L., Liu, Q.-B., Yu, W.-H., Wu, Z.-Q., & Liu, Y.-M. (2021). A Review of Solvent Freeze-Out Technology for Protein Crystallization. *CrystEngComm, 23*, 2723.

Mitsuda, H., & Yasumatsu, K. (1955). Crystallization of Animal Catalase and Studies on its Optimum Temperature. *Journal of the Agricultural Chemical Society of Japan, 19*(3), 200-207. doi:10.1080/03758397.1955.10857289

Mohamed Azarkan, Garcia-Pino, A., Dibiani, R., Wyns, L., Lorisband, R., & Baeyens-Volant, D. (2006). Crystallization and Preliminary X-ray Analysis of a Protease Inhibitor from the Latex of Carica Papaya. *Structural Biology and Crystallization Communications, F62*, 1239–1242. doi:10.1107/S1744309106046367

Moraes, D., Levenhagen, M. A., Costa-Netto, A. P. d., Costa-Cruz, J. M., & Rodrigues, R. M. (2016). In Vitro Efficacy of Latex and Purified Papain from Carica Papaya Against Strongyloides Venezuelensis Eggs and Larvae. *Inst Med Trop São Paulo, 59*(e7), 1-6. doi:http://dx.doi.org/10.1590/S1678-9946201759007

Motoki, M., & Seguro, K. (1998). Transglutaminase and Its Use for Food Processing. *Trends food sci&technology, 9*(5), 204-210. doi: 10.1016/S0924-2244(98)00038-7

Müller, C., Liu, Y., Migge, A., Pietzsch, M., & Ulrich, J. (2011). Recombinant L-Asparaginase B and its Crystallization – What is the Nature ofProtein Crystals? *Chemical Engineering&Technology, 34*(No. 4), 571–577. doi:10.1002/ceat.201000504

Mullin, J. W. (2001). *"Crystallization," 4th Edition*.

Nekoueinaeini, S. M., Aliahmadi, A., & Soleimani, N. (2024). An Overview of Papain Enzyme Characteristics, Applications and Production. *Plant, Algae, and Environment, 8*(2), 1505-1527. doi:10.48308/jpr.2024.235806.1080

Noor, S. Z. M., Camacho, D. M., Ma, C. Y., & Mahmud, T. (2020). Effect of Crystallization Conditions on the Metastable Zone Width and Nucleation Kinetics of p-Aminobenzoic Acid in Ethanol. *Chem. Eng. Technol, 43*(6), 1105–1114. doi:10.1002/ceat.201900679

Nyvlt, J. (1984). Nucleation and Growth Rate in Mass Crystallization. *Crystal Growth and Charact., 9*, 335-370.

Parsaeimehr, A., Chen, Y.-F., & Sargsyan, E. (2014). Bioactive Molecules of Herbal Extracts with Anti-Infective and Wound Healing Properties. *Microbiology for Surgical Infections*, 209. doi:http://dx.doi.org/10.1016/B978-0-12-411629-0.00012-X

Qi Hao, Pan Guo, Honghai Wang, Min Su, Chunli Li, Yuqi Hu, & Su, W. (2024). Synergistic Precipitant Powered Self-Assembly of Papain for Cross-Linked Enzyme Crystals Preparation. *Particuology, 85*, 102-112. doi:https://doi.org/10.1016/j.partic.2023.03.023

Roy, J. J., & Abraham, T. E. (2003). Strategies in Making Cross-Linked Enzyme Crystals. *Chemical Review, 104*(no 9), 3706-3722. doi:10.1021/cr0204707

Ruth, A. (1970). The Cysteine Proteases: Papain. *In Methods in Enzymology; Perman, G.E., Lorand, L., Eds.; Elsevier, 19*, 226–244.

Ryu, B. H., & Ulrich, J. (2018). Protein Crystallization by Solvent Freeze-Out for Industrial Application. *Cryst. Growth Des, 18*, 6765−6776. doi:10.1021/acs.cgd.8b01027

Sacher, J. B., Bolf, N., & Sejdi, M. (2024). Batch Cooling Crystallization of a Model System Using Direct Nucleation Control and High-Performance In Situ Microscopy. *Crystals, 14*, 1079. doi:https://doi.org/10.3390/cryst14121079

Schmidt, S., Havekost, D., Klaus Kaiser, Kauling, J., & Henzler, a. H.-J. (2005). Crystallization for the Downstream Processing of Proteins. *Eng. Life Sci., 5*(No.3). doi:10.1002/elsc.200500116

Sirirak, J., Tamdee, P., Sawatthitileat, P., Thaithong, J., & Sirasunthorn, N. (2025). Papain-Catalyzed Hydrolysis of N**α**-Benzoyl–arginine–p-nitroanilide in an

Aqueous–Organic Medium. *ACS Omega, 10*, 8601–8610. doi:https://doi.org/10.1021/acsomega.4c11059

Tam, S. K., Chan, H. C., & Ng, K. M. (2011). Design of Protein Crystallization Processes Guided by Phase Diagrams. *Industrial & Engineering Chemistry Research, 50*, 8163-8175. Retrieved from https://pubs.acs.org/doi/pdf/10.1021/ie2002654

Tang, XH, Liu, JJ, & Zhang, Y. (2018). Study on the Influence of Lysozyme Crystallization Conditions on Crystal Properties in Crystallizers of Varied Sizes when Temperature is the Manipulated Variable. *Journal of Crystal Growth 498*, 186-196. doi:https://doi.org/10.1016/j.jcrysgro.2018.06.023

Ulrich, J., Bierwirth, J., & Henning, S. (1996). Solid Layer Melt Crystallization. *Separation & Purification Reviews, 25(1)*, 1-45. doi:10.1080/03602549608006625

Ulrich, J., & Stelzer, T. (2014). Chapter9: Melt Crystallization. *Cambridge Core terms of use*, 268. doi:https://doi.org/10.1017/9781139026949.009

Wang, Y., Li, N., Zhang, X., & Wang, Z. (2023). The Influence of Ionic Liquids on Solubility and Metastable Zone Width of Hen Egg Lysozyme. *Theoretical Foundations of Chemical Engineering, 57*(6), 1602–1609. doi:10.1134/S0040579523330102

Weber, P. C. (1997). Overview of Protein Crystallization Methods. *METHODS IN ENZYMOLOGY, 276*, 13-22. Retrieved from https://www.academia.edu/40780870/2_PROTEIN_CRYSTALLIZATION_METHODS_13_2_Overview_of_Protein_Crystallization_Methods

Wegner, C. H., Eming, S. M., Walla, B., Bischoff, D., Weuster-Botz, D., & Hubbuch, J. (2024). Spectroscopic Insights into multi-Phase Protein Crystallization in Complex Lysate using Raman Spectroscopy and a Particle-Free Bypass. *Front. Bioeng. Biotechnol, 12*, 1397465. doi:10.3389/fbioe.2024.1397465

Wiencek, J. M. (1999). New Strategies for Protein Crystal Growth. *Annual. Review. Biomedical Engineering, 01*, 505-534. Retrieved from https://www.annualreviews.org/doi/10.1146/annurev.bioeng.1.1.505

Xiaoxi Yu, Jingkang Wang, & Ulrich, J. (2015). Solvent-Freeze-Out (SFO) Technology: A Controlled Crystallization Process—Case Study of Jack Bean Urease. *Chemical Engineering Science 135*, 137–144. Retrieved from http://dx.doi.org/10.1016/j.ces.2015.05.012

Y. Liu, M. Pietzsch, & Ulrich, J. (2013). Purification of L-asparaginase II by Crystallization. *Chem. Sci. Eng., 7(1)*, 37–42. doi:10.1007/s11705-013-1303-z

Yi-Bin Lin, Dao-Wei Zhu, Tao Wang, Jian Song, Yong-Shui Zou, Yong-Lian Zhang, & Lin, S.-X. (2008). An Extensive Study of Protein Phase Diagram Modification: Increasing Macromolecular Crystallizability by Temperature Screening. *Crystal Growth & Design, 8*(12), 4277–4283. doi:10.1021/cg800698p

Yu, X., Wang, J., & Ulrich, J. (2014). Purification of Lysozyme from Protein Mixtures by Solvent-Freeze-Out Technology. *Chemical Engineering&Technology, 37*(No. 8), 1353–1357. doi:10.1002/ceat.201300832

Yu, X., Wu, Y., Huang, F., Ulrich, J., & Wang, J. (2017). Purification of Recombinant L-Asparaginase II Using Solvent-Freeze-Out Technology. *Chemical Engineering&Technology, 41*(6), 1080–1085. doi:10.1002/ceat.201700569

APPENDIX A

SUPPLEMENTARY INFORMATION

A.1 The induction time measurement by PVM100 (easy-viewer by Mettler Toledo) for papain cooling crystallization.

Papain saturation at 30 degree C in water was cooling by a rate of 0.005 degree C/min to 9 degree C (30 hours usage) with 50-100 rpm agitation (magnetic stir bar) and easy-viewer probe was added for observation the cloud point. In Figure A.1(a) the easy-viewer monitor showed uncount particle and clearly solution and after 15 hours, the cloud point started counting in Figure A.1(b). So, the total induction time was approximately 35 hours to nucleation, about 7 hours to growth and for none agitation was usaged about 50 hours to nucleation.

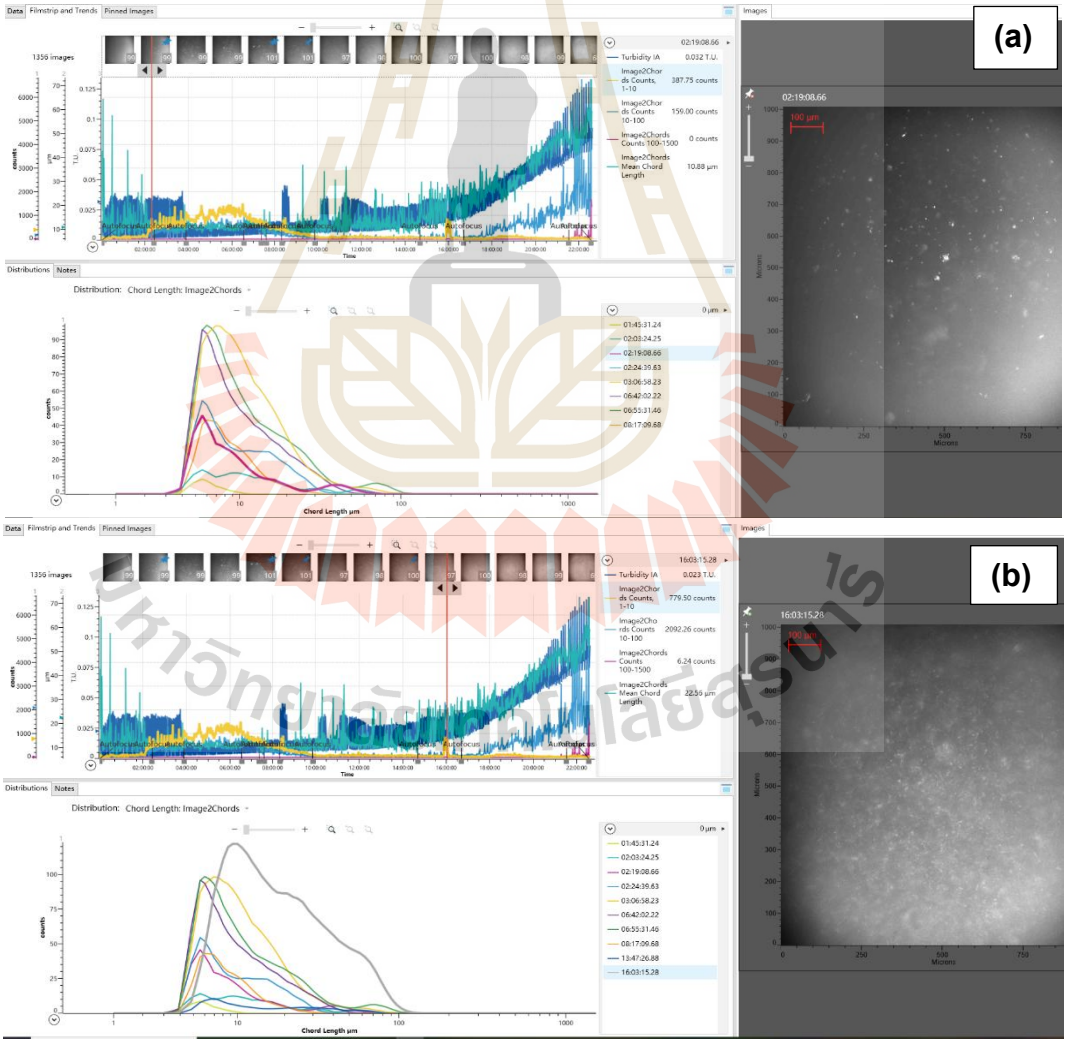

Figure A.1 Easy-viewer (100) probe observation the cloud point.

APPENDIX B

PUBLICATION AND PRESENTATIONS

B.1 List of publications

Chonut Xaiyathoumma, Penchit Chitnumsub and Lek Wantha (2025). Papain Crystallization Using Solvent Freeze-Out Crystallizer. **The 2025 Pure and Applied Chemistry International Conference (PACCON 2025),** E-proceeding April 30th, 2025.


CHEMISTRY FOR A CHANGING WORLD
PACCON
PURE AND APPLIED CHEMISTRY INTERNATIONAL CONFERENCE 2025
Pure and Applied Chemistry
International Conference 2025
PROCEEDINGS
Chemistry for a Changing World
Khao Yai Convention Center (KYCC),
Nakhon Ratchasima, THAILAND
February 13-15, 2025
https://paccon2025.sut.ac.th

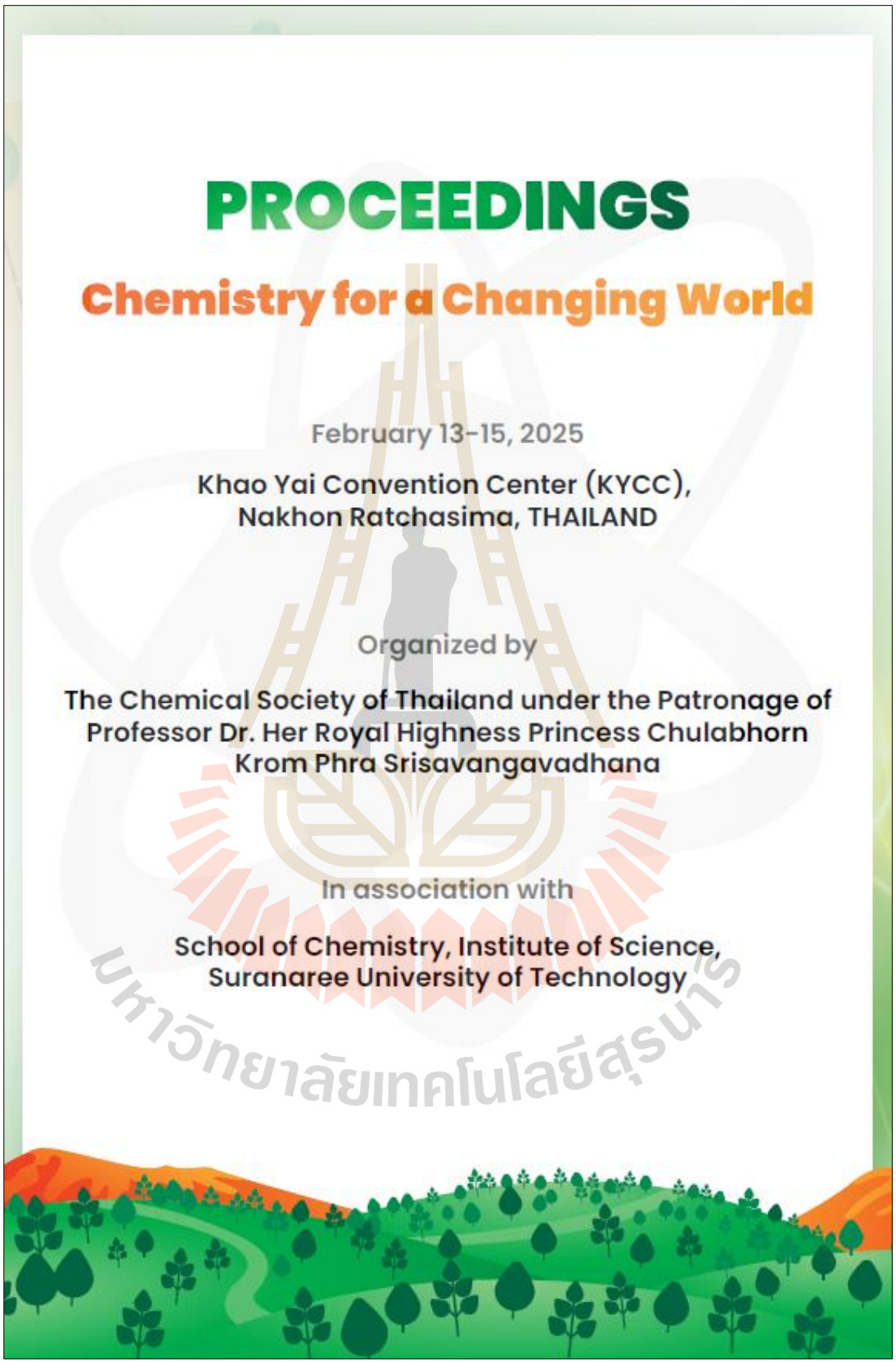

Pure and Applied Chemistry International Conference 2025 (PACCON 2025)

PROCEEDINGS

ISBN (e-book)	978-974-533-791-6
1st Edition	April 2025 (available in PDF version only)
Published by	The Chemical Society of Thailand under the Patronage of Professor Dr. Her Royal Highness Princess Chulabhorn Krom Phra Srisavangavadhana in association with the School of Chemistry, Institute of Science, Suranaree University of Technology

A CELEBRATION OF SUT 35TH ANNIVERSARY

NP-P-33

PACCON 2025 13-15 FEB 2025 VENUE @KYCC

Papain Crystallization Using Solvent Freeze-Out Crystallizer

Chonut Xaiyathoumma[1], Penchit Chitnumsub[2], and Lek Wantha[1]*

[1]*School of Chemical Engineering, Suranaree University of Technology, 111 University Avenue, Muang District, Nakhon Ratchasima 30000, Thailand*

[2]*Biomolecular Analysis and Application Research Team, National Center for Genetic Engineering and Biotechnology (BIOTEC), 113 Thailand Science Park, Phaholyothin Road, Khlong Luang, Pathum Thani 12120, Thailand*

**Corresponding author's e-mail address: lekwa@g.sut.ac.th*

Abstract:

To enhance the efficiency of industrial enzyme crystallization, important parameters such as the solubility curve must be understood. The solubility of papain was measured using the gravity method in an acetate buffer solution (pH 5) and in a buffer solution with methanol concentrations ranging from 0 to 0.6 weight fraction, while controlling the temperature at 20°C, 10°C, 0°C, and -8°C. Nucleation was studied by starting using saturated solutions. The solvent freeze-out (SFO) crystallization technique, conducted near the freezing point of water. The results showed that methanol reduced the solubility of crystalline papain, resulting in smaller nucleation at 0°C. Amorphous solid papain was obtained from the antisolvent crystallization. However, methanol had no effect on the enzyme activity of papain. Papain crystals obtained by the SFO method had a needle-like shape. The activity of the recovered papain crystals remained stable, with a 57% recovery, and 20% recovery for the saturation concentration of 0.4 g/mL and 0.33 g/mL, respectively.

1. Introduction

Crystallization enables the preservation of macromolecule properties and serves as an alternative method in the enzyme purification in food and pharmaceutical industries[1,2]. The crystallization of papain is quite challenging due to the various driving forces involved. Papain has an against microorganism ability and it is also intimate in the skincare's production area[3,4]. Therefore, it would be valuable if crystalline papain is incorporated into the supply chain. There are two mechanisms of crystallization including crystal nucleation and crystal growth. Nucleation is the initial stage of crystal formation. Supersaturation, agitation, time, and type or amount of anti-dissolution agent also affect nucleation[5,6]. Papain is also crystallized difficulty, but it has been successfully crystallized using methanol as a precipitant at pH5[7] with needle-like crystals[8]. Therefore, the methodology for crystallizing papain on an industrial scale should continue to be studied and refined. The effect of the amount of methanol on solubility should be considered before crystallization study. The solubility measurement using the gravimetric method is consistent, and nucleation studies by anti-solvent, monitoring by Focus Beam Reflectance Measurement (FBRM) or easy-viewer in solution, are also more suitable for industrial scale-up purposes[9]. However, from the preliminary crystallization of papain using methanol and measuring nucleation particles with FBRM, it was found that the solution sometimes becomes cloudy, but no particles were detectable. This is related to Andrea Sauter's criticism of the two-step nucleation process for some protein crystallizations[10]. In the first step, a solute or macroscopic dense liquid phase forms a metastable intermediate phase (nano-sized), followed by the second step, where nucleation occurs within that phase. This is consistent with a 2021 review that revises the solvent freeze-out (SFO) technology as an efficient method for protein crystallization[11]. The SFO process performs crystallization near the freezing point of water. The water content in protein/enzyme solution will be decreased by formation of ice on the freezing coil, which increases the solution concentration until the nucleation point is reached. However, this method has many parameters that need to be considered. In this study, a laboratory scale SFO crystallizer was set up. The cooling rate of freezing coil was fixed at 0.02°C/min as a step-down of temperature to avoid papain lost in ice[11]. The SFO process was prepared at close to 0°C saturation. The saturation of the solution was measured by the gravimetric method and with various methanol fraction. Supersaturation measurements using anti-solvent were also conducted and observed with an Easy-Viewer camera under the liquid. Methanol was added stepwise at a rate of 0.2 mL/20 min. It provides slow nucleation, to define first cloudy zone well and reduce wasting papain solution[12]. Therefore, this work focuses on nucleation points observation in the SFO process, and comparison products using methanol versus using the SFO method.

2. Materials and Methods

2.1 Materials

Crystalline papain (white powder) was purchased from Shaanxi Yuantai Biological Technology Co., Ltd (YT0829) and crystalline papain 2xUSP (14049) was purchased from Sisco Research Laboratories Pvt. Ltd (SRL). Sodium acetate trihydrate, ethylenediaminetetraacetic acid (EDTA), dimethylsulfide (DMSO), hydrochloric acid, and methanol were purchased from RCI LabscanLimited. Tris (hydroxymethyl-aminomethane) was from Carlo Erba. Glacial acetic acid was purchased from QReC New Zealand. Nα-Benzoyl-DL-arginine-4-nitroanilide-hydrochloride (BAPNA, B4875-1G) was purchased from Sigma-Aldrich. L-cysteine hydrochloride monohydrate (GRM046) was purchased from Himedia. All chemicals and reagents used were of analytical grade.

2.2 Solubility measurement

The solubility (saturation) was measured by the gravity method[12]. An excess amount of papain powder was dissolved in the acetate buffer solution (pH5) and in the buffer solution plus methanol at weight fractions of 0 to 0.6 while controlling the temperature at 20, 10, 0, and -8°C to observe the saturated points. The clear solution was sampled using syringe filters and monitored with a refractometer (Refractive Index, RI) every hour. The filtrated solution was then evaporated to dryness to determine the solution concentration.

2.3 Solvent Freeze-Out Crystallization

The solvent freeze-out (SFO) crystallization technique near the freezing point of water was conducted for papain solution at pH 5.[13]. The SFO crystallizer is a 50-mL jacket crystallizer assembly with a glass cold finger (freezing coil) that is temperature-controlled by a second thermostat. The setup is shown in Figure 1. The first thermostat controlled the jacket's temperature for saturation solution. The second thermostat manually lowered the temperature of the freezing coil at a rate not exceeding 0.20°C every 10 minutes (0.02°C/min), maintaining a stepwise reduction to the final temperature to prevent papain loss in the ice.[11, 14].

The final temperature of the freezing coil depended on the different saturation temperatures and continued freezing until the concentration of the papain solution reached supersaturation. Approximately 1-3 mL of the papain solution remained from the initial 7 mL, or about 14-42% of the final volume of solution. After crystallization occurred, the solution was maintained at the same nucleation temperature until growth ceased, and the papain crystals were harvested. The growth continued for approximately 72 hours. The weight of papain lost in the ice of the freezing coil and the recovery of papain crystals were calculated by Equations 1 and 2, respectively. The nucleation points, or supersaturation points, were marked on the phase diagram, as shown in Figure 3.

$$\text{Mass lost papain\%} = \frac{B}{i} \times 100\% \quad (1)$$

$$\text{Recovery\% of crystalline papain} = \frac{C}{i} \times 100\% \quad (2)$$

where B is the mass (g) of papain in ice per volume; i is the initial mass (g) of papain in saturated solution before the SFO process launching; C is dry mass (g) of papain crystal after the process. The crystal was captured by microscope.

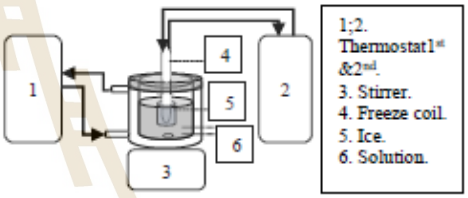

Figure 1. The SFO crystallizer set-up.

2.4 Assays of Enzymatic Activity and PXRD

The enzymatic activity of papain from commercials supplier, an anti-solvent, and the SFO process were measured by Anorn Ruth's method[15-17]. Crystalized papain was confirmed by powder X-ray diffraction (PXRD, D2-Phaser, BRUKER).

The substrate solution was prepared by dissolving 43.5 mg of BAPNA in 1 mL of DMSO and the volume was adjusted to 100 mL with Tris-buffer (0.05 M Tris, pH 7.5 by HCl, containing 0.005 M cysteine and 0.002 M EDTA). All the solid papain was dissolved in DI-water at a concentration of 30 mg/mL and measured by UV-vis spectroscopy (DR6000, Hach, Ames, IA, USA) at 280 nm (Quartz U-shaped cuvette, Di-water was blank), to confirm the concentration. One milliliter of the papain solution was reacted with 5 mL of the BAPNA substrate in test tubes at 25°C for 25 min. The reaction was stopped by adding 1 mL of 30%v/v acetic acid before measuring the absorbance by UV-vis at 410 nm (5 mL substrate + 1 mL acetic acid was used as the blank), corresponding to the liberated p-nitroaniline. The absorbance values of the product were used in calculation by Equation 3 for substrate hydrolysis (BAPNA Units) and specific activity as Units per mg of papain. In the same way, the BAPNA activity is

defined as the enzyme hydrolyzing 1 micromole of substrate per minute.

$$\text{BAPNA Units}=\frac{Abs_{410nm}}{25min}\times\frac{3\times1000}{8800} \quad (3)$$

$$\text{Specific activity}=\frac{\text{Units}}{mg}=\frac{\text{BAPNA Units}}{30mg} \quad (4)$$

where Abs_{410nm} is the absorbance of product p-nitroaniline (yellow); t is 25 min of enzymatic reaction; and 8800 M^{-1} cm^{-1} is the p-nitroaniline molar extinction coefficient at 410 nm. The enzyme activity was measured immediately after complete dissolution.

3. Results & Discussion

3.1 Solubility

The solubility of papain in mixture of acetate buffer (pH5) and methanol is illustrated in Figure 2. The result showed that the papain solubility decreased with increasing methanol weight fraction and decreasing temperature.

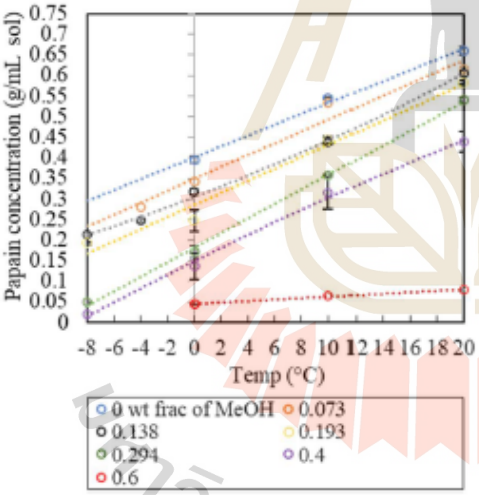

Figure 2. The solubility of papain at various temperatures and methanol fractions.

3.2 The SFO Crystallization

Solvent freeze-out crystallization was carried out at three concentration levels: supersaturation (0.472 g/mL), saturation (0.4 g/mL), and undersaturation (0.33 g/mL), respectively to observe the nucleation point with different temperatures (-1.5, -0.5, and 1°C). The phase diagram used for the SFO process of papain is shown in Figure 3. The nucleation point was quite high.

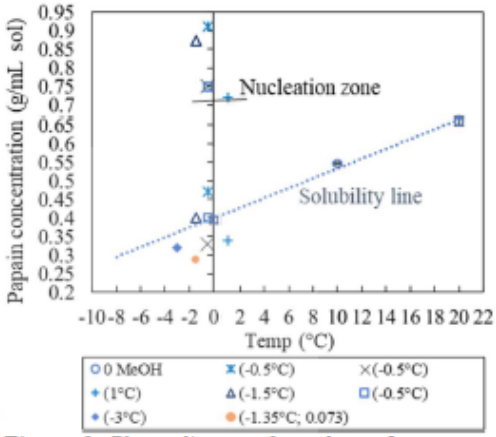

Figure 3. Phase diagram for solvent freeze-out crystallization of papain solutions.

Figure 4 describes the control of the freezing coil temperature and the solution temperature of the saturated papain solution (0.47 g/mL, 6.6 mL) from the point the coil was immersed in the solution (-3°C) until the freezing and nucleation occurred. Ice started to form on the freezing coil at -5°C, and ice growth continued at -6.8 °C until the final coil temperature reached -12.6 °C. The temperature was held constant at -12.6°C until the papain solution volume was reduced to 2-3 mL, at which point stirring was initiated at 120 rpm for 10 min. Then, the solution was kept until nucleation, which occurred at hour 188 (24 hours after stirring). At this point, the freezing coil was turned off. The solution concentration was measured immediately at the nucleation point by reflectometer and it was kept at constant temperature until growth stopped. Crystals harvesting and characterization followed this. The nucleation process, crystal growth images, and photomicrographs of papain crystals obtained from SFO crystallization are shown in Figure 5. At the time of nucleation, the final volume was 2.6 mL, and the nucleation concentration was 0.91 g/mL (Figure 3).

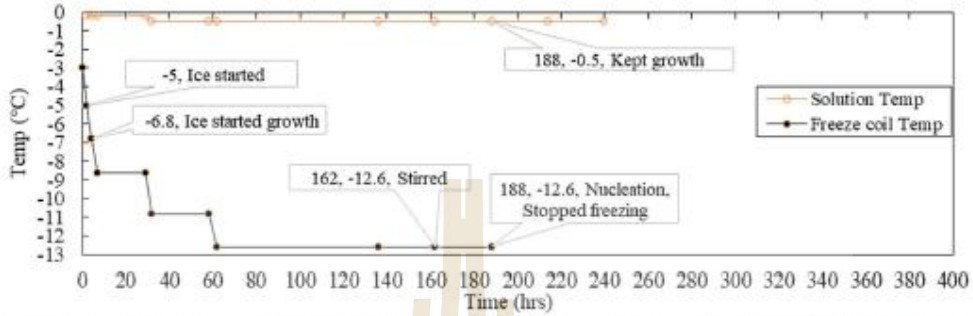

Figure 4. The temperature reduction profile of the freezing coil for initial 0.47 g/mL papain solution at -0.5°C.

Figure 5. The SFO crystallizer and photomicrographs of papain crystals obtained from SFO crystallization of initial 0.47 g/mL papain solution at -0.5 °C.

Figure 6 describes the control of the freezing coil temperature and the solution temperature of the saturated papain solution 0.4 g/mL (7 mL) from the point the coil was immersed in the solution (-3 °C) until the freezing and nucleation occurred. Ice started growing at -6.6 °C and continued until the final coil temperature reached -12.6 °C. The temperature was held constant at -12.6 °C, and stirring was initiated at 120 rpm for 10 min at hour 148. Then, the solution was observed for 72 hours and re-stirred at hour 233 due to no nucleation occurring. Nucleation started at hour 311 (3 days + 10 hours after stirring). It appeared a bit cloudy and was left for another 20 hours to confirm the process. The freezing coil was turned off at hour 331. At this point, the solution concentration was 0.7449 g/mL (2 mL), and it was maintained. The crystals were harvested after 72 hours. The nucleation process, crystal growth images, and photomicrographs of papain crystals obtained from SFO crystallization are shown in Figure 7.

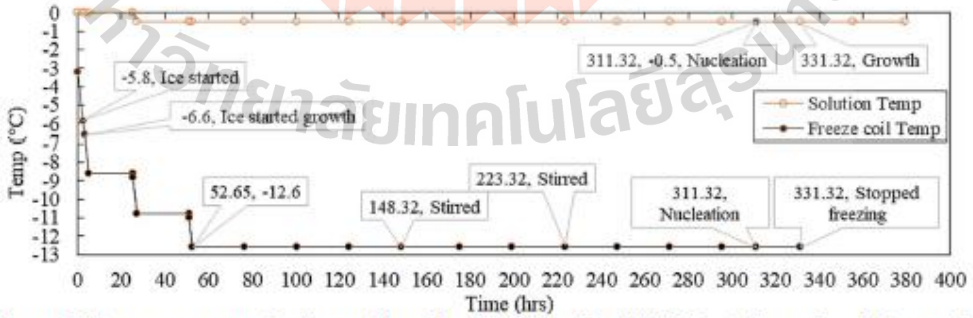

Figure 6. The temperature reduction profile of the freezing coil for initial 0.4 g/mL papain solution at -0.5°C.

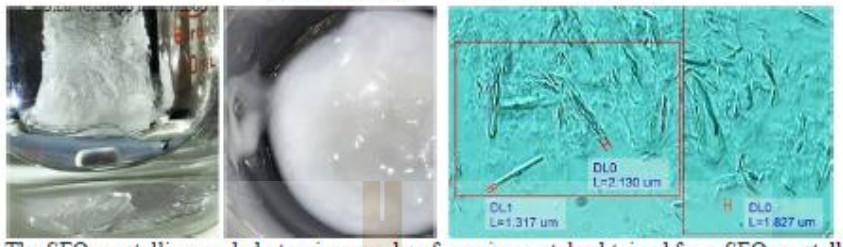

Figure 7. The SFO crystallizer and photomicrographs of papain crystals obtained from SFO crystallization of initial 0.4 g/mL papain solution at -0.5°C.

Figure 8 describes the control of the freezing coil temperature and the solution temperature of the saturated papain solution 0.33 g/mL (7 mL) from the point the coil was immersed in the solution (-3 °C) until the freezing and nucleation occurred. Ice started growing at -3.6 °C, and the final coil temperature reached -12.6 °C, at hour 60. The temperature was held constant at -12.6°C, and stirring started at hour 140 and re-stirred at 182. The solution was then observed for 72 hours and re-stirred at hour 254 due to no nucleation occurring, although it became slightly sticky. The freezing coil was turned off at hour 254, and the solution was stored. A slight nucleation was observed at hour 278. The solution concentration was 0.7482 g/mL (1.9 mL), and it was kept for further growth. The crystals were harvested after 72 hours. So, for this initial concentration the freezing coil should be turned off at around -12.2°C to avoid high viscosity. The nucleation process, crystal growth images, and photomicrographs of papain crystals obtained from SFO crystallization are shown in Figure 9.

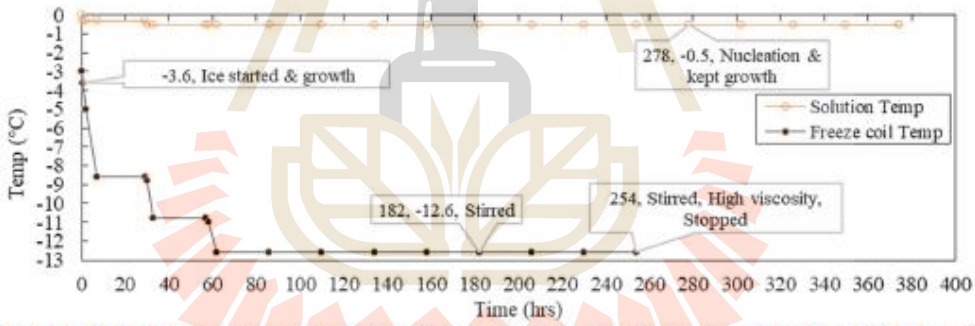

Figure 8. The temperature reduction profile of the freezing coil for initial 0.33 g/mL papain solution at -0.5°C.

Figure 9. The SFO crystallizer and photomicrographs of papain crystals obtained from SFO crystallization of initial 0.33 g/mL papain solution at -0.5°C.

The SFO process for 0.47, 0.4, and 0.33 g/mL initial papain concentration at -0.5°C influenced the percent recovery, as shown in Table 1. The percent recoveries were 64%, 57%, and 20% for 0.47 g/mL, 0.4 g/mL, 0.33 g/mL, respectively. However, all three concentrations unlost more than 26%, indicating that a freezing rate of 0.02°C/min[11] is effective. The initial

concentrations of 0.4 and 0.33 g/mL took time to nucleate more than 200 hours. However, at an initial 0.33 g/mL papain solution reached nucleation after the freezing coil was stopped, likely due to the high viscosity that developed on the surface of the papain solution. This is because the lower concentration allowed the ice to grow faster than at the higher initial papain concentration. Even though, all the recovered crystals exhibited a needle-like crystal shape and growth, which indicates the crystal shape of papain.[8]

Table 1. Comparison of the percent lost into the freezing coil and recovery of papain crystallization using SFO at solution temperature of -0.5 °C.

Initial Concentration, g/mL	Final Volume, mL	%Recovery	%Lost in Ice
0.47	2.6	64	21
0.4	2	57	26
0.33	1.9	20	21

3.3 The Enzymatic Activity and PXRD

The papain powder was dissolved in DI water, and its concentration was prepared and calculated from the prepared calibration curve shown in Figure 10. The calibration curve of papain was measured at 280 nm before reacting with the substrate. The parched crystalline papain, papain solid obtained from antisolvent crystallization using methanol, and papain crystals obtained from the SFO crystallization were each tested at 30 mg/mL for reaction with the substrate and the resulting product was measured at 410 nm, as shown in Figure 11. The activity was then calculated, and the specific activity is shown in Figure 12. The results showed no reduction in activity. This work was further examined using PXRD, as shown in Figure 13. The product obtained from the SFO process had high crystallinity, while the product obtained from anti-solvent crystallization was amorphous.

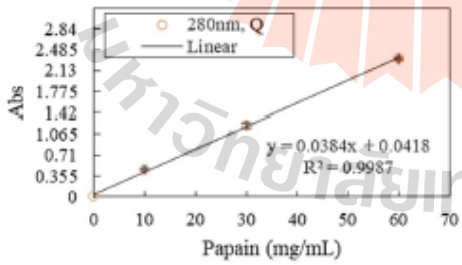

Figure 10. The calibration for determining the concentration obtained from UV-vis spectroscopy at 280 nm.

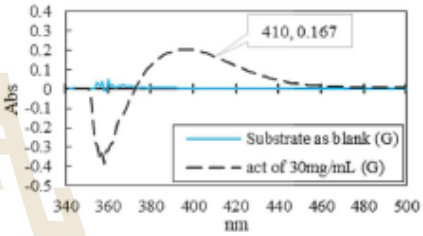

Figure 11. The product was analyzed using UV-vis spectroscopy at 410 nm.

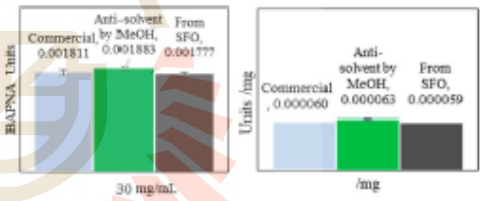

Figure 12. Enzyme activity of purchased papain (left), antisolvent crystallization (middle), and SFO (right).

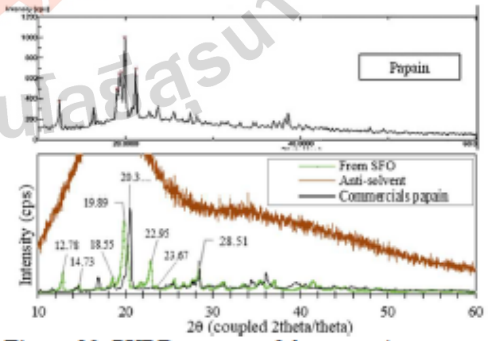

Figure 13. PXRD patterns of these papain crystals obtained from this work (Bottom) and previous work (Top)[18].

4. Conclusion

The SFO crystallization itself involves complex parameters that need to be controlled. However, this study successfully crystallized papain from solution at a solution temperature of -0.5°C, with concentrations ranging from 0.33 to 0.47 g/mL, and a final freezing coil temperature of -12.6°C. The crystals obtained from the SFO crystallization were needle-like. In contrast, antisolvent crystallization using methanol produced amorphous-like. Furthermore, the effect of methanol on the solubility of papain is consistent, and the specific activity remains stable.

Acknowledgments

We gratefully acknowledge the financial support of the National Science and Technology Development Agency (NSTDA) through the Thailand Graduate Institute of Science and Technology (TGIST) scholarship agreement (Grant Agreement No. SCA-CO-2563-12080-EN), and Suranaree University of Technology research fund. The authors also acknowledge the research funding from (i) Suranaree University of Technology (SUT), (ii) Thailand Science Research and Innovation (TSRI), and (iii) National Science, Research and Innovation Fund (NSRF)-Grant No. 195675.

References

1. Motoki, M.; Seguro, K., Transglutaminase and Its Use for Food Processing. *Trends Food Sci&Technology* **1998,** *9* (5), 204-210.
2. Tam, S. K.; Chan, H. C.; Ng, K. M., Design of Protein Crystallization Processes Guided by Phase Diagrams. *Industrial & Engineering Chemistry Research* **2011,** *50*, 8163-8175.
3. Amri, E.; Mamboya, F., Papain, A Plant Enzyme of Biological Importance: A Review. *American Journal of Biochemistry and Biotechnology* **2012,** *8* (2), 99-104.
4. Parsaeimehr, A.; Chen, Y.-F.; Sargsyan, E., Bioactive Molecules of Herbal Extracts with Anti-Infective and Wound Healing Properties. *Microbiology for Surgical Infections* **2014,** 209.
5. NyvIt, J., Nucleation and Growth Rate in Mass Crystallization. *Crystal Growth and Charact.* **1984,** *9*, 335-370.
6. Giulietti, M.; Seckler, M. M.; Derenzo, S.; Re, M. I.; Cekinski, E., Industrial Crystallization and Precipitation from Solutions: State of the Technique. *Brazilian Journal of Chemical Engineering* **2001**, 1-25.
7. Kamphuis, I. G.; Kalk, K. H.; Swarte, M. B. A.; Drenth, J., Structure of Papain Refined at 1.65 A Resolution. *Academic Press Inc. (London) Ltd.* **1984,** *179*, 233-256.
8. Harris, J. R., Electron Microscopy of Papain Crystals. *Printed in Great Britain, Micron.* **1983,** *14* (2), 147-164.
9. Kongsamai, P.; Wantha, L.; Flood, A. E.; Tangsathitkulchaia, C., In-situ Measurement of the Primary Nucleation Rate of the Metastable Polymorph B of L-histidine in Antisolvent Crystallization. *Elsevier Science Publishers B.V.* **2019,** *525*, 125209.
10. Andrea, S.; Felix, R. R.; Fajun, Z.; Gudrun, L.; Artem, F.; Robert, M. J.; Jacobse.; Frank, S., On the Question of Two-Step Nucleation in Protein Crystallization. *Faraday Discuss* **2015,** *179*, 41-58.
11. Ming, H.; Zhu, M.-F.; Li, L.; Liu, Q.-B.; Yu, W.-H.; Wu, Z.-Q.; Liu, Y.-M., A Review of Solvent Freeze-Out Technology for Protein Crystallization. *CrystEngComm* **2021,** *23*, 2723.
12. Yu, X.; Wu, Y.; Huang, F.; Ulrich, J.; Wang, J., Purification of Recombinant L-Asparaginase II Using Solvent-Freeze-Out Technology. *Chemical Engineering&Technology* **2017,** *41* (6), 1080–1085.
13. Borbon, V. P. D.; Ulrich, J., SFO-Solvent Freeze Out-Technology for Industrial Proteins. *Elsevier Science Publishers B.V.* **2013,** *373*, 38–44.
14. Ryu, B. H.; Ulrich, a. J., Protein Crystallization by Solvent Freeze-Out for Industrial Application. *Crystal Growth & Design* **2018,** *18*, 6765−6776.
15. Iván E. Moreno-Cortez; Jorge Romero-García; Virgilio González-González; Domingo I. García-Gutierrez; Marco A. Garza-Navarro; Cruz-Silva, R., Encapsulation and Immobilization of Papain in Electrospun Nanofibrous Membranes of PVA Cross-Linked with Glutaraldehyde Vapor. *Materials Science and Engineering* **2015,** *C* (52), 306–314.
16. Boonkerd, S.; Wantha, L., Antisolvent Crystallization of Papain. *ChemEngineering* **2024,** *8* (4).
17. Ruth, A., The Cysteine Proteases: Papain. *In Methods in Enzymology; Perman, G.E., Lorand, L., Eds.; Elsevier* **1970,** *19*, 226–244.
18. Chandran, S. P.; Nachimuthu, K., Formulation and Characterization of Papain Loaded Solid Lipid Nanoparticles Against Human Colorectal Adenocarcinoma Cell Line. *Asian J Pharm Clin Res* **2018,** *11* (10), 393-399.

B.2 List of presentations

Chonut Xaiyathoumma, Penchit Chitnumsub and Lek Wantha (2022). Preliminary Study of Lysozyme Crystallization in Ammonium Sulfate Solution using Solvent Freeze-Out Crystallizer. **The 31st Thai Institute of Chemical Engineering and Applied Chemistry Conference (TIChE2022),** which held online on March 15th-16th, 2022, organized by The Thai Institute of Chemical Engineering and Applied Chemistry (TIChE) and the Department of Chemical Engineering, Naresuan University, Thailand. (Poster presentation)

Chonut Xaiyathoumma, Penchit Chitnumsub and Lek Wantha (2023). The Study of α-amylase Crystallization from Commercializes α-amylase Broth with various Salt Precipitants. **The 32nd Thai Institute of Chemical Engineering and Applied Chemistry Conference (TIChE2023)**, Nakhon Pathom, Thailand, March 16th-17th, 2023, organized by The Thai Institute of Chemical Engineering and Applied Chemistry (TIChE) and the Department of Chemical Engineering, Silpakorn University. (Oral presentation)

Chonut Xaiyathoumma, Penchit Chitnumsub and Lek Wantha (2023). The Nucleation Zone Screening of Crystalline Papain from Solution by Dropwise Methanol Cooling Crystallization. **The 12th International Symposium on Nano & Supramolecular Chemistry (ISNSC-12) & The 3rd Thailand Biorefinery Symposium (TBioS-3)**, Chiang Mai, Thailand, July 23rd-26th, 2023, organized by Thammasat University's Faculty of Science and Technology. (Oral presentation)

Chonut Xaiyathoumma, Penchit Chitnumsub and Lek Wantha (2023). Nucleation of Papain using Methanol as Precipitant. **The 6th Asian Crystallization Technology Symposium (ACTS2023), (Virtual Conference),** Taipei, Taiwan, September 25th-26th, 2023, organized by National Central University, National Taiwan University, National Taipei University of Technology, and Chang Gung University. (Oral presentation)

Chonut Xaiyathoumma, Penchit Chitnumsub and Lek Wantha (2024). Effect of Methanol on the Solubility and Nucleation Point of Papain. **The 33rd Thai**

Institute of Chemical Engineering and Applied Chemistry International Conference (TIChE2024), Krungsri River Hotel Ayutthaya, Thailand, March 7th-8th, 2024, organized by Rajamangala University of Technology Thanyaburi. (Oral presentation)

Chonut Xaiyathoumma, Penchit Chitnumsub and Lek Wantha (2024). Effect of Methanol on the Solubility and Nucleation Point of Papain. **The 4th Thailand Biorefinery Symposium (TBioS-4)**, pullman Khon Kaen Raja Orchid hotel, Thailand, June 13rd-14th, 2024, organized by Faculty of Engineering, Khon Kaen University. (Oral presentation)

Chonut Xaiyathoumma, Penchit Chitnumsub and Lek Wantha (2024). Effect of Methanol on the Solubility and Nucleation Point of Papain**. The 15th International Workshop on Crystal Growth of Organic Materials (CGOM15),** Phuket, Thailand, July 23rd-26th, 2024, organized by School of Chemical Engineering, Suranaree University of Technology. (Poster presentation)

Chonut Xaiyathoumma, Penchit Chitnumsub and Lek Wantha (2025). The full article Papain Crystallization Using Solvent Freeze-Out Crystallizer. **The 2025 Pure and Applied Chemistry International Conference (PACCON 2025),** Khao Yai Convention Center, Nakhon Ratchasima, Feb 13th-15th, 2025, online E-proceeding April 30th, 2025, organized by Chemical society of Thailand and Suranaree University of technology. (Poster presentation)

Chonut Xaiyathoumma, Lek Wantha and Hongxun Hao (2025). A Comparative Study of Solvent Freeze-Out, Cooling, and Antisolvent Techniques for Papain Crystallization. **7th Asian Crystallization Technology Symposium (ACTS2025),** Pukyong National University, Busan, Republic of Korea, 12th-14th, November, organized by Asian Crystallization Society, Pukyong National University, The Division of Separation Technology, Korean Institute of Chemical Engineers and Institute of Energy Converting Soft Materials (IECSM), Chung-Ang University. (Oral presentation)

BIOGRAPHY

Chonut Xaiyathoumma was born on September 28, 1997, in HouaPhanh province, Laos PDR. He completed his primary education at Ban ThatMueang School, ThatMueang village, HouaPhanh province, in the academic year 2007. For his secondary and upper secondary education, he attended ChanSawang secondary&high School, Sikhottabong district, Vientiane Capital, in the academic year 2015. He pursued his bechelor's degree in chemical engineering at National University of Lao, Vientiane Capital and graduated in academic year 2019. His undergraduate research focused on the design of vacuum bio-oil evaporator and bio-fuel characteristic study of evaporated oil from Yang-Na-oil. During his studies, he completed two internships, first at Beer-Laos brewery CO., Ltd for 45days, in line of production and waste water treatment & bio-gas, second at Bio-diesel plant of Lao-Agrotech public company (Laos). He also achieved two exchange programs, first was Erasmus plus to study in Babes-Bolyai University (Bio-Chem & Chemical engineering lab) and second was trainee in Toyohashi University of Technology (fluid mechanic lab) by JICA in 2019. He continued his education by pursuing a master's degree in chemical engineering at Suranaree University of Technology, starting in the academic year 2020. During his master's studies, he conducted research on papain crystallization using solvent freeze-out technique. Additionally, he presented his research findings at international conferences such as...TIChE2022, TIChE2023, Thailand, ISNSC-12&TBioS-3, 2023, Chiang Mai, ACTS2023 (Virtual Conference), Taiwan, TIChE2024, Ayutthaya, TBioS-4, 2024, Khon Kaen, the 2025 Pure and Applied Chemistry International Conference (PACCON2025), on Feb 13rd-15th, 2025, Nakhon Ratchasima, Thailand, and 7th ACTS2025, Busan, Korea. Furthermore, he actively engaged in various research activities such as an Exchange program on March 1st to June 1st, 2025, National Engineering Research Center of Industrial Crystallization Technology (NERCICT), Tianjin University, China and he also served as a teaching assistant, contributing to the enhancement of knowledge and research development in SUT.